

Forsmark site investigation

The character and kinematics of deformation zones (ductile shear zones, fracture zones and fault zones) at Forsmark – report from phase 2

Aline Saintot, Øystein Nordgulen
Geological Survey of Norway

October 2007

Svensk Kärnbränslehantering AB

Swedish Nuclear Fuel
and Waste Management Co
Box 5864
SE-102 40 Stockholm Sweden
Tel 08-459 84 00
+46 8 459 84 00
Fax 08-661 57 19
+46 8 661 57 19



Forsmark site investigation

The character and kinematics of deformation zones (ductile shear zones, fracture zones and fault zones) at Forsmark – report from phase 2

Aline Saintot, Øystein Nordgulen
Geological Survey of Norway

October 2007

Keywords: Forsmark, AP PF 400-06-109, Structural geology, Deformation zone, Shear zone, Fracture zone, Fault zone, Mylonite, Cataclasite, Fault breccia, Kinematics.

This report concerns a study which was conducted for SKB. The conclusions and viewpoints presented in the report are those of the authors and do not necessarily coincide with those of the client.

Data in SKB's database can be changed for different reasons. Minor changes in SKB's database will not necessarily result in a revised report. Data revisions may also be presented as supplements, available at www.skb.se.

A pdf version of this document can be downloaded from www.skb.se.

Abstract

This report presents the results of a study of predominantly brittle structures, i.e. faults and fractures, observed within 34 deformation zones of nine boreholes at Forsmark. The work expands on previously reported studies and aims to document the character. Including the kinematics of the brittle deformation zones.

Structural data were obtained from selected, previously defined possible deformation zones of drill cores from nine boreholes (KFM01C, KFM01D, KFM06C, KFM07B, KFM07C, KFM08C, KFM09A, KFM09B and KFM10A). The character of each deformation zone is described in terms of fracture frequency, the distribution of transition zones and fault core and kinematics. Polished thin sections from samples collected from the drill cores were studied using standard petrographic techniques, and in some cases also SEM (backscatter). Observations from thin sections combined with data from drill cores form the basis for the conclusions of this study.

The investigated structures different types of cataclasite, and some breccias cemented by various minerals. In most drill cores, there are abundant fractures, commonly with kinematic indicators. These are in most cases coated or filled with a range of different minerals reflecting the changing conditions during successive brittle events. The amount and quality of acquired kinematic structural data are quite variable. However, in many cases excellent data were obtained, and in general this manner of obtaining data adds substantially to the value of structural information that can be effectively retrieved from the drill cores.

The main set of brittle structures recorded in this study are sinistral, steep, strike-slip faults oriented NW-SE to NNW-SSE. A possibly conjugate set of ENE-WSW dextral, steep, minor faults is also encountered along the investigated drill cores. In addition, gently south-dipping, reverse, minor faults oriented NE-SW to ENE-WSW are present in several drill cores. Striations on minor fault planes along the drill cores are observed on chlorite, hematite and calcite. Calcite steps on fault planes are also common and allow exact determination of the sense of shear. Epidote- and quartz-filled fractures are among the oldest brittle structures observed. Fault rocks occur as mainly laumontite-cemented cataclasites and breccias post-dated by veins sealed with calcite, prehnite and laumontite.

In total, considerable amounts of new data have been acquired that pertain to the understanding of the structural evolution of faults and fractures on a local and regional scale. Combining the new data with those previously collected from surface outcrops and from deformation zones in drill cores, provides valuable input to a kinematic study of the brittle deformation products at the Forsmark site.

Sammanfattning

Denne rapporten presenterer resultatene fra en undersøkelse av i hovedsak sprø strukturer, dvs forkastninger og sprekker, gjennomført på 34 deformasjonssoner i 9 borehull i Forsmark. Arbeidet er en forsettelse av tidligere undersøkelser der det viktigste målet er å dokumentere geometri og kinematikk relatert til sprø deformasjon.

Strukturdata ble samlet inn fra utvalgte, tidligere definerte deformasjonssoner i kjerner fra 9 borehull (KFM01C, KFM01D, KFM06C, KFM07B, KFM07C, KFM08C, KFM09A, KFM09B og KFM10A). Hver deformasjonssone er beskrevet med hensyn til sprekkefrekvens, fordeling av overgangssoner (transition zones) og forkastningskjerner (fault core), og kinematikk. Polerte tynnslip fra borekjernene ble studert ved hjelp av standard petrografiske teknikker, og i noen tilfeller ved bruk av SEM (backscatter). Observasjoner fra tynnslip sammen med data fra borekjerner danner basis for konklusjonene i dette arbeidet.

De undersøkte strukturene omfatter flere typer kataklasitt, og breksjer som er sementert av ulike mineraler. I de fleste borekjerner fins det flere sprekkesett, i mange tilfeller med kinematiske indikatorer. Sprekkene er i de fleste tilfeller dekket eller fylt med ulike mineraler som reflekterer forholdene under flere deformasjonshendelser. Mengde og kvalitet på kinematiske data varierer. I mange tilfeller ble det samlet inn en betydelig mengde nye data som vil øke nytten av den strukturelle informasjonen som blir samlet inn fra borekjerner.

De viktigste sprø strukturene observert i denne undersøkelsen er sinistrale, steile, sidelengs forkastninger orientert NV-SØ til NNV-SSØ. Et mulig konjugert sett med dekstrale steile forkastninger orientert ØNØ-VSV ble også observert. I tillegg fins det i flere borekjerner en del reversforkastninger orientert NØ-SV til ØNØ-VSV. Slickensides på forkastningsplan er definert av kloritt, hematitt og kalkspat. Kalkspat danner i mange tilfeller steg på forkastningsplanet og gir dermed mulighet for å avklare relativ bevegelse langs forkastningen. Epidot- og kvartsfylte sprekker er de eldste observerte sprø strukturene. Forkastnings-bergarter fins i hovedsak som laumontitt-sementerte kataklasitter og breksjer gjennomsett av yngre årer forseglet med kalkspat, prehnitt og laumontitt.

Til sammen er det samlet inn en betydelig mengde nye data som har betydning for forståelsen av den strukturelle utviklingen langs forkastninger og sprekker på lokal og regional skala. Ved å sammenstille nye data med det som tidligere er innsamlet fra overflaten og fra deformasjonssoner i borehull, vil det gi et viktig bidrag til studiet av den kinematiske utviklingen av de sprø deformasjonsstrukturene i Forsmark.

Contents

1	Introduction	7
2	Objective and scope	9
3	Equipment	11
3.1	Description of equipment	11
4	Execution	13
4.1	Nomenclature	13
4.2	Working procedure	16
4.3	Analysis and interpretation	17
4.4	Data handling and processing	18
4.5	Nonconformities	18
5	Results	19
5.1	Drill core investigations	19
5.1.1	Investigated drill cores	19
5.1.2	KFM01C	20
5.1.3	KFM01D	28
5.1.4	KFM06C	31
5.1.5	KFM07B	43
5.1.6	KFM07C	45
5.1.7	KFM08C	52
5.1.8	KFM09A	58
5.1.9	KFM09B	71
5.1.10	KFM10A	83
5.2	Summary of the results of the borehole data	89
	References	91
	Appendix 1 Samples for microscope studies	93

1 Introduction

This document reports the results of a study of the character and kinematics of a number of deformation zones at the Forsmark site. This study forms one of the activities performed within the site investigation work at Forsmark (Figure 1-1). The work was carried out in accordance with activity plan AP PF 400-06-109. Controlling documents for performing this activity are listed in Table 1-1. Both activity plan and method descriptions are SKB's internal controlling documents.

Original data from the reported activity are stored in the primary database Sicada, where they are traceable by the Activity Plan number (AP PF 400-06-109). Only data in SKB's databases are accepted for further interpretation and modelling. The data presented in this report are regarded as copies of the original data. Data in the databases may be revised, if needed. Such revisions will not necessarily result in a revision of the P-report, although the normal procedure is that major data revisions entail a revision of the P-report. Minor data revisions are normally presented as supplements, available at www.skb.se.

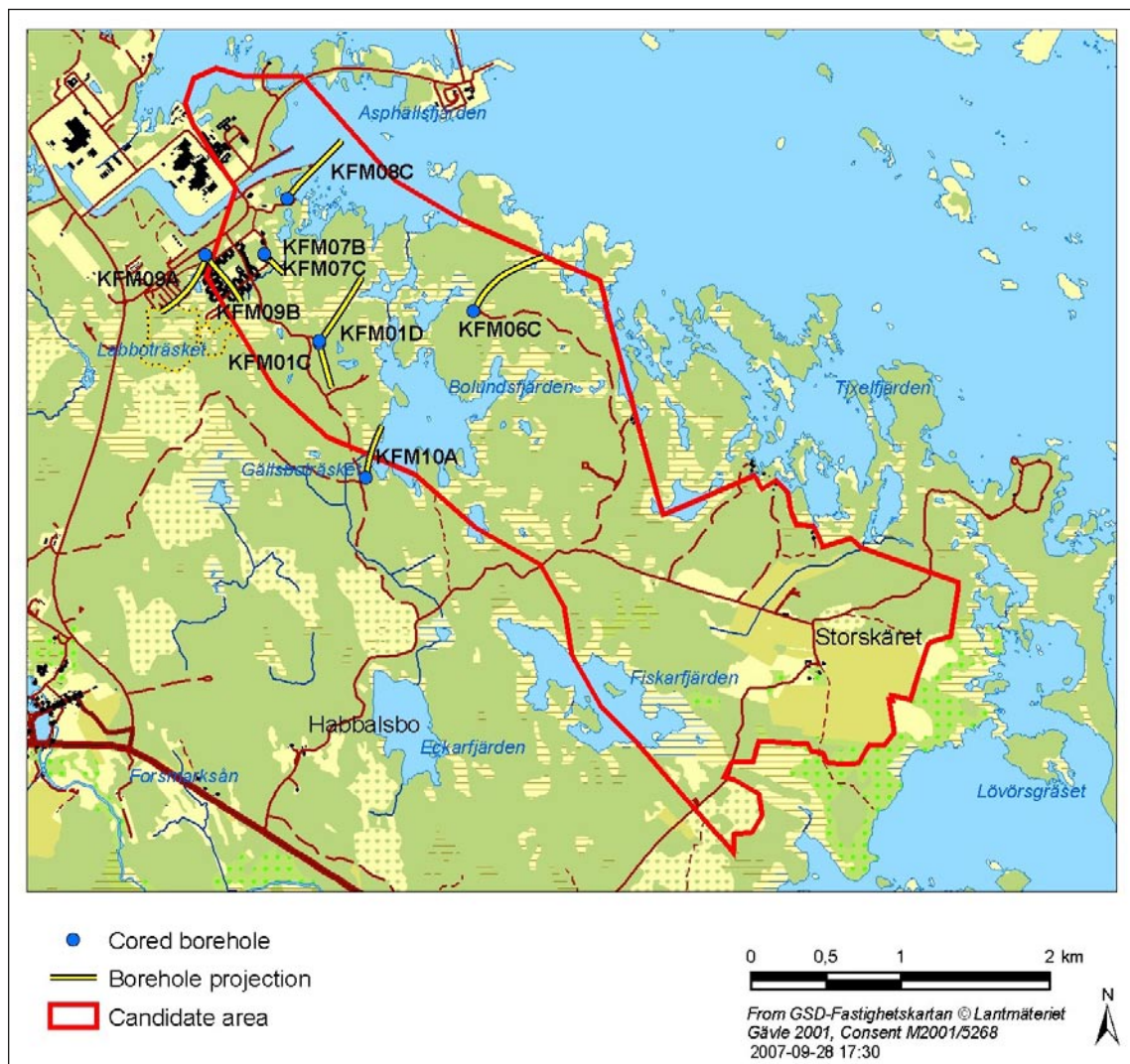


Figure 1-1. General overview of the Forsmark site investigation area. The locations of the boreholes used for obtaining the structural data are shown.

Table 1-1. Controlling documents for the performance of the activity.

Activity plan	Number	Version
Karaktärisering av spröda deformationszoner, steg 2	AP PF 400-06-109	1.0
Method description	Number	Version
Metodbeskrivning för geologisk enhålstolkning	SKB MD 810.003	3.0
Methodology referenses used in this study		
/Braathen 1999/	Tectonophysics 302, 99–121.	
/Braathen et al. 2002/	Norwegian Journal of Geology, 82, 225–241.	
/Braathen et al. 2004/	Tectonics, 23, TC4010, doi:10.1029/2003TC001558.	
/Nordgulen et al. 2002/	Norwegian Journal of Geology, 82, 299–316.	
/Osmundsen et al. 2003/	Journal of the Geological Society, London 160, 1–14.	
/Petit 1987/	Journal of Structural Geology 9, 597–608.	

2 Objective and scope

The aim of this study is to describe and document the characteristic properties, including the kinematics, of deformation zones in boreholes. Fault rocks were investigated in order to improve our understanding of the deformation mechanisms that controlled the local brittle structural history. Observations from thin sections combined with data from drill cores form the basis for the conclusions of the study.

This study is the second phase of the work carried out in accordance with activity plan AP PF 400-06-109. The first phase of the study is reported in the SKB P-report 06-212 /Nordgulen and Saintot 2006/, and this expanded on the preliminary work carried out in the pilot project in 2005 /Nordgulen and Braathen 2005/.

A total of 34 deformation zones from 9 drill holes (KFM01C, KFM01D, KFM06C, KFM07B, KFM07C, KFM08C, KFM09A, KFM09B and KFM10A) were studied with the aim of providing a description of the nature of each deformation zone, and to examine faults and fractures searching for features that potentially would have significance for the understanding of the kinematic history of the faults. The deformation zones were selected by SKB based on the single-hole interpretation of individual boreholes. Most zones that were assigned the highest confidence (3) are included in the study. The drill holes and deformation zones that were inspected are listed in Table 5-1.

3 Equipment

3.1 Description of equipment

During inspection, the standard equipment for structural investigations was used, including compass, hand lens, diluted HCl, and digital camera. Samples collected from drill cores were cut in the core laboratory, and selected chips were correctly marked (felt pen) and sent for preparation of polished thin sections. The thin sections were petrographically analysed and some selected sections were analysed using SEM in backscatter mode

4 Execution

4.1 Nomenclature

Faults occur on all scales in the lithosphere. They contribute to the spatial arrangement of rock units, may affect the topography, control the permeability of rocks and sediments and, more importantly, create deformation (strain, plus rotation plus translation) during plate interaction and intraplate movements. The term fault zone is generally used for brittle structures in which loss of continuity and slip occurs on several discrete faults within a band of definable width. Shear zones, on the other hand, are ductile structures, across which a rock body does not lose cohesion so that strain is progressively distributed across a band of definable width. Based on this definition, a fault zone is a volume of rock where strain is highly localized.

Commonly fault zones can be divided into a series of distinctive constituent elements. These are 1) the *undeformed host rock*, 2) the *transition zone* /Munier et al. 2003/ (corresponding to the “damage zone” of /Gudmundsson et al. 2001/) and 3) the proper *fault core* /e.g. Caine et al. 1996, Evans et al. 1997, Braathen and Gabrielsen 2000/. The host rock consists of undisturbed rock with a low fracture frequency of < 4 fractures/m /Munier et al. 2003/ (Figure 4-1). The transition zone still contains undeformed rock, but the fracture frequency generally increases up to 9 fractures/m (Figure 4-1). Narrow zones or bands of fault rock may occur, especially closer to the transition to the fault core. The width of the transition zone varies with the size of the fault zone and the style of deformation, and can range from a few metres to tens of metres. The fault core is identified by the occurrence of fault rock or intensively fractured rock (Figure 4-1 and 4-2). Fault rocks may occur in lenses alternating with pods of relatively undeformed rock /Caine et al. 1996, Braathen and Gabrielsen 2000/. The width of the fault core may vary from a few centimetres to a few metres /Braathen and Gabrielsen 2000/. The deformation zones reported in this study exhibit minor occurrence of fault rocks, mainly in the form of narrow zones with cataclasite and cemented breccias. Fault core is therefore expressed as highly fractured rocks that may form zones of sealed fracture networks.

Rocks that occur within fault zones provide primary evidence for the processes that occur there. It is therefore of great importance to characterize fault rock occurrences so as to better understand faulting processes at all scales. Fault rocks form in response to strain localization within fault and shear zones and reflect the interplay of a variety of physical and environmental parameters

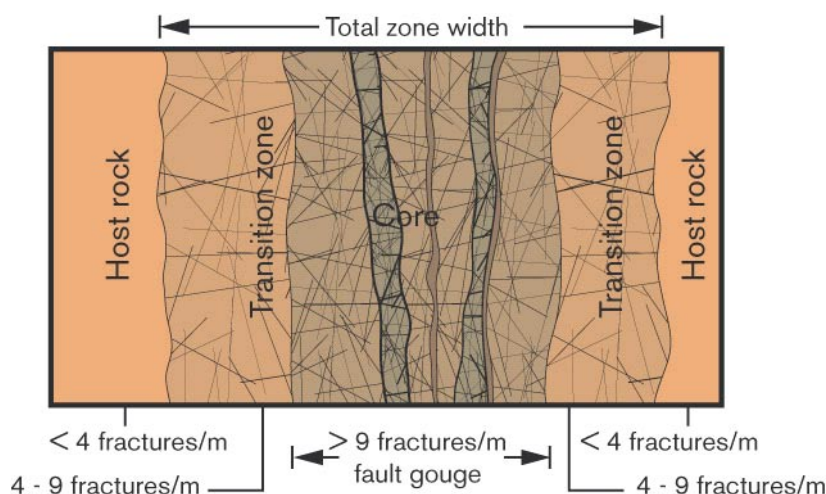


Figure 4-1. Schematic illustration of a brittle deformation zone according to SKB definition /after Munier et al. 2003/.

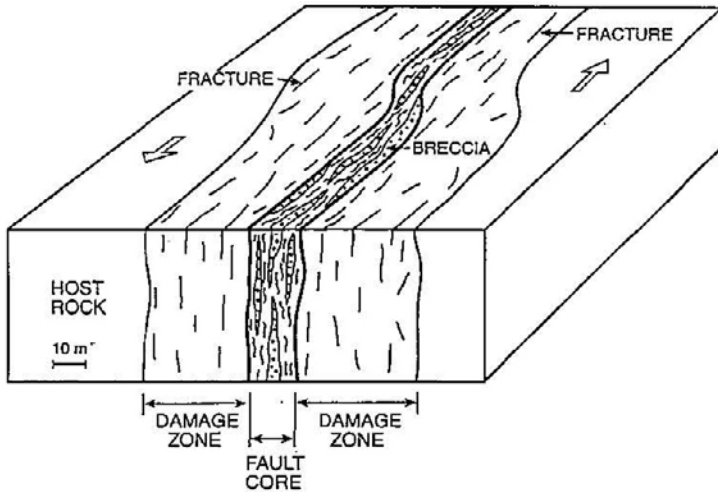


Figure 4-2. Schematic illustration of the architecture of an idealized fault zone /Gudmundsson et al. 2001/. Note that the term “damage zone” corresponds conceptually to the term “transition zone” of Figure 4-1.

such as the finite amount of strain, lithology, style of deformation (i.e. frictional or plastic flow), presence or absence of fluids, strain rate, temperature, pressure and so on. Figure 4-3 shows the classification scheme suggested by /Braathen et al. 2004/ that we will use in this study to classify fault rock occurrences.

Brittle		← Deformation style →						Ductile	
		← Dominant deformation mechanism →			Plastic flow				
Frictional flow		Secondary cohesion		Primary cohesion				% matrix and grain-size	
Non-cohesive		Cemented HB	Indurated HB	> 50% phyllosilicate		< 50% phyllosilicate			
Hydraulic breccia (HB)	Breccia series	Proto-breccia	Cemented proto-breccia	Indurated proto-breccia	Cataclasite series	Proto-cataclasite	Proto-phylionite	Proto-mylonite	0-50% matrix
		Breccia	Cemented breccia	Indurated breccia		Cataclasite	Phylionite	Mylonite	50-90% matrix
		Ultra-breccia	Cemented ultra-breccia	Indurated ultra-breccia		Ultra-cataclasite	Ultra-phylionite	Ultra-mylonite	90-100% matrix
	Gouge	Cemented gouge	Indurated gouge					Sub-microscopic matrix	
		Pseudotachylyte							

Figure 4-3. Fault rock classification scheme proposed by /Braathen et al. 2004/. A brief explanation of some of the terms is given in Table 4-1.

Table 4-1. Schematic description of different types of fault rocks classified according to /Braathen et al. 2004/.

Term	Description	Note
Fault rocks or fault-related rocks	Commonly formed through strain concentration within a tabular or planar zone that experiences shear stress.	1
Frictional flow	Pressure, subordinate temperature and fluid controlled deformation mechanisms which have a brittle style: granulation of grains by inter, intra and transgranular micro fracturing, and intra or intergranular frictional sliding with abrasion of fracture walls and grain margins	2
Plastic flow	Mainly thermally activated, continuous deformation without rupture, with a ductile style of deformation: dislocation creep and glide, solid state diffusion creep, diffusional mass transfer, and viscous grain boundary sliding	
Non-cohesive	Not consolidated	3
Secondary cohesion	Consolidated after formation, either through cementation of the matrix, or through compaction, recrystallisation or neo-mineralisation (see indurated)	
Primary cohesion	Cohesion preserved during formation	3
Hydraulic fracturing	Fracturing caused by fluid pressure: commonly random orientation of fractures and rough fracture surfaces. The resulting hydraulic breccia may not be tabular or planar, however, it is tectonically induced and frequently fault-related.	4
Cemented	Consolidated through mineral precipitation in pores of the matrix	
Indurated	Consolidated basically by compaction due to directed pressure, annealing by recrystallisation of grains, or neomineralisation (e.g., muscovitisation, silicification, albitisation, epidotisation, saussuritisation). The term disregards cementation unless related to general neomineralisation	
Phyllosilicate content	Content of sheet-minerals (characterised by weak '001' bonds) of the phyllosilicate group	5
Matrix	Fine-grained material in a fault rock formed by granulation or dynamic recrystallisation of grains, filling the interstices between larger clasts of original rock	
Breccia	Mainly chaotic, non-cohesive fault rock, generated by frictional flow	3
Cataclasite	Mainly chaotic fault rock that developed with cohesion, which is generated by mainly frictional flow	6
Phyllonite	Phyllosilicate-rich fault rock with distinct mineral fabric, and dominated plastic flow	7
Mylonite	Fault rock with distinct mineral fabric, and dominated by plastic flow	8
Blasto-mylonite	Fault rock in which dynamic recrystallisation and/or neomineralisation causing grain-size increase of clasts, outpace grain-size reduction	8
<ol style="list-style-type: none"> 1. For classification of fault rocks, see: <i>Higgins</i> [1971], <i>Bell & Etheridge</i> [1973], <i>Zeck</i> [1974], <i>Sibson</i> [1977a], <i>Wise et al.</i> [1984], <i>Schmid & Handy</i> [1991]. 2. Term introduced by <i>Schmid & Handy</i> [1991]. See also description of <i>Bell & Etheridge</i> [1973]. 3. Concept introduced by <i>Higgins</i> [1971]. 4. For hydraulic breccias, see e.g. <i>Clark & James</i> [2003]. 5. Clay content as factor in classification of faults rocks in sedimentary units, e.g. <i>Fisher & Knipe</i> [1998]. 6. Possible application of phyllosilicate content in the sub-division of fault rocks in sedimentary rocks, e.g. <i>Fisher & Knipe</i> [1998]. 7. Definitions following <i>Knopf</i> [1931], however, adding a limit to the phyllosilicate content. 8. See definitions of <i>Sibson</i> [1977a]. 		

This study deals not only with faults, but also with brittle structures in general. It is therefore appropriate that the terminology that is used is clarified.

Fractures are all planar brittle structures.

Joints are extensional fractures (with the minimum stress axis perpendicular to the surface) along which no displacement can be observed with unaided eyes. The term is unfortunately not well constrained and the above definition is according to /Twiss and Moores 1992/: ‘Most outcrops of rocks exhibit many fractures that show very small displacement normal to their surfaces and no, or very little, displacement parallel to their surfaces. We called such fractures joints.’ The authors also noted at this point: ‘Unfortunately, there is no universally accepted

definition of the term joint. The definition set down here is conservative in that fractures satisfying this definition would be called joints by every other definition of the term’.

Note that the term ‘*shear joints*’ is also used when two sets of joints are at 60 degrees from each other. It implies that the maximum stress axis is the bisector of the acute angle, the minimum stress axis the bisector of the obtuse angle, and the intermediate stress axis is parallel to the intersection of the joints. Here also, it is stipulated that no displacement can be observed with unaided eyes.

The term ‘*vein*’ is descriptive and used for a body, that compared to its width, has great lateral extent in a given host rock. A vein can be rock-filled, like a granitic vein, or mineral-filled, like a calcite vein.

The term *tension gash* is genetic and interpretative. Tension gashes are inferred to be extensional fractures with a clear displacement normal to their sides (i.e. the minimum stress axis is roughly perpendicular to their sides, or there is little or no evidence of shearing acting along their sides). They are generally mineral-filled and commonly have mineral fibres that grew parallel to the tension axis. In this study, this term has therefore been used only if mineral fibres have been observed in the fracture, allowing for an estimate of the orientation of the minimum stress axis.

Mineral-filled fracture is a very general term that is used to describe fractures with at least some displacement normal to their sides (allowing mineral growth to take place). Provided that a shear component is documented, this would be a fault coated with minerals. This term is descriptive and non-genetic. It is used to describe a fracture with mineral coating on which the orientation of mineral fibres cannot be observed with the unaided eye, i.e. the orientation of the minimum stress axis remains uncertain. With the aided eye, it may be possible to distinguish between a tension gash (with the minimum stress axis roughly perpendicular and fibres parallel to the minimum stress axis) and a fault (shear fracture, with fibres oblique to the fractures).

4.2 Working procedure

Investigation of drill cores was conducted during two periods: December 11–14, 2006 and February 19–21, 2007. The standard procedure for obtaining the true orientation of linear structures (slickensides, striations, etc) on fault surfaces in drill cores with known orientation is as follows:

1. Fractures of potential interest were identified by visual inspection of drill cores from selected deformation zones, as defined previously by SKB.
2. Individual fractures were identified on the BIPS image of the borehole wall, which provided a mirror image of the core itself. Care had to be taken to ensure that the fracture selected on the image matched the one from the drill core. In some cases, this was challenging, particularly where abundant fractures cut the core at different angles. Independent checks that the correct fracture was selected could be carried out using data in the drill core database. These included the properties of the fracture itself, the acute angle α between the fracture and the drill core axis, and the angle β , which is the angle (measured counter-clockwise) from the lower intersection of the fracture with the drill core wall, to the top of the drill core.
3. Having identified the fracture of interest, the top of the drill core was marked based on visual inspection of the BIPS image and on the angle β . For each fracture, its orientation (strike and dip) was obtained using the information contained in the drill core database.
4. The drill core was positioned the right way up and at the true inclination using a core holder supplied by SKB. This device allowed the accurate adjustment of the drill core inclination as given in the database.
5. The orientation of the linear structure was determined by measuring its plunge direction (azimuth) and plunge.
6. When the sense of slip could be determined with confidence, the true movement of the hanging wall with respect to the footwall of the fault was established.
7. Relevant data were recorded in a database.

Eleven samples for thin section preparation were collected. The sections were studied at the Geological Survey of Norway (Trondheim) using standard petrographic techniques. These sections add to the 33 polished sections collected during phase 1 and during the pilot study.

At the Geological Survey of Norway (NGU) in Trondheim, structural data were analysed and plotted using standard techniques. The thin sections were analysed in several steps:

1. Scanning at high resolution of the entire section using a standard slide scanner.
2. Printing of the scanned jpg-images as A4 colour prints that greatly aid in establishing general relationships and locating critical features for detailed study.
3. Petrographic analysis and documentation of textural and micro-structural relations using a digital camera attached to the microscope (Leitz).
4. Detailed studies of specific mineralogical and textural details using SEM in backscatter mode.

4.3 Analysis and interpretation

The methods employed for drill core investigations through structural data analysis and petrographic work are based on those described in /Braathen 1999, Braathen et al. 2002, Nordgulen et al. 2002, Osmundsen et al. 2003/. In this report, definition of fault rocks is according to the classification in /Braathen et al. 2004/. Criteria for identifying the slip-direction on slickenside surfaces is presented in /Petit 1987/.

A systematic analysis of fault slip data at the micro-scale to meso-scale has been made, which aims to establish an improved understanding of the kinematic pattern in the area of interest. It consists of the analysis of strike and dip of fault planes and of azimuth and plunge of their striae. It also provides the basis for paleo-stress inversion calculations that can aim at the reconstruction of the stress field evolution through time. Figure 4-4 provides the key to read stereoplots used throughout this report that represent the orientation and the kinematics of individual fault plane/striation pairs.

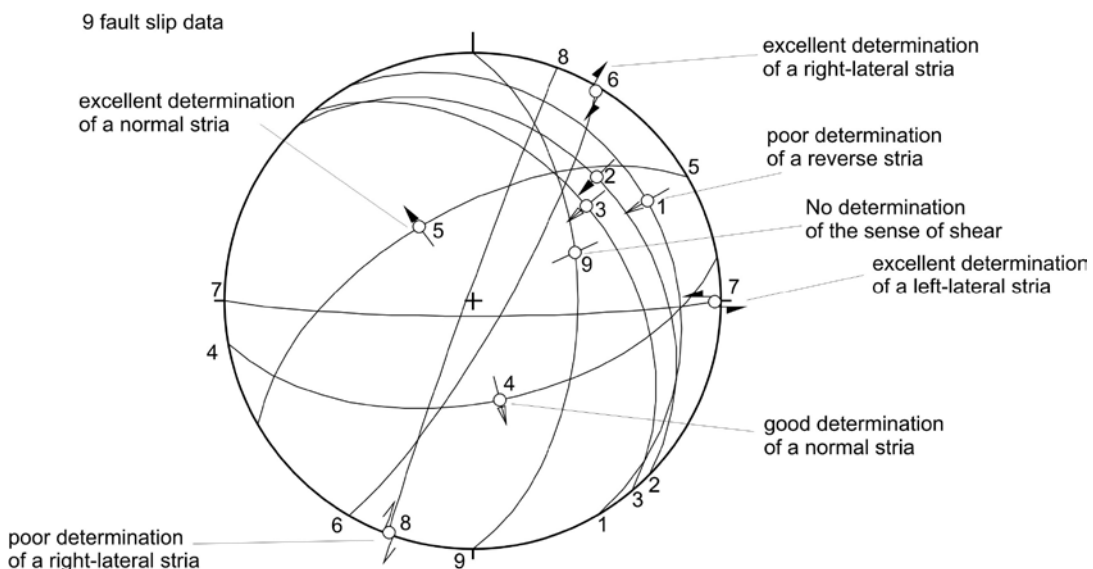


Figure 4-4. Example of a stereonet used for plotting kinematic information obtained from striated fault planes, Schmidt's projection, lower hemisphere. Keys for striae: outward directed arrow: normal striae (numbers 4 and 5 on stereonet); inward directed arrow: reverse striae (numbers 1, 2 and 3); couple of arrows: strike-slip striae (numbers 6, 7 and 8); full black arrow: excellent constraints on the sense of shear (numbers 2, 5, 6 and 7); empty arrow: good constraints on the sense of shear (numbers 3 and 4); simple arrow: poor constraints on the sense of shear (numbers 1 and 8); thin line without any arrowhead: no constraints on the sense of shear (number 9).

4.4 Data handling and processing

The data obtained in the study are transferred to SKB in a specified format that allows for transfer of the data to the internal database structure at SKB.

4.5 Nonconformities

No nonconformities have been noted.

5 Results

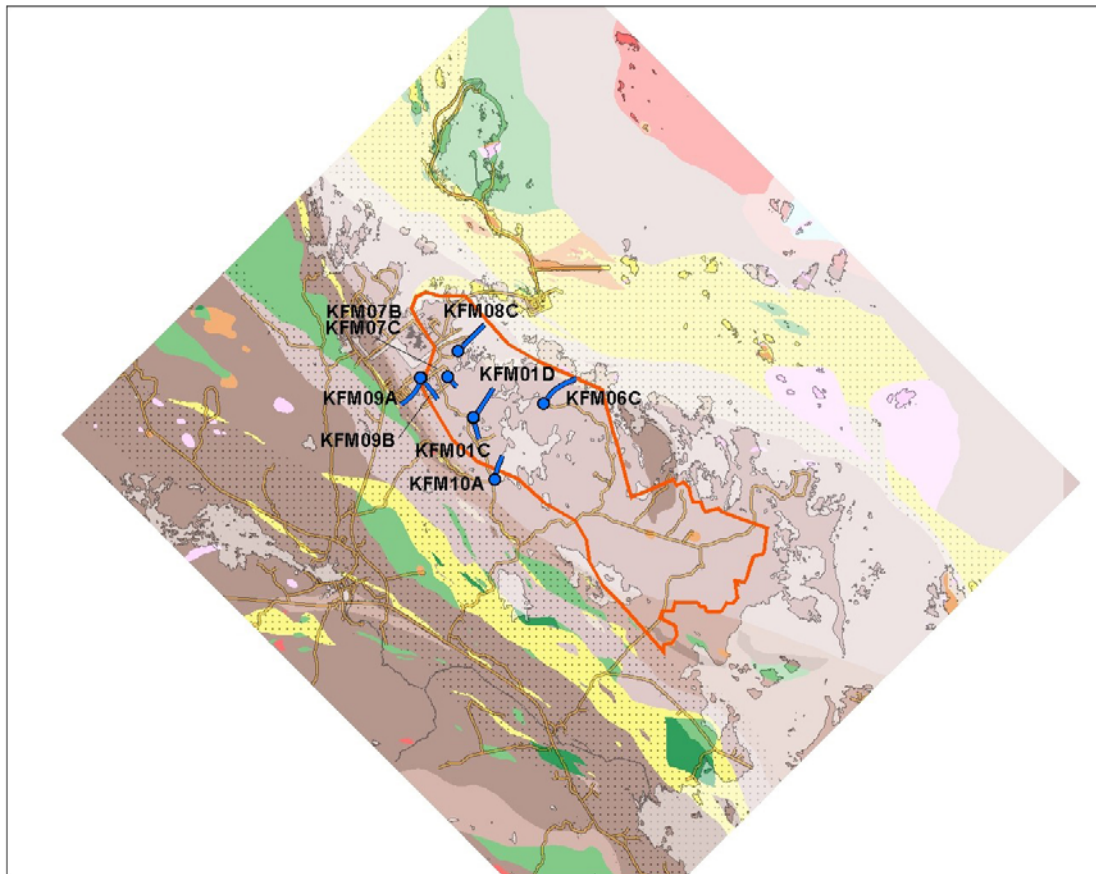
5.1 Drill core investigations

5.1.1 Investigated drill cores

34 selected sections from 9 drill holes were inspected with the aim of investigating the style of deformation in the previously defined deformation zones (DZ) classified with uncertainty 3 in the respective single-hole interpretations (Table 5-1). The geographic location of the drill holes is shown in Figure 5-1. During this investigation, samples for petrographic analysis were collected from characteristic fault rocks (see sample list in Appendix 1). The detailed studies of fracture mineralogy by /Sandström et al. 2004, 2005/ were also used.

Table 5-1. Overview of drill cores inspected in the project.

Drill core	Length, direction	Deformation zone section	Deformation zone identification
KFM01C	450 m, 165/50	23–48 m 62–99 m 235–450 m	DZ1 /Carlsten et al. 2006d/ DZ2 /Carlsten et al. 2006d/ DZ3 /Carlsten et al. 2006d/
KFM01D	800 m, 035/55	176–184 m 411–421 m 488–496 m 670–700 m 771–774 m	DZ1 /Carlsten et al. 2006c/ DZ2 /Carlsten et al. 2006c/ DZ3 /Carlsten et al. 2006c/ DZ4 /Carlsten et al. 2006c/ DZ5 /Carlsten et al. 2006c/
KFM06C	1,000.4 m, 026/60	102–169 m 359–400 m 415–489 m 502–555 m	DZ1 /Carlsten et al. 2006b/ DZ2 /Carlsten et al. 2006b/ DZ3 /Carlsten et al. 2006b/ DZ4 /Carlsten et al. 2006b/
KFM07B	298.4 m, 135/54	51–58 m 93–102 m 225–245 m	DZ1 /Carlsten et al. 2006a/ DZ2 /Carlsten et al. 2006a/ DZ4 /Carlsten et al. 2006a/
KFM07C	500.7 m, 143/85	92–103 m 308–388 m 429–439 m	DZ1 /Carlsten et al. 2006e/ DZ2 /Carlsten et al. 2006e/ DZ3 /Carlsten et al. 2006e/
KFM08C	952 m, 036/60	161–191 m 419–542 m 673–705 m 829–832 m	DZ1 /Carlsten et al. 2006f/ DZ2 /Carlsten et al. 2006f/ DZ3 /Carlsten et al. 2006f/ DZ4 /Carlsten et al. 2006f/
KFM09A	799.5 m, 200/60	15–40 m 86–116 m 217–280 m 723–754 m 770–790 m	DZ1 /Carlsten et al. 2006a/ DZ2 /Carlsten et al. 2006a/ DZ3 /Carlsten et al. 2006a/ DZ4 /Carlsten et al. 2006a/ DZ5 /Carlsten et al. 2006a/
KFM09B	616.3 m, 141/55	9–132 m 363–413 m 520–550 m 561–564 m	DZ1 /Carlsten et al. 2006d/ DZ3 /Carlsten et al. 2006d/ DZ4 /Carlsten et al. 2006d/ DZ5 /Carlsten et al. 2006d/
KFM10A	500 m, 010/50	63–145 m 430–449 m 478–490 m	DZ1 /Carlsten et al. 2006f/ DZ2 /Carlsten et al. 2006f/ DZ3 /Carlsten et al. 2006f/



- Cored borehole
- Borehole projection
- ▭ Candidate area
- ⋯ Banded and/or strongly foliated bedrock (strong ductile deformation)
- Granite, fine- to medium-grained
- Pegmatite, pegmatitic granite
- Granite, granodiorite and tonalite, metamorphic, fine- to medium-grained
- Granite, metamorphic, aplitic
- Granite to granodiorite, metamorphic, veined to migmatitic, medium-grained
- Granite to granodiorite, metamorphic, medium-grained
- Granodiorite, metamorphic
- Tonalite to granodiorite, metamorphic
- Diorite, quartz diorite and gabbro, metamorphic
- Ultramafic rock, metamorphic
- Magnetite mineralisation associated with calc-silicate rock (skarn)
- Felsic to intermediate volcanic rock, metamorphic
- Sedimentary rock, metamorphic, veined to migmatitic

0 1 2 4 km
 © Lantmäteriverket Gävle 2007. Consent In 2007/1092.
 2007-06-28 10:00

Figure 5-1. Map of the Forsmark area showing candidate investigation area (red line) and the geographic location of the drill hole.

5.1.2 KFM01C

The drill site is located in the north-western part of the investigation area some distance to the east of the Eckarfjärden deformation zone (Figure 5-1). The drill hole has a length of 450 m and is oriented 165/50 /Carlsten et al. 2006d/. The main rock type is a medium-grained metagranite-granodiorite with subordinate occurrences of pegmatitic granite, amphibolite, fine- to medium-grained metagranitoid, felsic to intermediate metavolcanic rock and aplitic metagranite. Three deformation zones were investigated (DZ1, DZ2, DZ3).

32 striated faults have been measured along the three studied intervals of the drill core (Figure 5-2). Two sets of steep strike-slip faults are identified, one set trends NW-SE to NNW-SSE and is mainly sinistral, the other set is oriented NE-SW and probably dextral. Another set of probably reverse, gently south-dipping faults oriented WNW-ESE is also present (Figure 5-2).

KFM01C: 23–48 m – DZ1

Steeply dipping fractures that strike WSW and dip northwards as well as gently dipping to sub-horizontal fractures dominate in DZ1. The zone exhibits an increased frequency of open and sealed fractures (Figure 5-3). Sealed fracture networks with minor breccia contain mainly laumontite and some calcite (see photo inset in Figure 5-3). There is generally a low fracture frequency in the upper part of the zone. Three crush zones (30–40 cm) that represent fault core are present between 40 and 45 m (Figure 5-3). The most frequent fracture filling minerals include chlorite, clay minerals, hematite, calcite and laumontite. Prehnite, adularia and asphaltite occur sporadically. A 20 cm wide zone with epidote alteration occurs in the lowermost part of the zone. DZ1 is a transition zone with short intervals of fault core (i.e. the crush zones) according to the definition of /Munier et al. 2003/.

Only four striated faults have been measured along DZ1 (Figure 5-4). Two types of fault planes are present: two sub-horizontal south-dipping planes and two steep north-dipping planes, all striking roughly ENE-WSW. No consistency exists in the set of striae (Figure 5-4). Shearing is displayed by grooves on calcite (number 1, Figure 5-4); by striations of clay minerals, hematite (numbers 2 and 3, Figure 5-4; the fault planes are also coated with prehnite and asphaltite); by striations of clay minerals and calcite (number 4, Figure 5-4). The dip-slip striation on the south-dipping plane appears to be reverse (number 4, Figure 5-4). Strike-slip, dip-slip and oblique-slip are apparent on the other three fault planes.

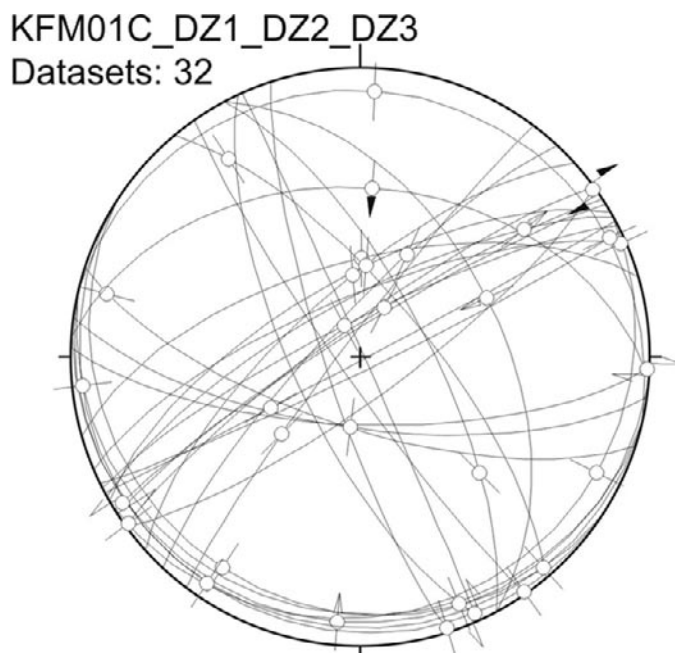


Figure 5-2. Stereoplot showing all the fault slip data collected along all the studied DZ in drill core KFM01C.

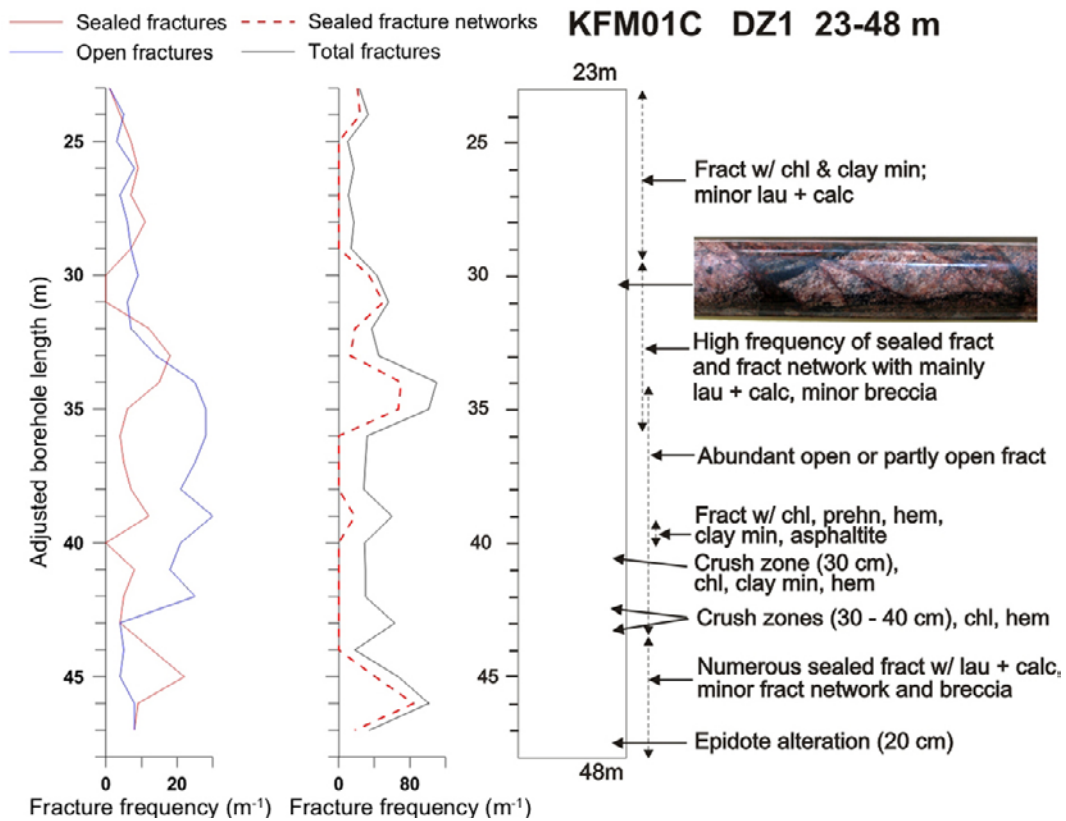


Figure 5-3. Simplified drawing of DZ1 showing the most prominent brittle structures. At approximately 30.3 m there is an interval with laumontite-sealed fractures (see photo inset). Three crush zones (30–40 cm) that represent fault core are present between 40 and 45 m. Abbreviations used throughout the report: Calc=calcite, Chl=chlorite, Corr=corrensite, Ep=epidote, Fract=fracture(s), Hem=hematite, Lau=laumontite, Ox=oxides, min or mnl=mineral, Py=pyrite, Qtz=quartz, w/=with.

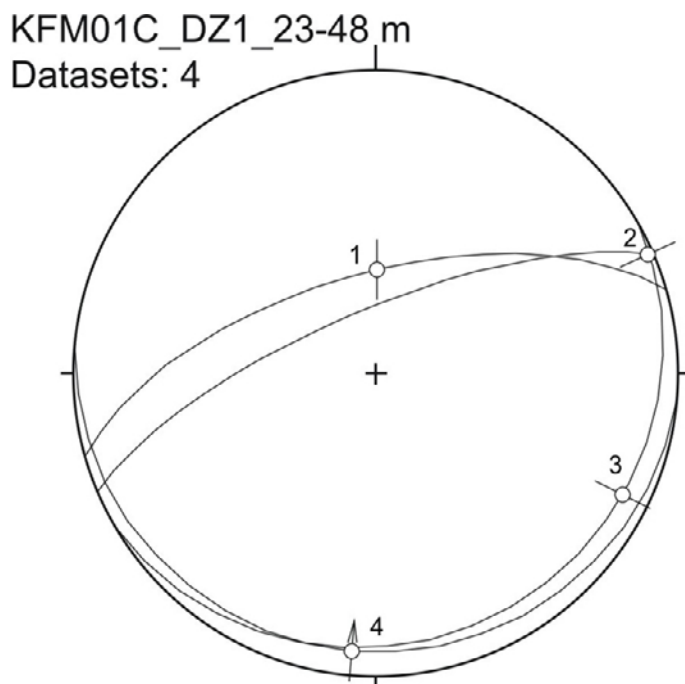


Figure 5-4. Stereoplot of fault slip data in DZ1 (KFM01C).

KFM01C: 62–99 m – DZ2

DZ2 transects medium-grained metagranite-granodiorite with subordinate pegmatite and amphibolite. The predominant brittle structures are steeply dipping fractures that strike WSW and dip northwards as well as gently dipping to sub-horizontal fractures. The most frequent fracture filling minerals include chlorite, calcite, clay minerals, hematite, and asphaltite. The highest fracture frequencies occur in the central interval of the zone (Figure 5-5). At ca 69.7 m, cross-cutting relationships define the following sequence of events: 1) Chlorite + calcite + hematite on uneven fractures sub-parallel to the foliation in the metagranite; 2) Hairline fractures with minor laumontite; 3) Calcite-sealed, 1–2 mm wide fractures. At 77 m, fractures with chlorite, hematite and calcite are cut by calcite-sealed fractures. The DZ is generally considered a transition zone according to the definition of /Munier et al. 2003/. Strong fracturing and partial core loss characterize the interval at 84.5–86 m; this section constitutes a fault core /Munier et al. 2003/.

Twelve striated faults are present in DZ2 along KFM01C (Figure 5-6). As in DZ1, DZ2 is characterised by sub-horizontal fault planes displaying mainly dip-slip striae. A set of NNW-SSE steep strike-slip faults is also present with one sinistral sense of shear of medium quality indicated by striae on hematite. The striations are mainly on hematite and/or chlorite and/or clay minerals. The fault planes have later been coated by calcite, laumontite, adularia and chlorite.

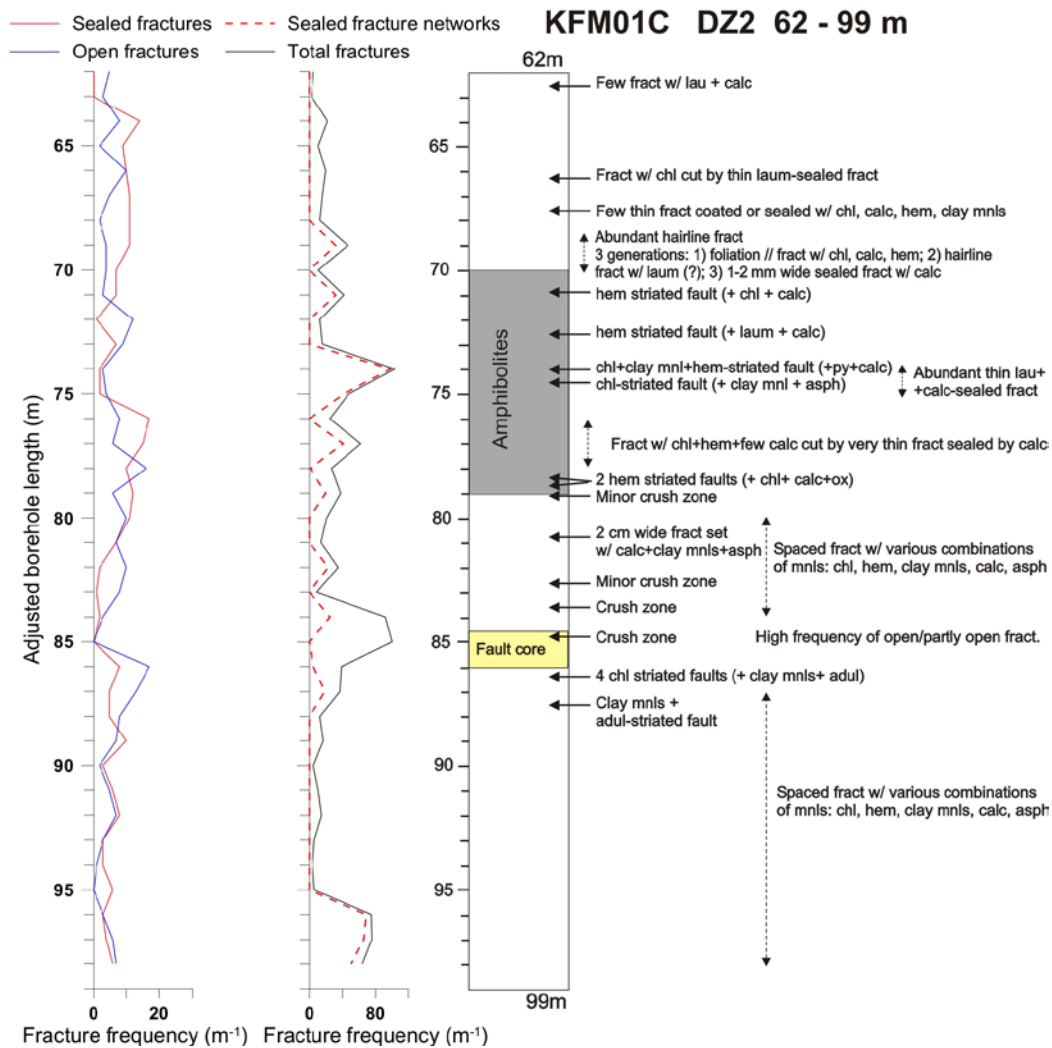


Figure 5-5. Simplified drawing of DZ2 showing the most prominent brittle structures. Note cross-cutting relationships at 69.7 m and at 77 m, and crush zone with partial core loss defined as fault core at 84.5–86 m. Abbreviations as in Figure 5-3.

KFM01C_DZ2_62-99 m
 Datasets: 12

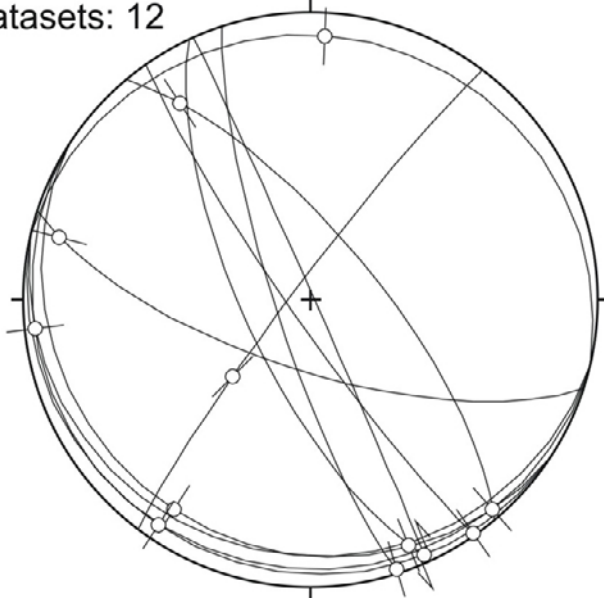
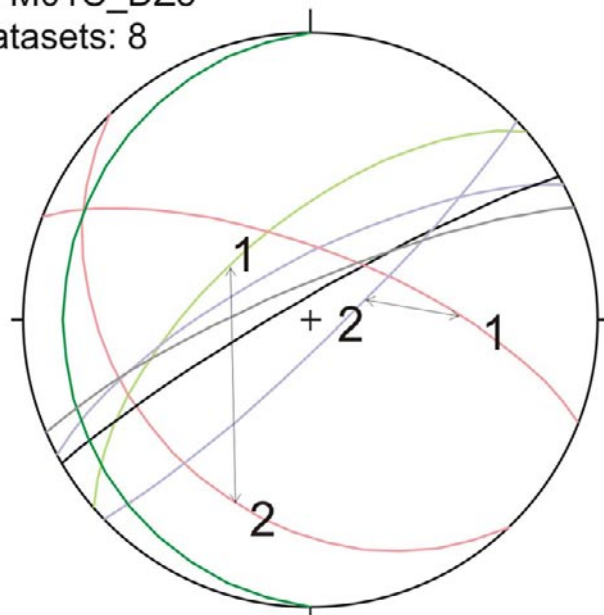


Figure 5-6. Left: Stereonet of the 12 striated faults measured along DZ2 in KFM01C. Right: two examples of fault surfaces are shown. Striae on chlorite and clay minerals, unknown sense of shear (strike/dip angle/pitch: 145/84/0) (74.56 m) at the left side. Striae on hematite and coating of calcite and laumontite, unknown sense of shear (strike/dip angle/pitch: 162/80/2) (72.40 m) at the right side.

KFM01C: 235–450 m – DZ3

DZ3 along KFM01C exhibits an increased frequency of predominantly sealed fractures and sealed fracture networks. Common fracture filling minerals include laumontite, calcite and chlorite. As in DZ1 and DZ2, the predominant fractures strike WSW to SW and dip steeply northwards; gently dipping to sub-horizontal fractures are also common (Figure 5-7). Steeply dipping fractures that

KFM01C_DZ3
 Datasets: 8



- Epidote-filled vein in pale green
- Laumontite-sealed veins in pink
- Calcite-filled veins in mauve
- Chlorite-sealed vein in green
- Network of chlorite, calcite, pyrite, prehnite in black
- Network of calcite, quartz, hematite, iron hydroxyde in grey

Figure 5-7. Stereonet for DZ3 in KFM01C showing the orientation of some of the predominant structures observed brittle structures (1 and 2 linked by a double arrow are for the chronology between the brittle structures, 1 being the oldest).

strike NW are also present. Networks, epidote-filled veins and calcite-filled veins are parallel to the main population of NE-SW steep faults. Laumontite-sealed veins are oblique to these faults and strike NW-SE to WNW-ESE with dips to the NE or SW (Figure 5-7). Some relative chronologies have been identified using these mineral-filled or -coated brittle structures. The NE-SW steep epidote-filled veins are cut by laumontite-sealed veins that dip 35 degrees SW. Furthermore, NE-dipping laumontite-sealed veins, which form a possible conjugate system with the SW-dipping veins, are cut by NE-SW steep calcite-filled veins. This implies the successive reactivation of the system of steep NE-SW fractures related to polyphase tectonics.

The zone shows different characteristics in its upper and lower parts (Figures 5-8 and 5-9). The upper part, between 235 and 340 m (Figure 5-8), has a variable, but generally a moderately high

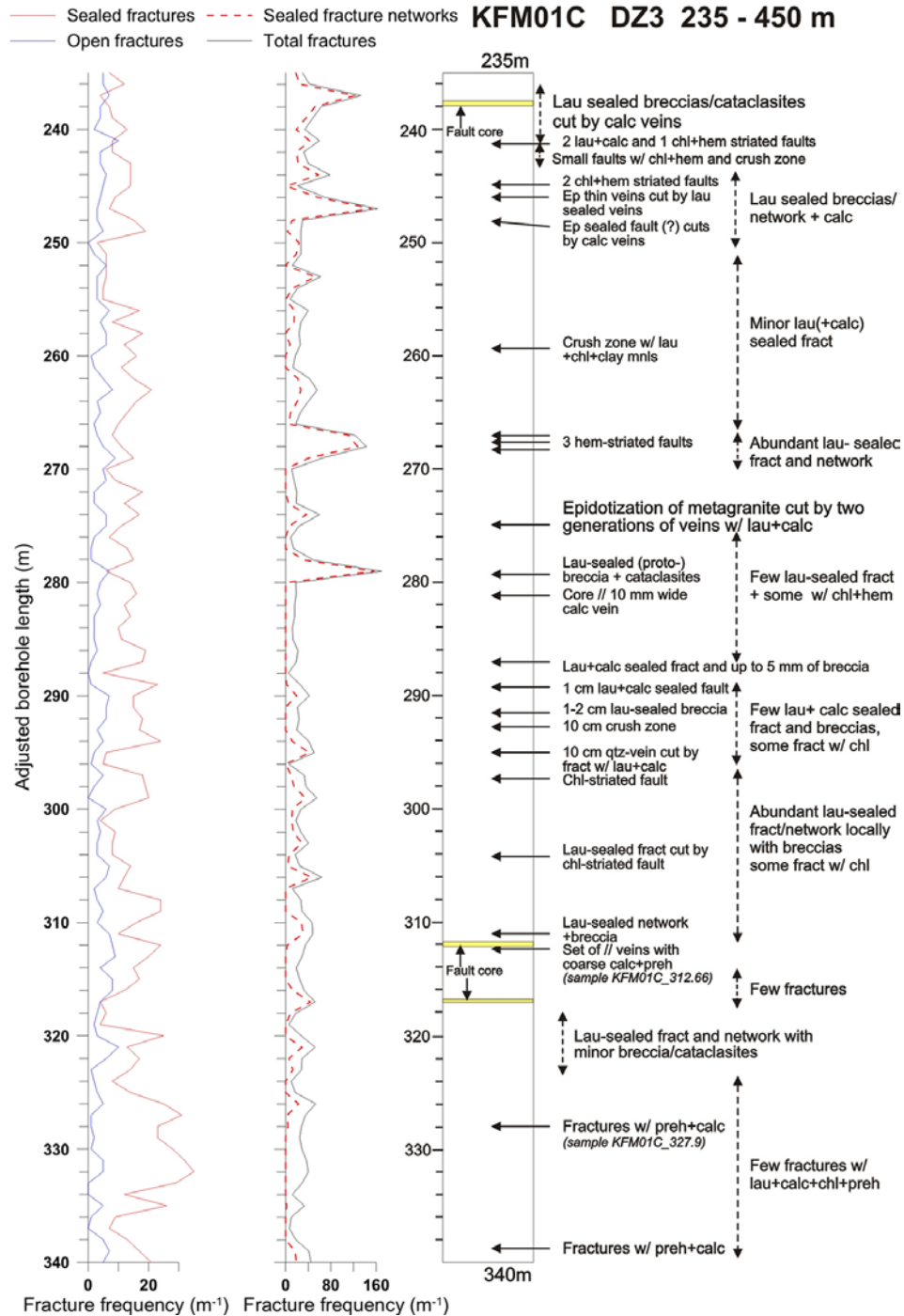


Figure 5-8. Simplified drawing of DZ3 showing the most prominent brittle structures in the upper part of the zone (235–340 m). Abbreviations as in Figure 5-3.

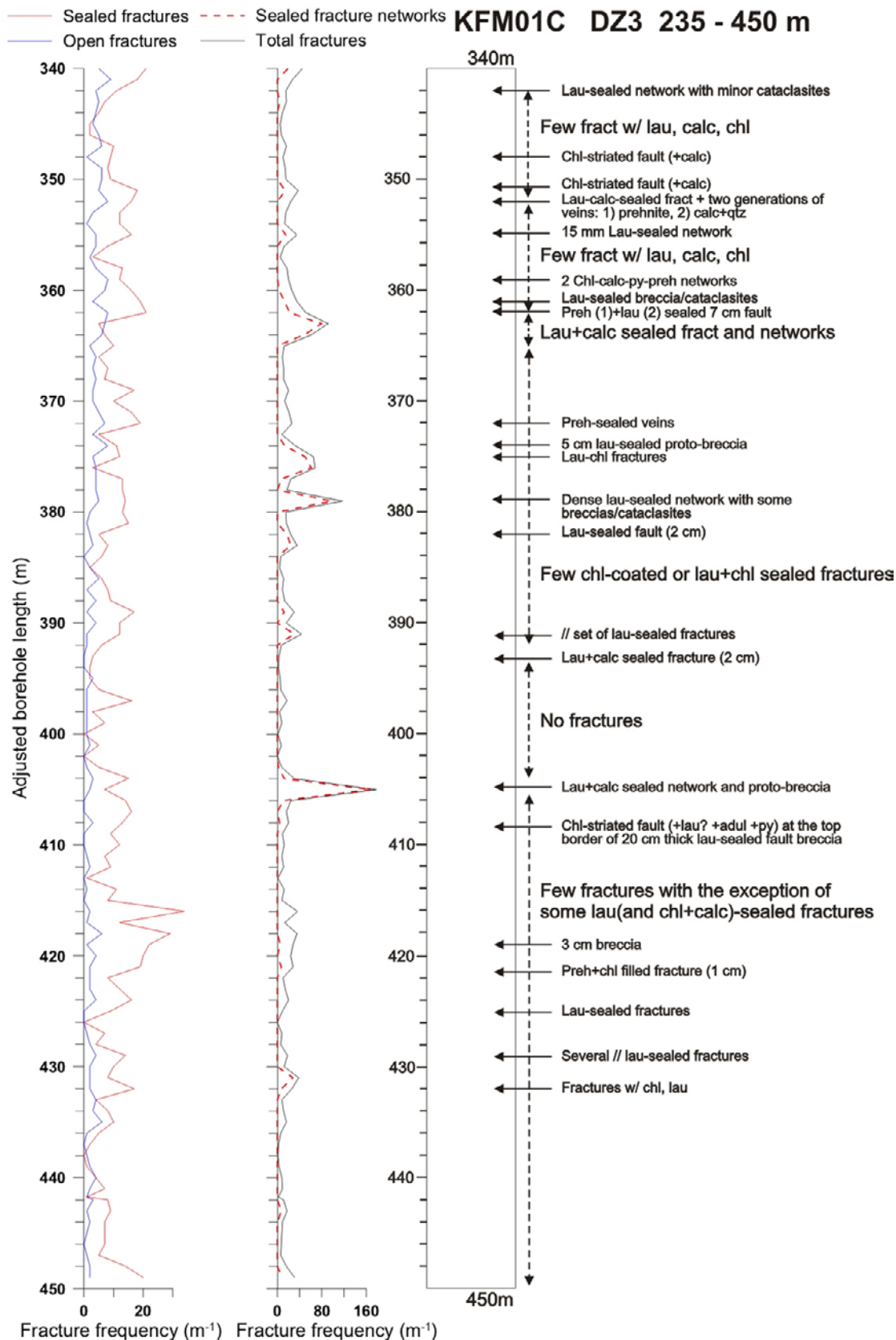


Figure 5-9. Simplified drawing of DZ3 showing the most prominent brittle structures in the lower part of the zone (340–450 m). Abbreviations as in Figure 5-3.

frequency of fractures with numerous occurrences of sealed fracture networks with laumontite and calcite. Minor laumontite-sealed breccias are associated with these fractures. The structural relationships are illustrated by the drill core section shown in Figure 5-10. Notice reddish oxidation of the host rock and distribution of fractures and minor faults and fracture networks. The structural history derived from this section is based on cross-cutting relationships. At ca 248 and 275 m, the NE-SW epidote-sealed veins and epidote-altered metagranite are cut by veins sealed with calcite and laumontite (Figures 5-7 and 5-8). At 312.6 and 327.9 m, ca 5 cm wide veins with euhedral calcite and prehnite cut chloritised metagranite. A sample collected for thin section at 312.66 m shows that the vein is composed of variably sized euhedral crystals of prehnite and calcite (Figure 5-11). In general, the upper part of the DZ is considered a transition zone /Munier et al. 2003/ with short sections of fault core associated with the occurrences of sealed fracture networks and breccias.

The lower part of DZ3, between 340 and 435 m (Figure 5-9), shows a somewhat lower background fracture frequency and some intervals exhibit frequencies below the levels required for a transition zone /Munier et al. 2003/. Nevertheless, some sections show a higher concentration of mainly sealed fractures and some fracture networks similar to those in the upper part of the deformation zone (Figure 5-8). Minor local fault core are associated with the occurrences of sealed fracture networks and breccias (not shown on Figure 5-9). At ca 419 m, a sealed fault with calcite, quartz and hematite cut fractures and veins filled with quartz and chlorite.

Example of drill core from DZ3 and a photomicrograph is shown in Figure 5-10 and Figure 5-11, respectively.



Figure 5-10. Example of drill core from DZ3 of KFM01C (312.4–323.2 m). Notice reddish oxidation of the host rock and distribution of fractures and minor faults and fracture networks. Minor laumontite-sealed breccias are associated with some of the sealed fractures. Photo: Alf Sevastik, SKB.

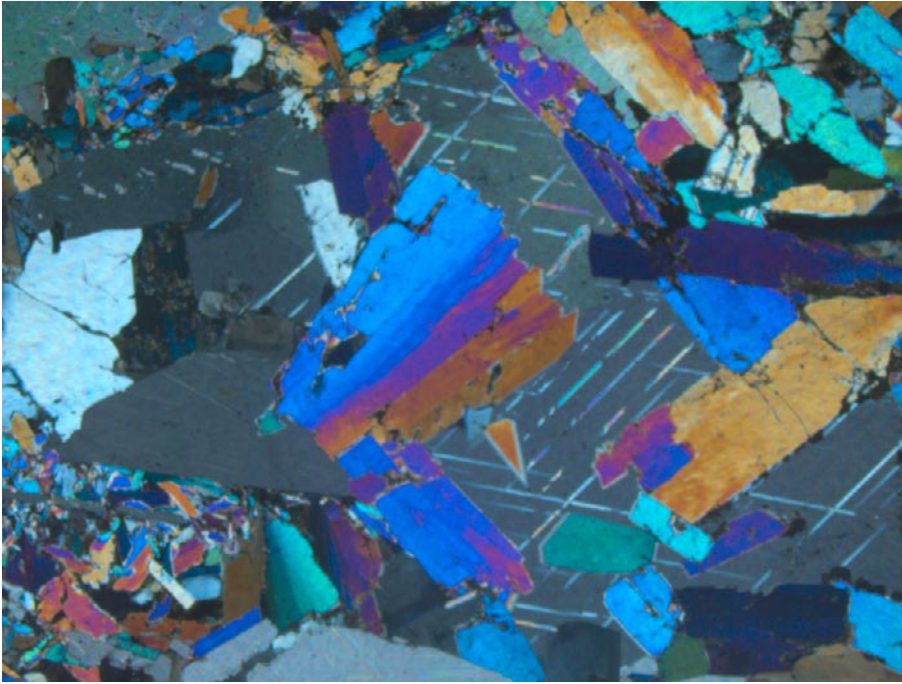


Figure 5-11. Photomicrograph of thin section from sample KFM01C_312.66. The sample was collected from a 5 cm wide vein composed of variably sized euhedral crystals of prehnite and calcite. The field of view is ca 5 mm wide.

In DZ3 along KFM01C, 16 striated faults have been measured (Figure 5-12). The frequency of striated faults in DZ3 is the highest encountered in this study with one fault per metre of drill core on average. The zone is dominated by steep fault planes trending NE-SW. They display both strike-slip and dip-slip striae. Among the strike-slip striae, a dextral sense of shear has been clearly identified with steps of chlorite. An E-W 40 degrees north-dipping fault displays a reverse sense of shear with striations of chlorite and hematite, and with calcite steps. Two other E-W faults have the attitude of conjugate faults with a dip angle of 50 to the south and roughly dip-slip striae. Most of the fault surfaces exhibit striations of hematite, chlorite, and clay minerals and are coated with calcite, oxides, laumontite, pyrite, and adularia.

5.1.3 KFM01D

The drill site is located in the north-western part of the investigation area some distance to the east of the EDZ (Figure 5-1). The drill hole has a length of 800 m and is oriented 035/55. The main rock type is a medium-grained metagranite-granodiorite with subordinate occurrences of pegmatitic granite, fine- to medium-grained metagranitoid, amphibolite, felsic to intermediate metavolcanic rock and aplitic metagranite /Carlsten et al. 2006c/. Five deformation zones were investigated (DZ1, DZ2, DZ3, DZ4, DZ5).

KFM01D: 176–184 m – DZ1

Zone DZ1 shows some increase in the frequency of open, and to some extent also sealed fractures. Fractures are present mostly as sporadic single structures and are commonly gently dipping; steep fractures strike NW to NNW. The fractures are filled and/or coated mainly by chlorite, calcite, laumontite, clay minerals and adularia. A sealed fault (182.5 m) with chlorite and hematite striation occurs along the upper surface of strongly sheared mafic lithology (Figure 5-13). The DZ is considered a transition zone according to /Munier et al. 2003/.

Only one 65 degrees WSW-dipping fault has been measured along DZ1 in KFM01D. It displays dip-slip slickensides on hematite and chlorite (Figure 5-14).

KFM01C_DZ3_235-450 m
Datasets: 16

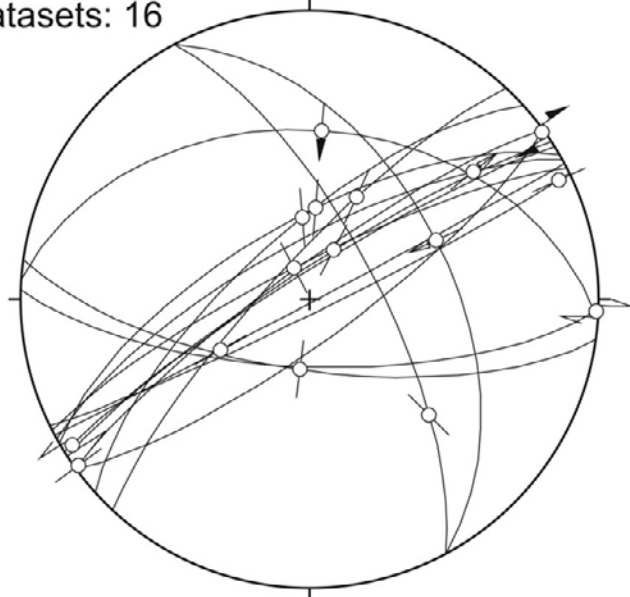


Figure 5-12. Stereonet of striated faults along DZ3 in KFM01C.



Figure 5-13. Photo showing highly sheared and oxidised mafic lithology and metagranites. A fault with striation (chlorite+hematite) occurs along the upper surface (to the left).

KFM01D_DZ1_176-184 m
Datasets: 1

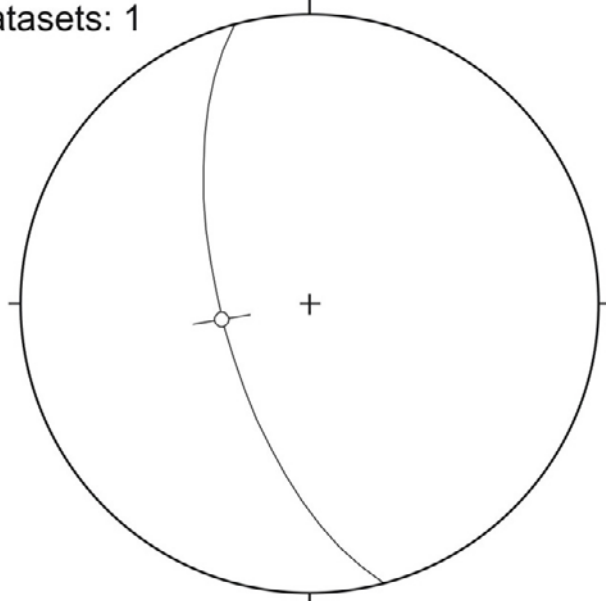


Figure 5-14. Stereoplot of fault slip data in DZ1 (KFM01D).

KFM01D: 411–421 m – DZ2

Zone DZ2 mainly consists of fractures that strike NNE and dip steeply east; some gently dipping fractures are also present. The fractures are sealed with laumontite, calcite, chlorite and minor hematite. In the central part of the zone (ca 416 m), a 10 cm wide fracture network with laumontite and secondary calcite veins is present. No fault slip data have been identified in the zone. The DZ is considered a transition zone according to /Munier et al. 2003/.

KFM01D: 488–496 m – DZ3

Zone DZ3 mainly consists of sporadic fractures and minor sealed networks that strike SSE and dip steeply westwards; some gently dipping fractures are also present. The fractures are sealed with calcite, chlorite and minor hematite and adularia. At ca 489 m, there is a minor ductile shear zone with epidote + quartz and with chlorite + hematite on fracture surfaces. The DZ is considered a transition zone according to /Munier et al. 2003/.

Only one NNW-SSE steep fault has been measured along DZ3 in KFM01D (Figure 5-15). It is sub-parallel to the measured fault along DZ1 in the same drill core (see above). The striation is rather oblique, with a pitch of 48 degrees to the NW and displayed by slickensides on chlorite and hematite.

KFM01D: 670–700 m – DZ4

Zone DZ4 exhibits a moderately increased frequency of sealed and open fractures (Figure 5-16). Gently dipping fractures and fractures dipping steeply SE and NE dominate. Chlorite-sealed veins are vertical and strike NNE-SSW. The most frequent fracture filling minerals are calcite, chlorite, laumontite and some clay minerals and quartz. Fractures with calcite, quartz and pyrite post-date fractures sealed with calcite and laumontite (Figure 5-16). At ca 686 m, a NE-SW-oriented steep network of parallel fractures sealed with laumontite and calcite that are cut by calcite veins constitutes a thin fault core. Otherwise the DZ is considered a transition zone /Munier et al. 2003/. Late calcite veins (2–5 mm wide) in the upper part of the zone trend NNE with steep dips. No fault slip data have been identified in the zone.

KFM01D_DZ3_488-496 m

Datasets: 1

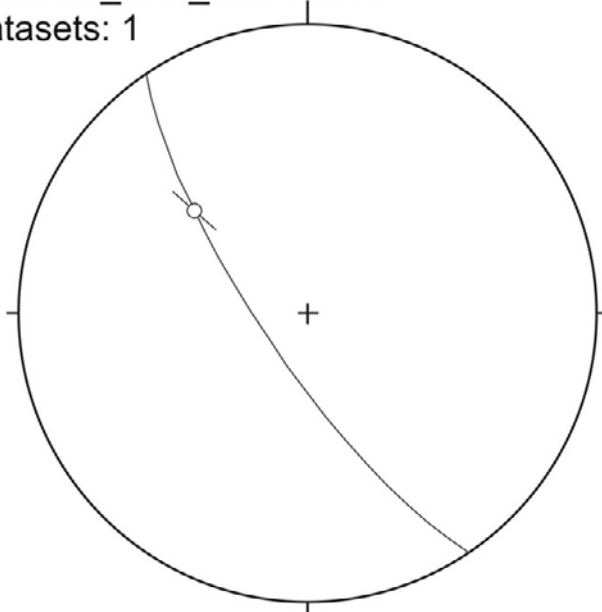


Figure 5-15. Stereoplot of fault slip data in DZ3 (KFM01D).

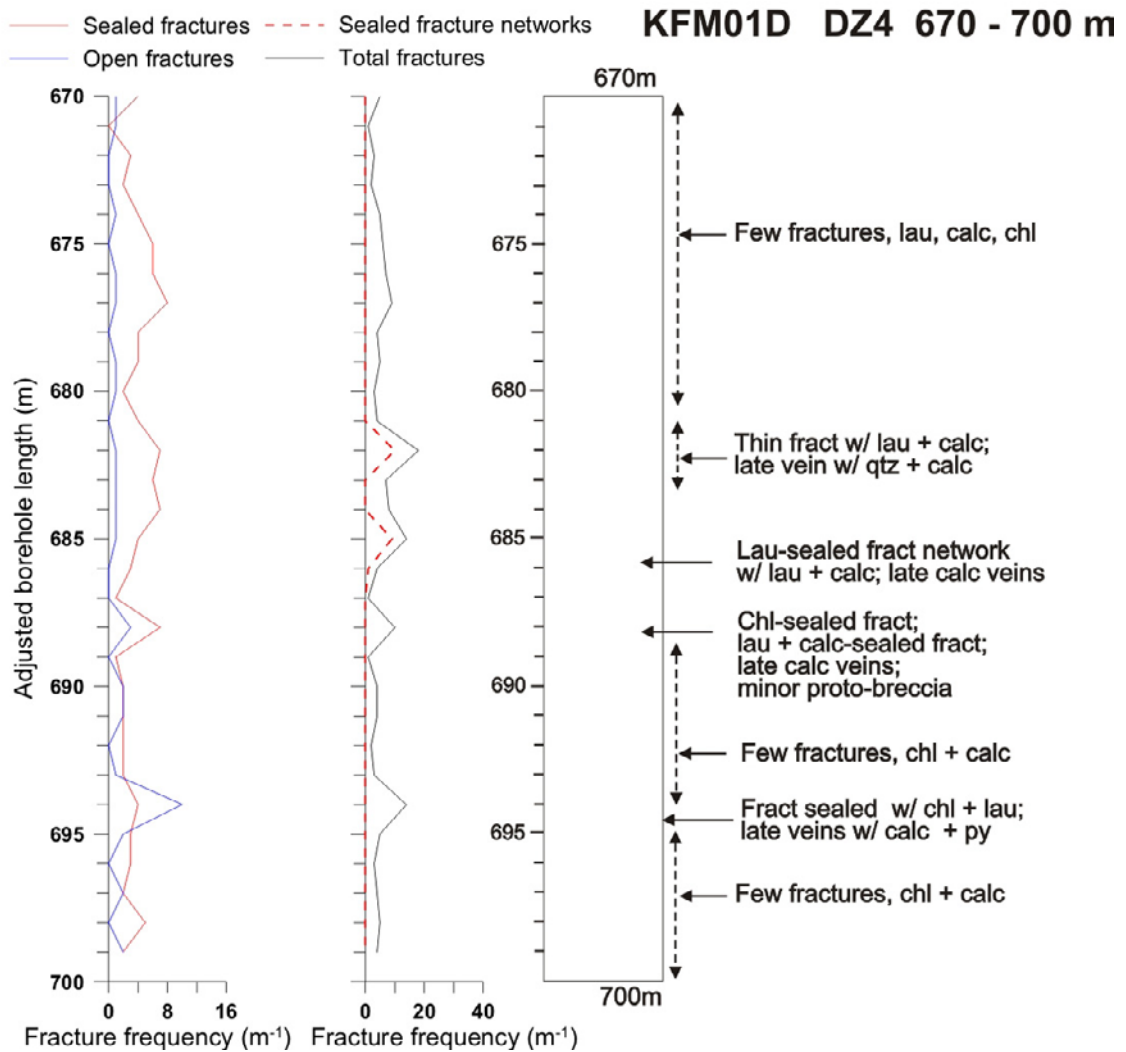


Figure 5-16. Simplified drawing of DZ4 showing the most prominent brittle structures in the zone. Abbreviations as in Figure 5-3.

KFM01D: 771–774 m – DZ5

Short interval with chlorite, clay minerals and calcite on open and some sealed fractures. At ca 772 m, there is 2–3 cm wide calcite-sealed fault with chlorite on broken surfaces. It trends ENE-WSW parallel to abundant wide calcite-filled veins. Calcite steps superimposed on the chlorite-striated surface define dextral movement on the fault (Figure 5-17). In general, the DZ exhibits moderate fracture frequencies and is considered a transition zone /Munier et al. 2003/.

5.1.4 KFM06C

This drill hole is located in the central southeast part of the investigation area (Figure 5-1). The drill hole is oriented 026/60 and has a length of 1,000.4 m /Carlsten et al. 2006b/. Four deformation zones with a total length of 235 m were investigated.

15 striated faults are collected along all the studied DZ in drill core KFM06C (Figure 5-18). A predominant feature is the NNE-SSW, probably sinistral, set of faults. Two sets of some gently to moderately E- and S-dipping faults are also observed. Oblique- to dip-slip displacement, including a reverse dip-slip component, is apparent in these two sets.

KFM01D_DZ5_771-774 m
Datasets: 1

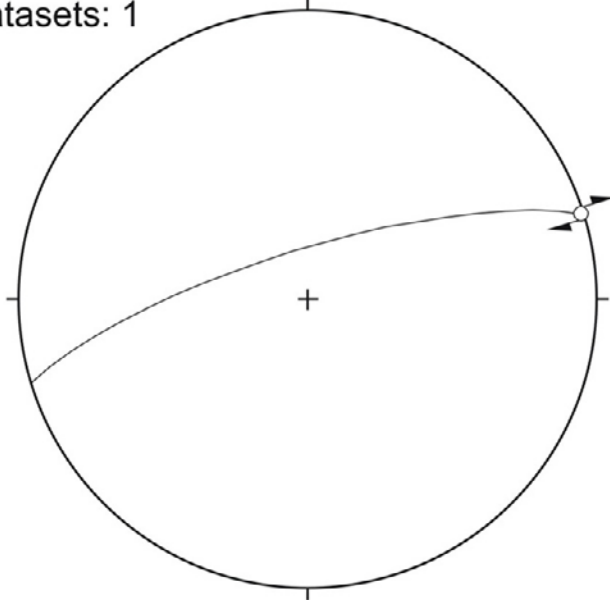


Figure 5-17. Stereoplot of fault slip data in DZ5 (KFM01D).

KFM06C_DZ1_DZ2_DZ3_DZ4
Datasets: 15

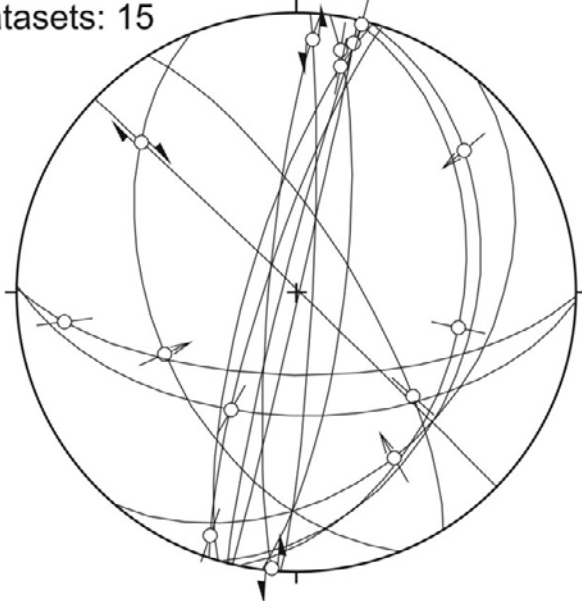


Figure 5-18. Stereoplot showing all the fault slip data collected along all the studied DZ of drill core KFM06C.

KFM06C: 102–169 m – DZ1

Metagranite with pegmatite and some amphibolite are the most common rocks along the DZ1 of core KFM06C. The upper 30 metres contains the main brittle deformation products. Based on the fracture frequencies and distribution of brittle features, this part of the DZ is considered a transition zone /Munier et al. 2003/. Little brittle deformation can be observed from ca 130 m to the base of the zone (Figure 5-19). This part of the DZ is also a transition zone; however, the intervals ca 130–140 m and ca 155–169 m have very few fractures and may be therefore

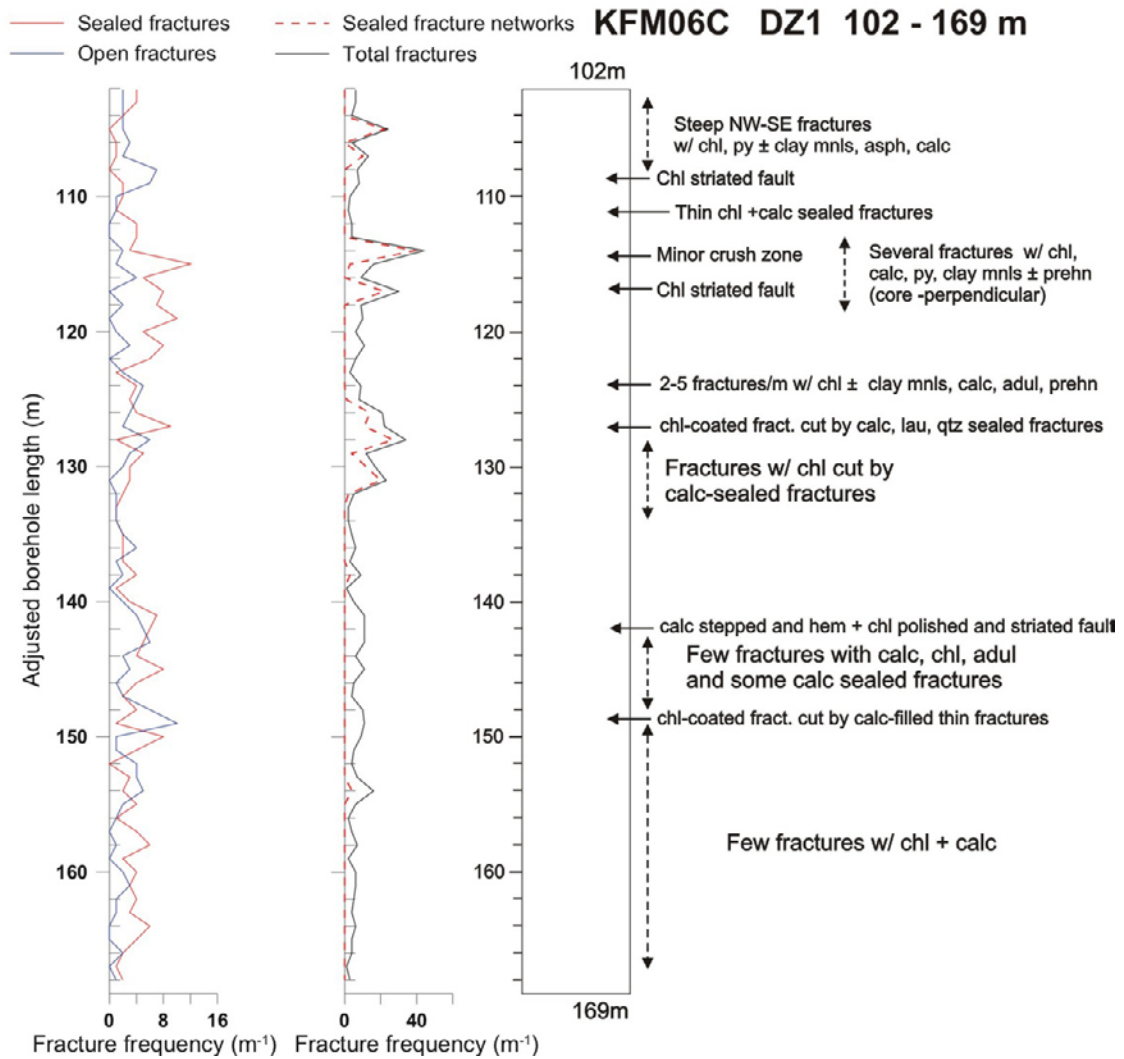


Figure 5-19. Simplified drawing of DZ1 showing the most prominent occurrences of brittle structures. Abbreviations as in Figure 5-3.

be considered undisturbed host rock. Minerals coating/filling the fractures are chlorite, calcite, pyrite, clay minerals, prehnite, adularia, laumontite, quartz and asphaltite.

The top of the zone is characterised by few NW-SE, steep calcite-chlorite-asphaltite-pyrite-sealed networks (Figure 5-20). Fracture density increases (1) between 110 and 120 m with several drill core-perpendicular chlorite-calcite (-pyrite-clay minerals-prehnite) fractures and a crush-zone at 114.50 m and (2) between 125 and 132 m with chlorite-coated fractures and calcite-filled veins. The chlorite-coated fractures are cut by NW-SE calcite-laumontite-quartz sealed fractures at 127 m (Figure 5-20 and 5-21) and by calcite-sealed veins at ca 130 m. The picture of Figure 5-21 is an example at 162 m of the few roughly N-S trending calcite-fluorite-quartz-pyrite-filled fractures present at the base of the DZ (Figure 5-20).

Three striated faults have been recorded along DZ1 in KFM06C (Figure 5-22). One is probably a dip-slip reverse fault, 47 degrees WSW-dipping with striations on chlorite. Clay minerals and a coating of prehnite are also visible on the plane. The two other faults are strike-slip faults, roughly N-S and steep. One of these faults show sinistral displacement (Figure 5-22).

KFM06C_DZ1_102-169 m
Datasets: 3

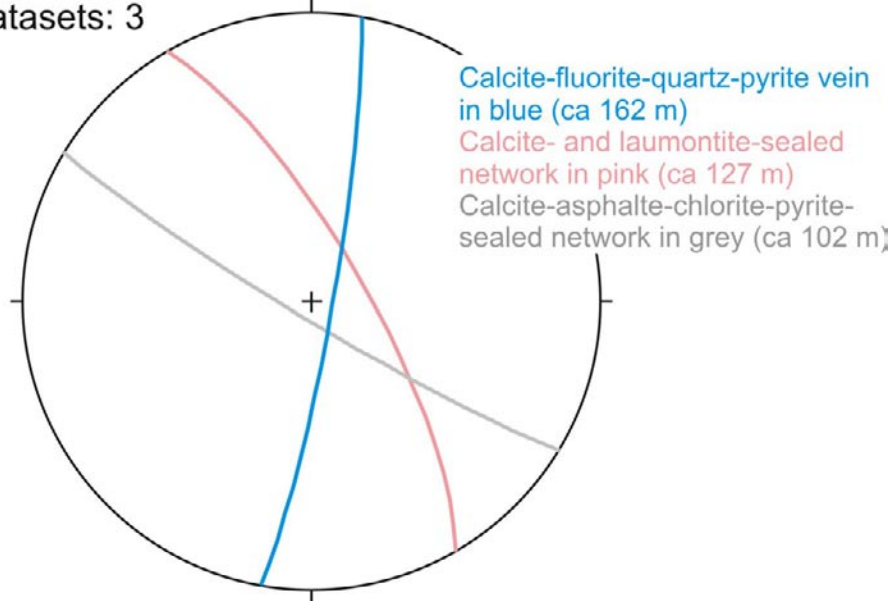


Figure 5-20. Stereoplot of some main fractures observed along DZ1 in KFM06C.



Figure 5-21. To the left: Thin NW-SE calcite-laumontite-quartz-sealed fracture at 127 m (pink colours on stereoplot in Figure 5-20) that cuts a chlorite-coated fracture. To the right: N-S calcite-fluorite-quartz-pyrite-filled fracture as an example of the few fractures present at the base of the DZ at 162 m (blue colour on stereoplot in Figure 5-20).

KFM06C_DZ1_102-169 m
Datasets: 3

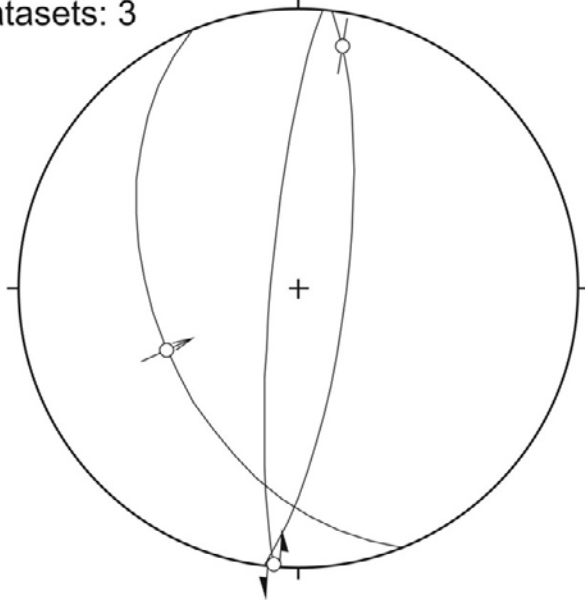


Figure 5-22. Left: Stereoplot of fault slip data along DZ1 in KFM06C. Right: Example of fault surface with striae on hematite and chlorite, and sinistral steps of calcite showing sinistral sense of slip (strike/dip angle/pitch: 185/82/0) (142.10 m).

KFM06C: 359–400 m – DZ2

The rocks along DZ2 in KFM06C are mainly medium to fine-grained, grey-pink metagranite that displays a strong foliation. Several intervals of pegmatite occur between 370 and 377 m and a 50 cm wide amphibolite is present at ca 383.50 m.

In general, fracture frequencies are moderate and the zone is considered a transition zone /Munier et al. 2003/. Undisturbed host rock with few fractures occurs between 370 and 376 m (Figure 5-23). Thin hairline fractures may locally contribute to an increased frequency in sealed fractures. The top of the zone from 359 to ca 370 m is characterised by (1) a minor crush zone at 361.20 m (Figure 5-23) (2) nearly horizontal epidote-chlorite-calcite-filled veins and NE-SW steep laumontite-chlorite filled fractures (Figure 5-23 and 5-24). Beneath 375 m, the fracture density increases and attains a maximum at 394–395 m. Fractures are coated by chlorite, clay minerals and calcite, with thin epidote- and laumontite-sealed fractures around 390 m (Figure 5-23).

Three fault slip data have been measured along DZ2 (Figure 5-25). One is a NW-SE, vertical dextral strike-slip fault with striae plunging 24 degrees towards the NW on the surface. This steep dextral fault occurs at the top of the amphibolite at 383.44 m. The fault plane is stepped and contains striations marked by chlorite. The two other fault slip data were obtained from gently E-dipping planes; one holds a probably oblique reverse striation with a pitch of 40 degrees to the N, and the other a dip-slip striation of uncertain shear sense.

KFM06C: 415–489 m – DZ3

The rocks along DZ3 in KFM06C are strongly foliated greyish-pink metagranite with minor amphibolite in the top of the zone, vuggy granite at ca 452 m, and metadiorite with granite and pegmatite from 467 to 470 m.

The zone is mainly characterised by networks of sealed fractures with primarily adularia as well as some open fractures with chlorite ± clay minerals. Two brecciated zones have been observed along the core at 429.5 and 442 m.

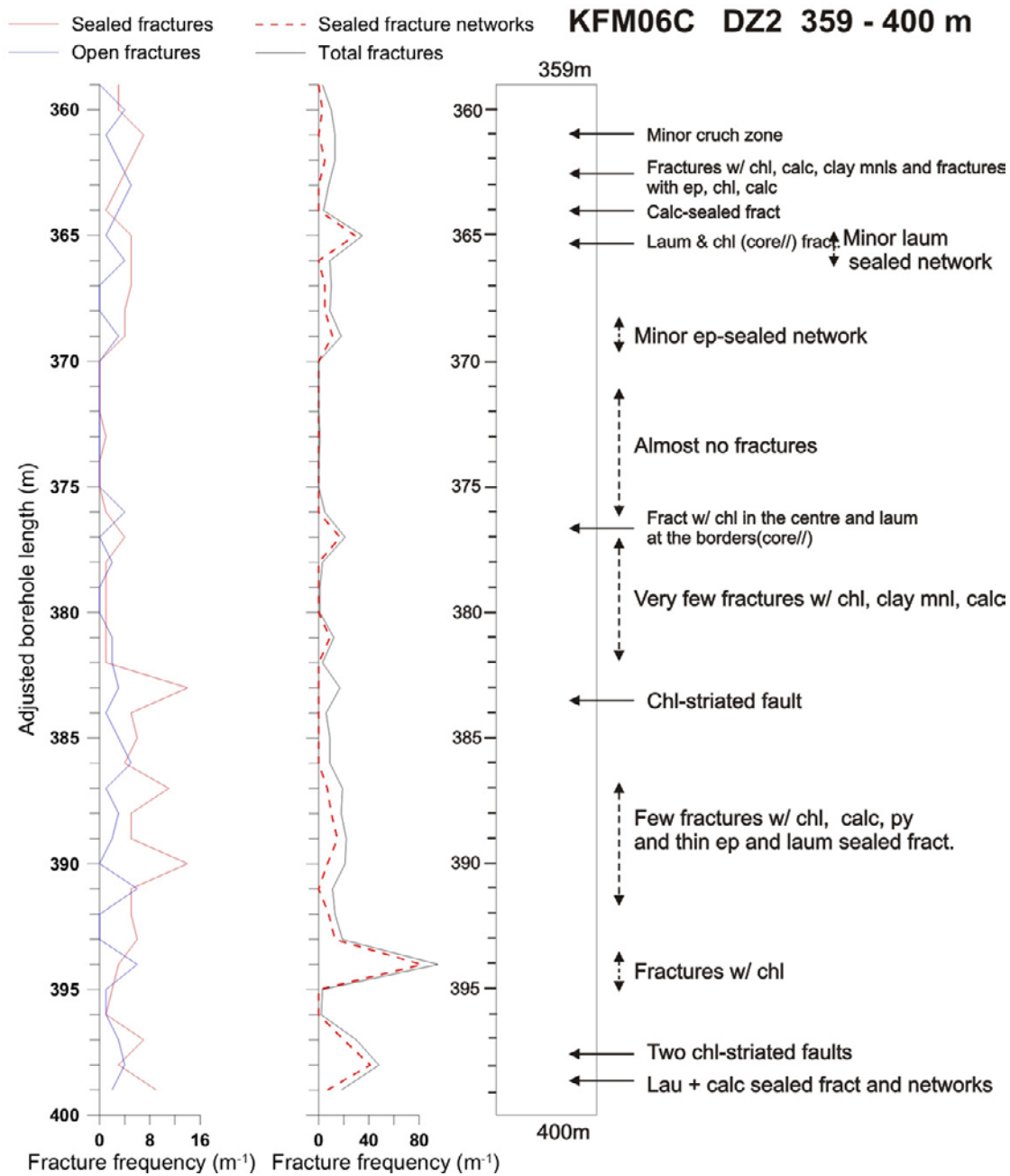


Figure 5-23. Simplified drawing of DZ2 showing the most prominent brittle structures. Abbreviations as in Figure 5-3.

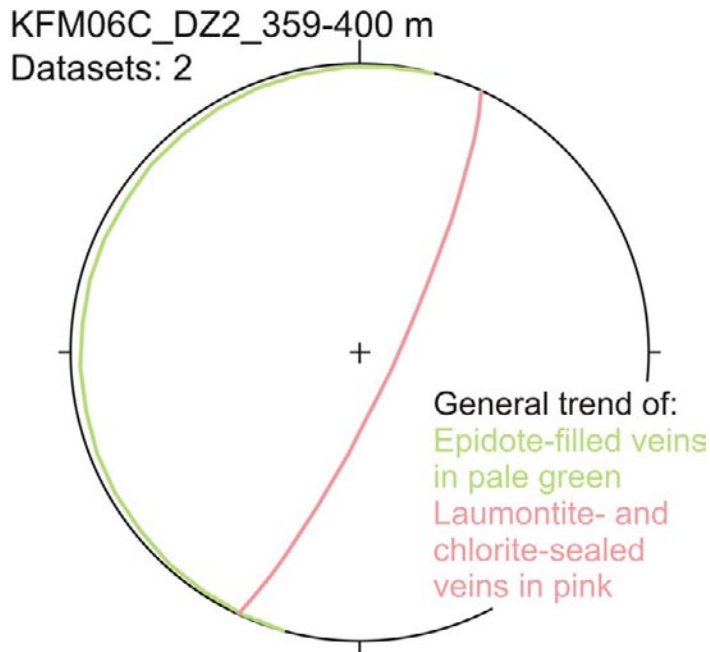


Figure 5-24. Stereoplot of flat-lying epidote-chlorite-calcite filled fractures at 362.50 m and NE-SW steep laumontite-chlorite-filled fractures at ca 365 m. DZ2 along KFM06C.

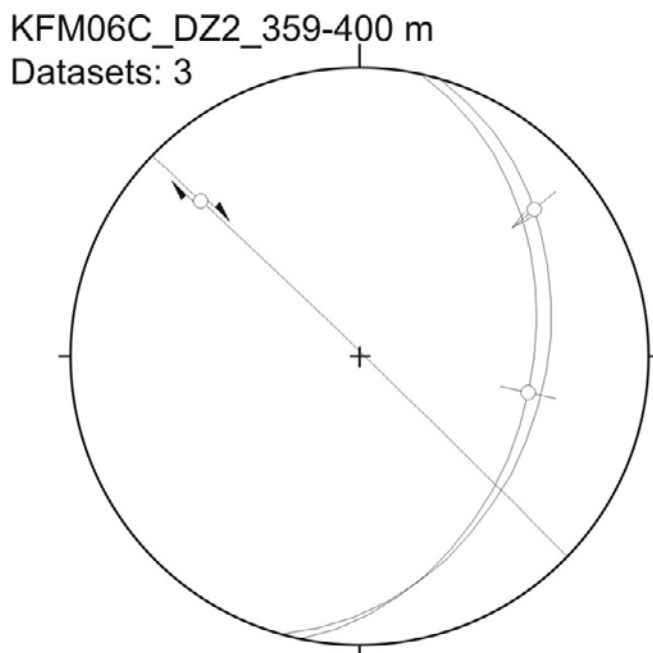


Figure 5-25. Stereoplot of fault slip data in DZ2 (KFM06C).

The top of the zone is characterized by networks of hairline fractures with adularia \pm calcite, chlorite and hematite (Figure 5-26). Figure 5-27 displays two pictures of the brittle structures encountered at the top of the zone: to the left, a steep and wide NE-SW fracture sealed with adularia, calcite and chlorite observed at 416 m (see also stereonet of Figure 5-28), and to the right, the network of thin adularia-sealed fractures around 420 m.

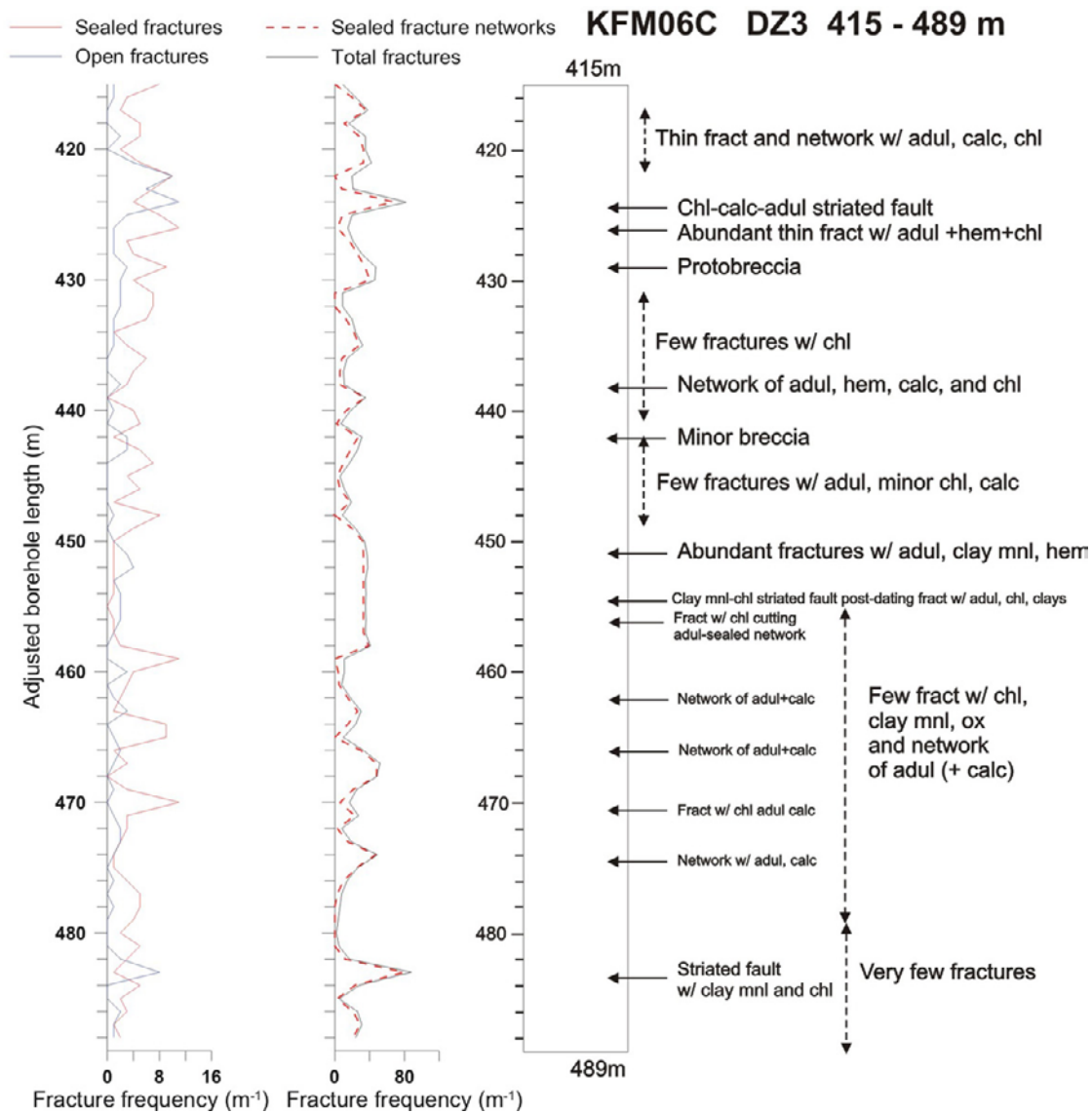


Figure 5-26. Simplified drawing of DZ3 showing brittle structures. Abbreviations as in Figure 5-3.



Figure 5-27. Left: Steep and wide NE-SW fracture sealed with adularia, calcite and chlorite observed at 416 m (see also stereoplot in Figure 5-28). Right: Network of thin adularia-sealed fractures around 420 m.

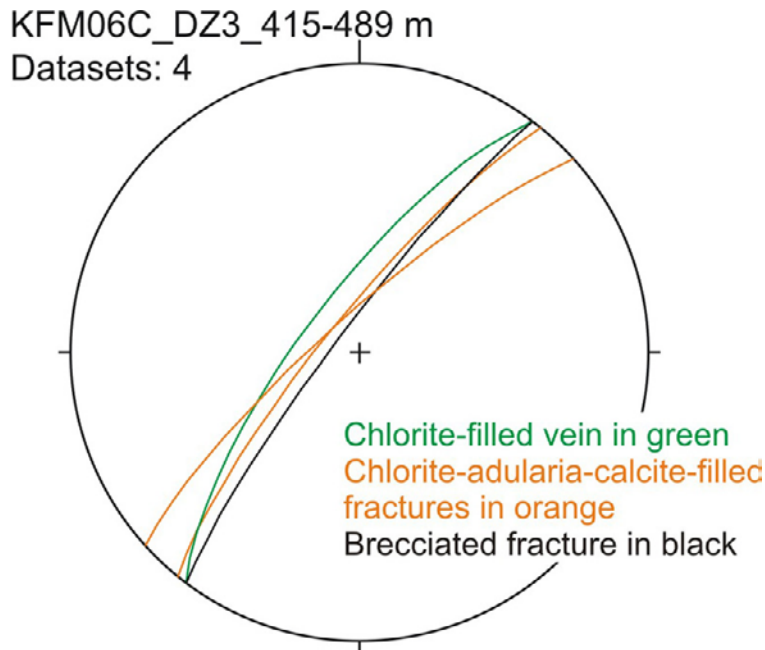


Figure 5-28. Stereonet showing the parallel trends of typical brittle structures along DZ3 in KFM06C: a wide adularia-calcite-chlorite filled fracture at 416 m (see also Figure 5-27), a chlorite-filled vein at 429.40 m that corresponds to the top border of a breccia (Figure 5-29), and a breccia at 442 m.

From 429 to 440 m, there is a reduced frequency of fractures with chlorite. One of the chlorite-filled veins is NE-SW and steep (Figure 5-28) and corresponds to the top border of a brecciated zone with laumontite, adularia and some calcite. The breccia has been sampled and consists of variably sized angular fragments in a fine-grained cataclasite matrix with laumontite and with some adularia and calcite (Figures 5-29 and 5-30).



Figure 5-29. Laumontite- and adularia-rich brecciated zone at 429.50 m limited by two NE-SW chlorite-filled veins (the top most is plotted on the stereonet in Figure 5-28).

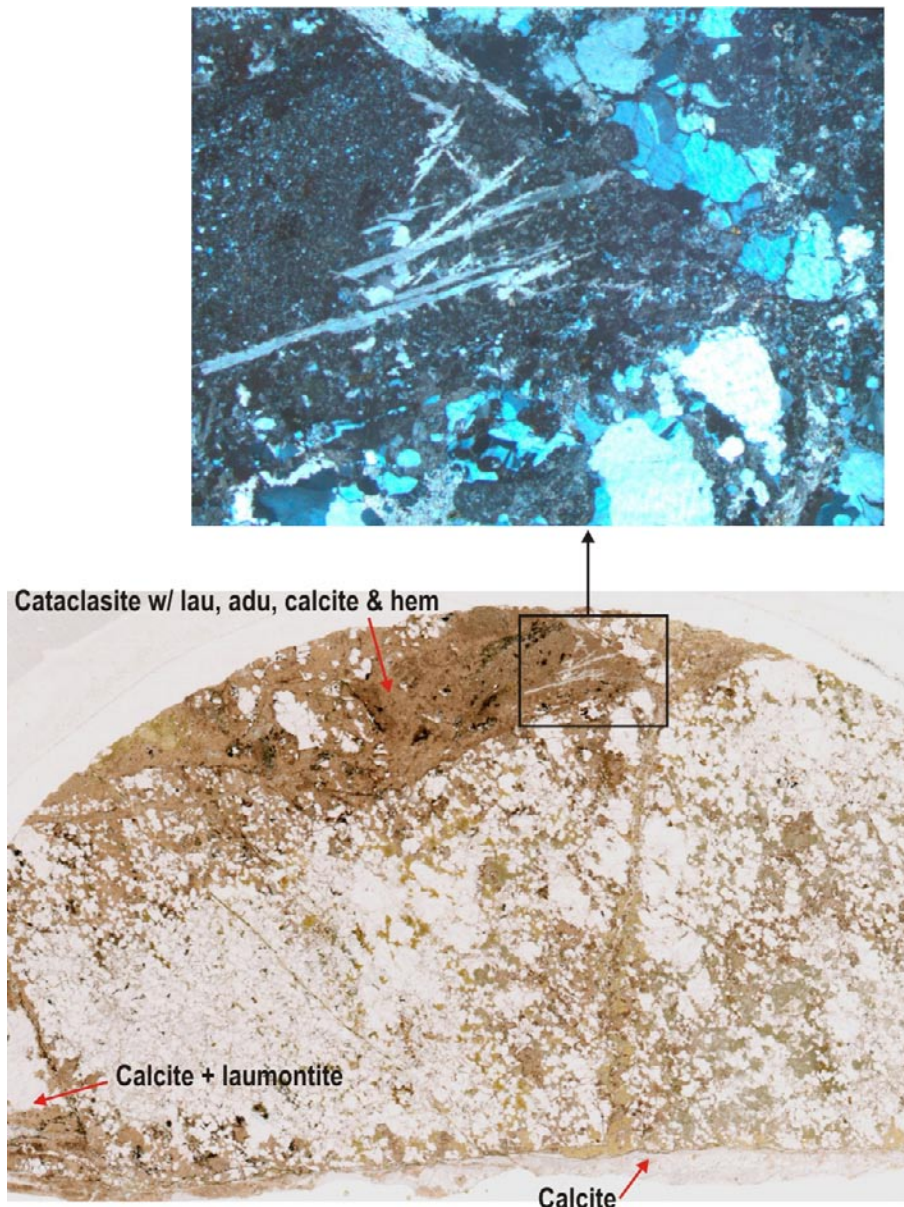


Figure 5-30. Scanned thin section (below) and photomicrograph (above) of sample KFM06C_429.4. The thin section (width of view is 25 mm) shows altered metagranite with some epidote and chlorite in the central part. At the base and to the left, calcite and laumontite-sealed veins cut the metagranite. In the upper part there is a fine-grained laumontite-rich (ultra-)cataclasite with adularia and calcite present as euhedral crystals. Hematite is present as small dusty specks. The photomicrograph shows a detail from the thin section. Blade-shaped, euhedral calcite occurs in fine-grained (ultra-)cataclasite. Width of view: 5.5 mm.

At 442 m, a minor brecciation is observed along a NE-SW steep fracture (see stereonet in Figure 5-28). From this point to the bottom of the zone, the brittle deformation is again characterised by adularia-rich networks (Figure 5-31) with some calcite and to some extent by chlorite-filled fractures. Fractures with chlorite and clay minerals cut the adularia-sealed fracture networks. Examples of this occur at 454.50 m (chlorite-striated fault as displayed on picture of Figure 5-32) and 455.50 m. The DZ is considered a transition zone /Munier et al. 2003/.

Three striated faults characterize DZ3 in KFM06C (Figure 5-32). They do not display any consistent pattern. One is probably a reverse dip-slip fault dipping gently to the SE, striations are on chlorite and clay minerals; quartz and calcite coat the plane. There is further an E-W steep plane showing strike-slip striae affecting chlorite and hematite; adularia and calcite are

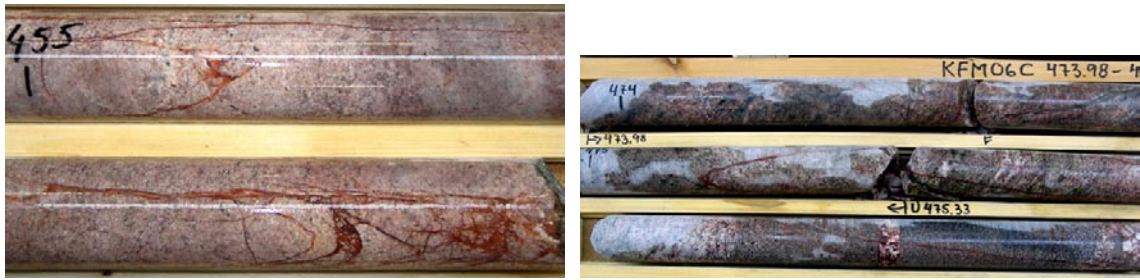


Figure 5-31. Left: adularia-rich network with some calcite as observed all along the DZ3, here in the 455–457 m interval. Right: network of adularia and hematite-filled fractures in the 474–476 m interval.

KFM06C_DZ3_415-489 m
Datasets: 3

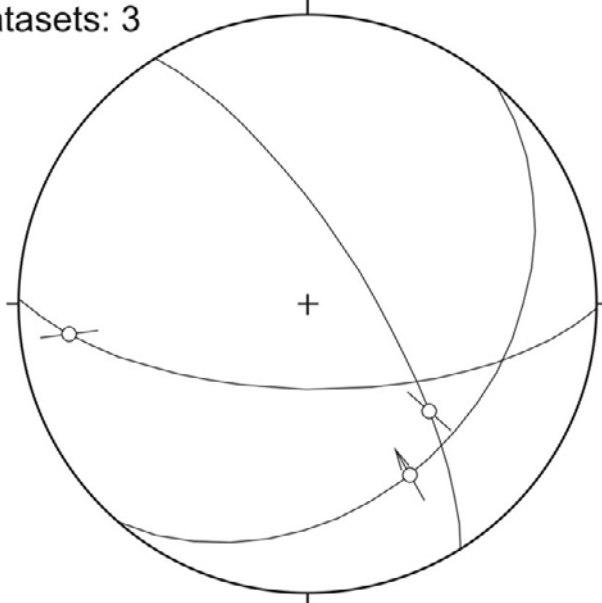


Figure 5-32. Left: Stereoplot of fault slip data along DZ3 in KFM06C. Right: Example of fault surface in KFM06C_DZ3 with striae on clay mineral and chlorite, unknown sense of shear (strike/dip angle/pitch: 328/73/-46) (454.47 m).

also observed on the fault surface. Finally, there is a NW-SE steep plane with oblique striae on chlorite and clay minerals (Figure 5-32).

KFM06C: 502–555 m – DZ4

The rock types along DZ4 in KFM06C are mainly a fine-grained greyish white to pinkish metagranite with a few minor bodies of amphibolite from 532 to 536 m.

Along the interval between 525 and 538 m, including the section where the amphibolites are present, this zone has a moderate to high fracture frequency (Figure 5-33). A ca 3 m long section occurring at 535–538 m, that has a high frequency of broken fractures including some thin crush zones, may tentatively be termed a fault core (Figure 5-34). Apart from this, DZ4 is considered a transition zone /Munier et al. 2003/. Fracture minerals are predominantly chlorite, clay minerals, calcite and oxides.

From the top of the zone to 530 m, the fractures are mainly chlorite-calcite-clay-rich (Figure 5-33). At ca 518 m, on nearly N-S trending steep fractures, two successive opening and subsequent mineralization events can be documented. The first infill was adularia and the youngest one chlorite and calcite.

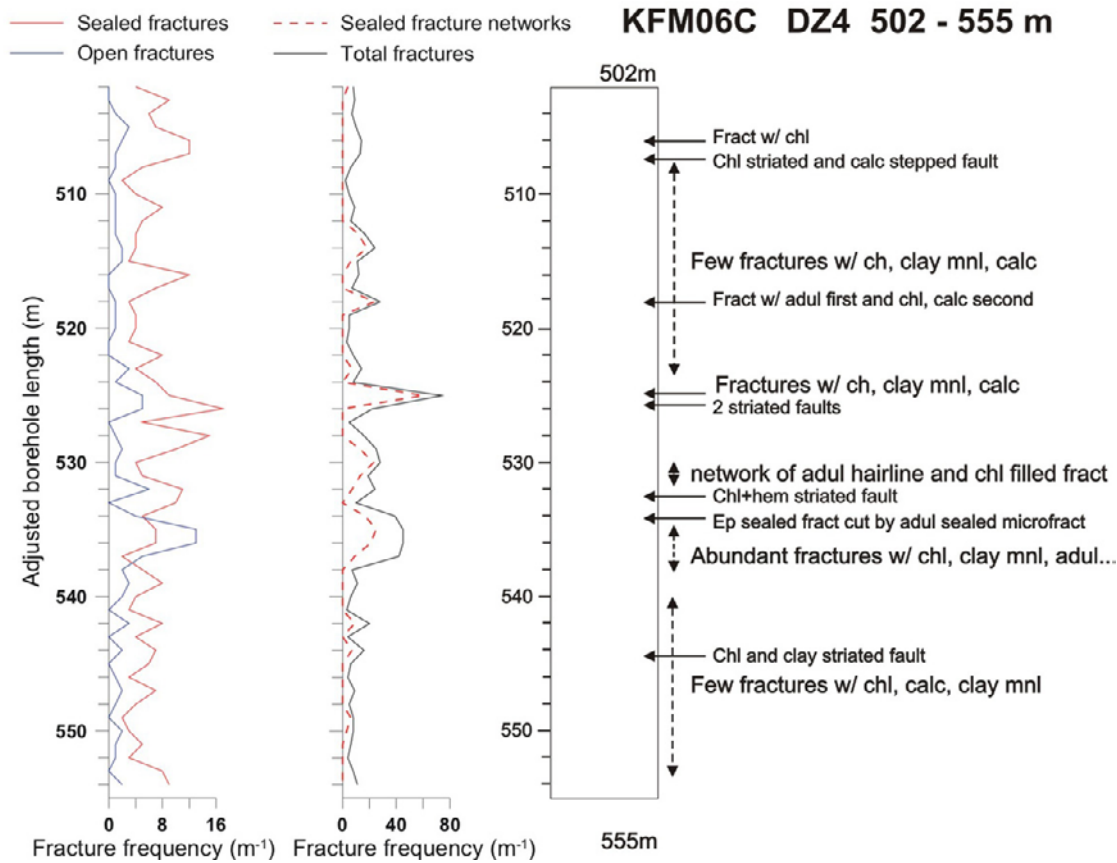


Figure 5-33. Simplified drawing of DZ4 showing brittle structures. Abbreviations as in Figure 5-3.



Figure 5-34. Left: notable increase in broken fracture frequency in the interval from 535 to 538 m, tentatively forming a fault core according to the definition of /Munier et al. 2003/. Right: an enlarged view of the picture to the left with the trend of the epidote-sealed veins underlined in green.

From 530 to 538 m, the broken fractures are quite abundant (Figures 5-33 and 5-34). Most of them are coated by chlorite but some clay minerals, calcite and adularia are also filling the fractures. Epidote-sealed veins are also present in this section and show a different trend (Figure 5-34). One of the epidote veins is cut by an adularia-sealed fracture.

Six fault slip data are present along DZ4 in KFM06C (Figure 5-35). Striations are on chlorite, hematite and clay minerals. A population of steep N-S striking strike-slip faults predominate. One certain sinistral sense of shear has been observed on one of the planes with calcite steps and striations on chlorite. One gently S-dipping dip-slip fault is also present and occurs along the upper contact of an amphibolitic body at ca 532.50 m.

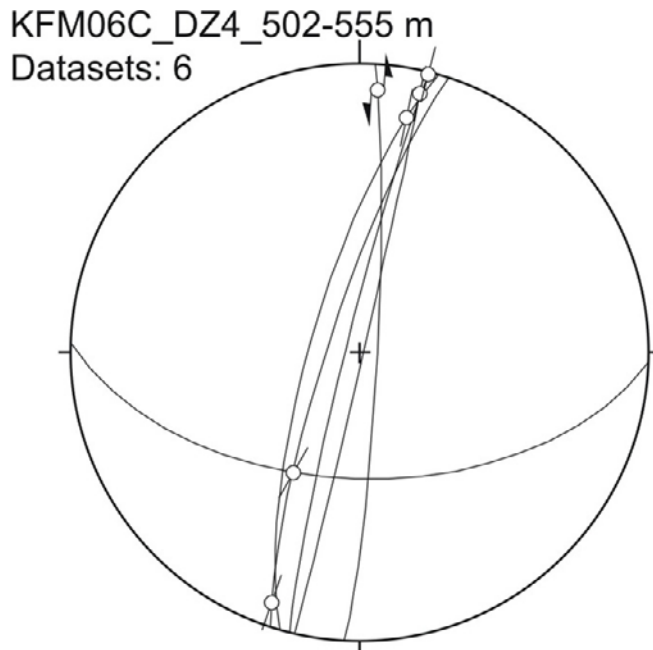


Figure 5-35. Stereoplot of fault slip data in DZ4 (KFM06C).

5.1.5 KFM07B

This inclined borehole is oriented 134/54 starting from a location in the northwestern part of the investigation area (Figure 5-1). The borehole has a length of 298.3 m /Carlsten et al. 2006a/. Three deformation zones (DZ1, DZ2 and DZ4) with a total length of 36 m were investigated.

KFM07B: 51–58 m – DZ1

This is a short deformation zone in foliated, medium-grained greyish pink metagranite to metagranodiorite with some amphibolite and minor pegmatite. Evidence of brittle deformation is mainly in the form of sub-parallel fractures with mainly chlorite and calcite. Some pyrite and hematite is also present. Abundant open fractures are predominantly gently dipping and occur particularly at 52–53 m and especially at 55–56 m (Figure 5-36). However, the general nature of the DZ is that of a transition zone /Munier et al. 2003/. At ca 56.5 m, a strong ductile fabric post-dated by brittle fracturing occurs in mafic amphibolite. A quartz vein with some chlorite is cut by a calcite-sealed vein at ca 56 m.

One flat NNW-SSE dip-slip fault of unknown sense of shear has been measured along DZ1 in KFM07B (Figure 5-37). Striae are on chlorite and later pyrite crystallized on the fault surface.

KFM07B: 93–102 m – DZ2

The rock type in this zone is a foliated, medium-grained greyish pink metagranite to metagranodiorite with some amphibolite and minor pegmatite. Open fractures are predominantly gently dipping whereas steep fractures have a variety of orientations. Open fractures are abundant at ca 95–96.5 m. Outside of this interval, the fracture frequencies are moderate. Predominant fracture minerals are chlorite, calcite, hematite, adularia. A laumontite-sealed network is oriented ca 020/70 at ca 93.5 m (Figure 5-38). The deformation zone shows the character of a transition zone /Munier et al. 2003/. Striated faults were not observed.



Figure 5-36. Photograph of the core in the upper part of DZ1. Note abundant fractures at 52–53 m and especially at 55–56 m. Photo: Alf Sevastik, SKB.

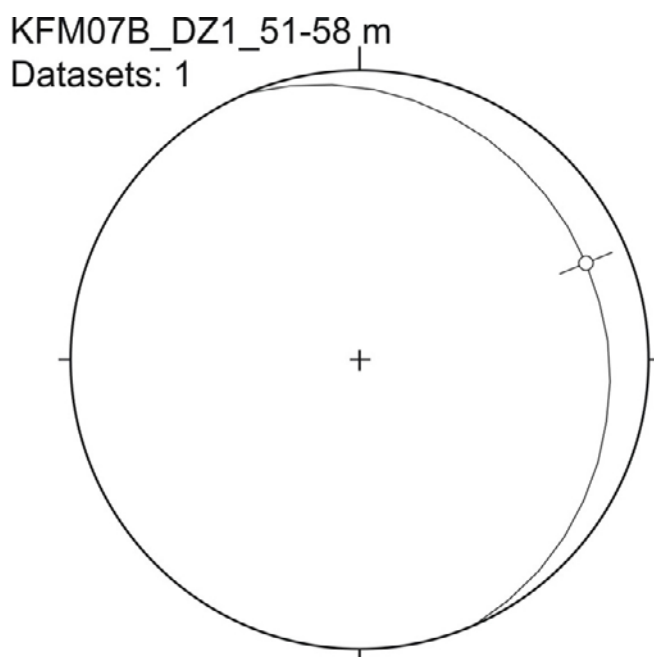


Figure 5-37. Stereoplot of fault slip data in DZ1 (KFM07B).



Figure 5-38. The upper part of DZ2 (92–95 m) exhibits moderate fracture frequency. Note relatively abundant open fractures at 95–96 m. A set of parallel laumontite-sealed fractures form a network at ca 93.5 m. Photo: Alf Sevastik, SKB.

KFM07B: 225–245 m – DZ4

The rock type in this zone is a foliated, medium-grained greyish pink metagranite to metagranodiorite with some amphibolite and minor pegmatite. Fractures are predominantly steep and strike SSE and NE. Some gently-dipping fractures are also present. Fractures are sealed/coated with chlorite, calcite, laumontite and minor hematite; reddish oxidation occurs along some fractures. At 234–235 m, a complex sequence of fault rock development is observed (Figure 5-39). Fine-grained cataclasite with altered plagioclase, epidote and chlorite is cut by NW-SE steep younger fractures and veins sealed with laumontite with some calcite. Following the definition of /Munier et al. 2003/, this zone shows the character of a transition zone with a short interval of fault core at 234–235 m (Figure 5-40). No fault slip data were obtained.

5.1.6 KFM07C

The borehole has a length of 500.3 m and the direction at the start is 143/85 /Carlsten et al. 2006e/. Three deformation zones (DZ1, DZ2 and DZ3) with a total length of 101 m were investigated.

KFM07C: 92–103 m – DZ1

This deformation zone is defined as 11 m wide occurring in pink and grey metagranite with minor pegmatite.

Most fractures strike NE-SW and show variable dip angles. Some fractures strikes NW-SE and dip moderately to steeply to the SW. The most frequent fracture filling minerals are chlorite and calcite. The steep fractures with chlorite and calcite cut gently-dipping fractures filled with chlorite and clay minerals (Figure 5-41). Thin calcite-filled veins oriented perpendicular to the drill core are also common (Figure 5-41). In general, the zone has the character of a transition zone /Munier et al. 2003/.

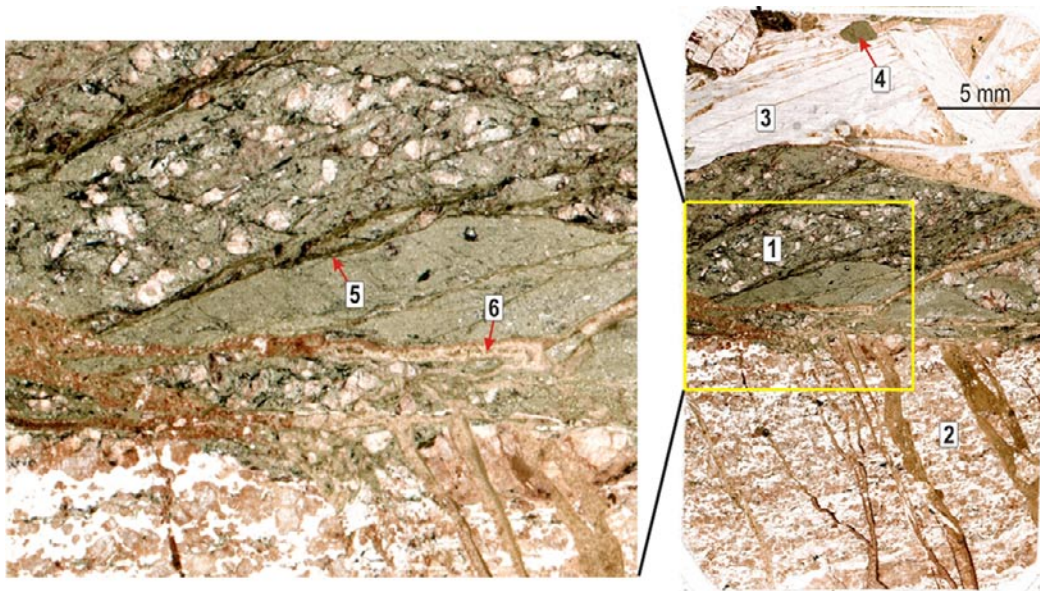


Figure 5-39. To the right: Scanned thin section KFM07B_234.2. Fine-grained, weakly foliated greenish cataclasite with altered plagioclase, epidote and chlorite (1) is cut by younger fractures. Below, a foliated metagranite is cut by laumontite + calcite-sealed fractures containing cataclasite (2). These fractures also cut the greenish cataclasite (see B). Above, a vein sealed with euhedral calcite and some laumontite is present (3). Note angular fragments of fine-grained dark cataclasite and fine-grained proto-cataclasite (4). Hairline fractures that do not contain any mineral fill are the last generation of structures. To the left: Detail from the central-left part of the scanned thin section. Greenish cataclasite with altered plagioclase, epidote and chlorite exhibits marked zones of very fine-grained ultra-cataclasite (?) oriented parallel to each other (5). This fault rock is cut by laumontite-rich, fine-grained cataclasite forming vein-like structures in the rock (6).

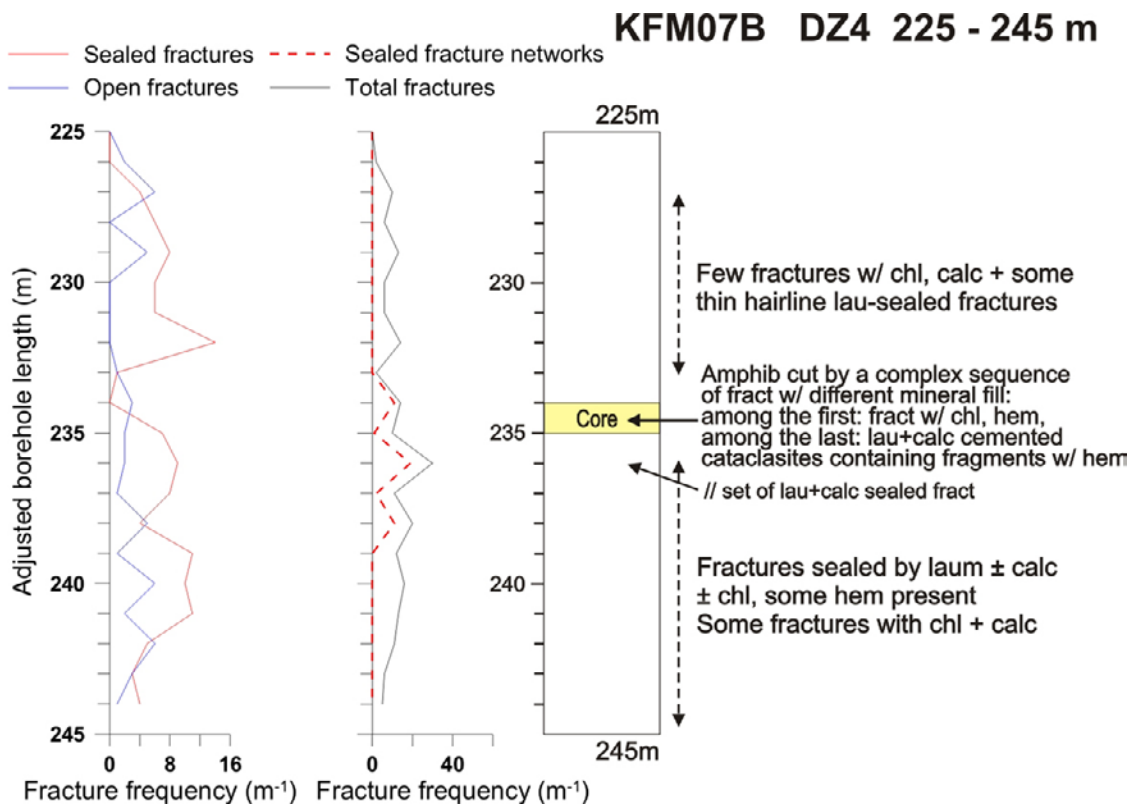


Figure 5-40. Simplified drawing of DZ4. Abbreviations as in Figure 5-3.



Figure 5-41. Overview of the brittle structures at the top of DZ1 in KFM07C. Steep chlorite-calcite filled fractures cut gently-dipping fractures filled with chlorite and clay minerals. Thin calcite-filled veins perpendicular to the drill core are also present.

KFM07C: 308–388 m – DZ2

DZ2 in core KFM07C consists of metagranite with several minor intervals of pegmatite and amphibolite. The brittle deformation is characterized by variable amounts of fractures with minor proto-breccia or cataclasites coated and sealed with chlorite, laumontite, calcite, and less commonly with hematite, corrensite and pyrite (Figure 5-42). Fractures that strike WSW-ENE and SW-NE and dip steeply to the NNW and to the NW, respectively, and fractures that are gently dipping to sub-horizontal dominate. Fractures with other orientations are also present. Most of the laumontite-sealed fractures are steep. However, gently-dipping laumontite-sealed fractures are also present. The DZ is mainly a transition zone /Munier et al. 2003/. Two intervals with fault core are present at 346.5–358 m and at 378.5–380.5 m (see below).

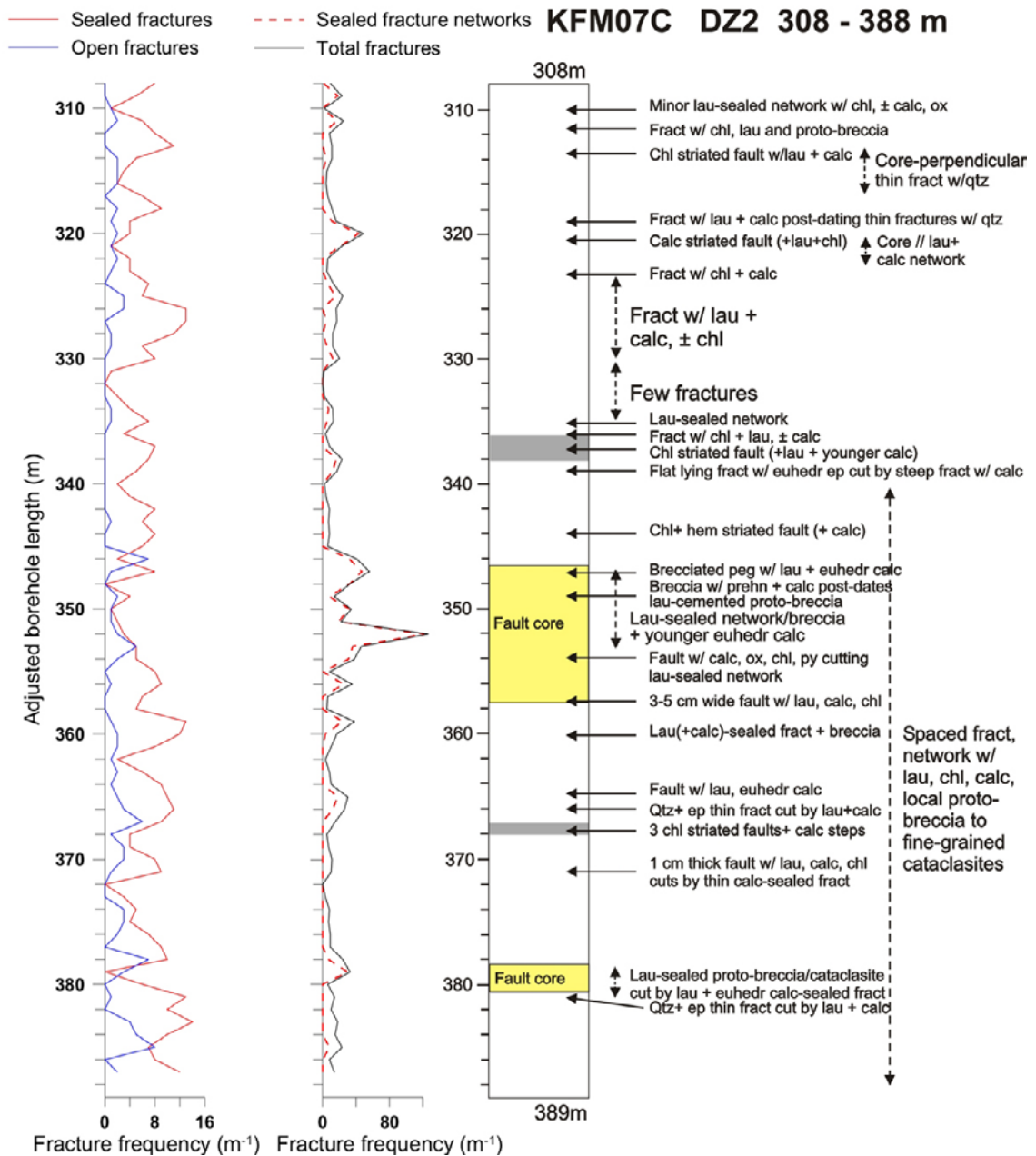


Figure 5-42. Simplified drawing of DZ2 showing brittle structures. Abbreviations as in Figure 5-3. Grey fields denote amphibolite.

The top of the zone is characterized by some laumontite-sealed networks and fractures with \pm calcite, chlorite and oxides (Figure 5-42). They post-date thin quartz veins oriented perpendicular to the drill core. The density of fractures increases at ca 320 m with the occurrence of laumontite–calcite-sealed network oriented parallel to the drill core (Figure 5-42).

From 320 m to 345 m, the brittle deformation is mainly characterized by fractures filled with laumontite, chlorite and calcite. The general pattern is chlorite at the border of fractures and laumontite on chlorite and an infill of calcite at the centre of the fractures. This may reflect the successive chronology of mineral infill of fractures with the oldest at the border and the youngest towards the centre. There are very few fractures in the interval 330–334 m.

A laumontite-sealed network is present at ca 335 m causing an increase in the fracture frequency. In the interval 336–338 m where the amphibolite is present, a slight increase in the amount of brittle structures is noted. At ca 339 m, flat-lying veins with euhedral epidote are cut by steep, calcite-filled fractures.

The central part of the zone (346.5–357.5 m) shows the highest fracture frequency (Figure 5-42) with the occurrence of two types of brittle structures (see overview of the interval on Figure 5-43). The older structures consist of a laumontite-cemented proto-breccia and associated sealed network. These are cut by numerous veins sealed with euhedral calcite and by an even younger calcite- and prehnite-cemented breccia at ca 349 m (Figure 5-44). The zone of contact between the two latter structures has been sampled (Figure 5-44). A similar chronology is observed at ca 354 m, with a strike-slip fault surface displaying calcite, oxides, chlorite and pyrite cutting across a laumontite-sealed fracture network. Based on the abundance of brittle deformation features, the interval 346.5–357.5 m is considered fault core following the definition of /Munier et al. 2003/.

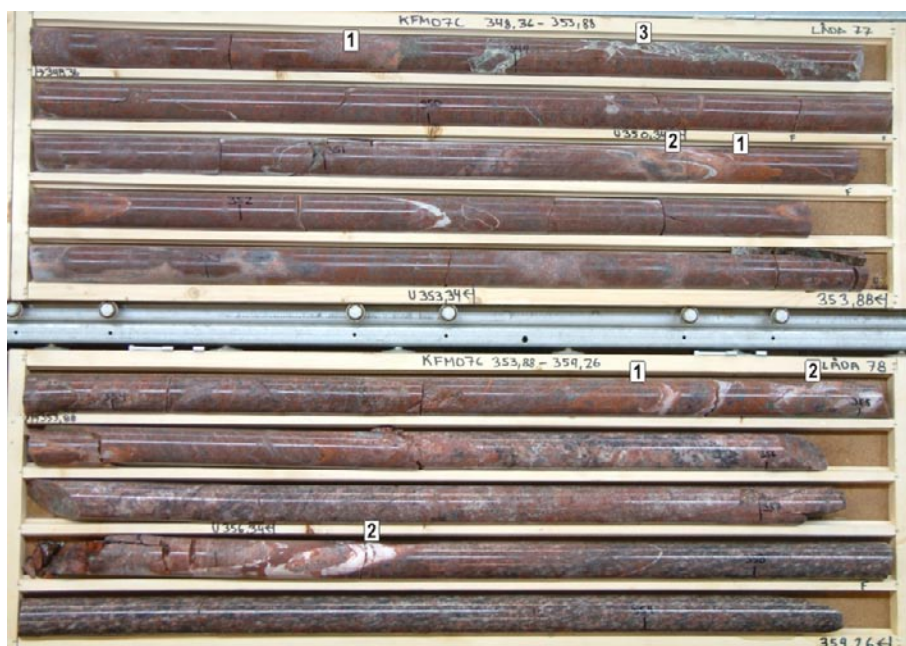


Figure 5-43. Drill core from the central part of DZ2. This part of the zone exhibits high fracture frequency with good examples of laumontite-cemented proto-breccia and laumontite-sealed network (1), post-dated by numerous occurrences of euhedral calcite-sealed veins (2) as well as proto-breccia with calcite + prehnite (3); see details from ca 349 m in Figure 5-44.



Figure 5-44. Left: Laumontite-cemented proto-breccia cut by a younger calcite- and prehnite-cemented breccia at 348.8 m. Right: The border between the two types of breccia and a thin vein that transect the laumontite-rich breccia (see details from thin section below).

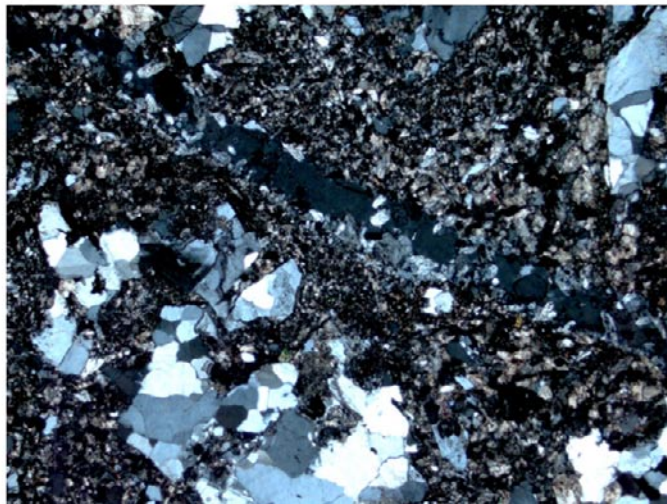
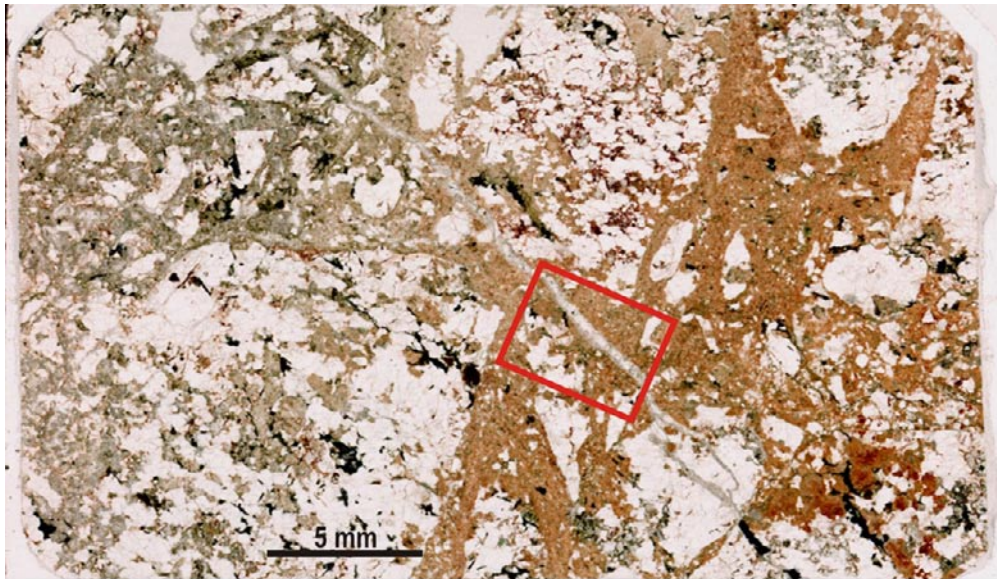


Figure 5-45. Above: scanned thin section of sample KFM07C_348.8 m. The brownish cataclasite consists of angular fragments of metagranite in a matrix of laumontite with some quartz and feldspar, and minor chlorite and epidote/zoisite. The metagranite is quartz-rich and mafic minerals are generally altered to chlorite + epidote. Note hairline vein that transects the cataclasite. Below: photomicrograph from the thin section (location shown by red frame) showing angular fragments of host metagranite in a laumontite-rich cataclasite. A thin vein that cuts across the cataclasite contains tiny, euhedral crystals of quartz that have grown perpendicular to the wall of the vein; the minerals in the central part of the vein are not preserved in the section.

Towards the base of the zone, there is again the same type of laumontite-rich fractures/networks with calcite and chlorite, and with local breccias and cataclasites (Figure 5-46). The cataclasites contain angular fragments of quartz and feldspar in a matrix of laumontite and minor epidote + zoisite. The interval 378.5–380.5 m is considered fault core according to /Munier et al. 2003/. At ca 379 m, a laumontite-calcite-filled fracture cuts across the laumontite-cemented proto-breccia (Figure 5-46). The upper border of the laumontite-rich cataclasite/proto-breccia at 380.6 m is a steep NE-SW trending plane. At ca 366 m and 380 m, thin veins with epidote and quartz are cut by laumontite-calcite-sealed fractures.

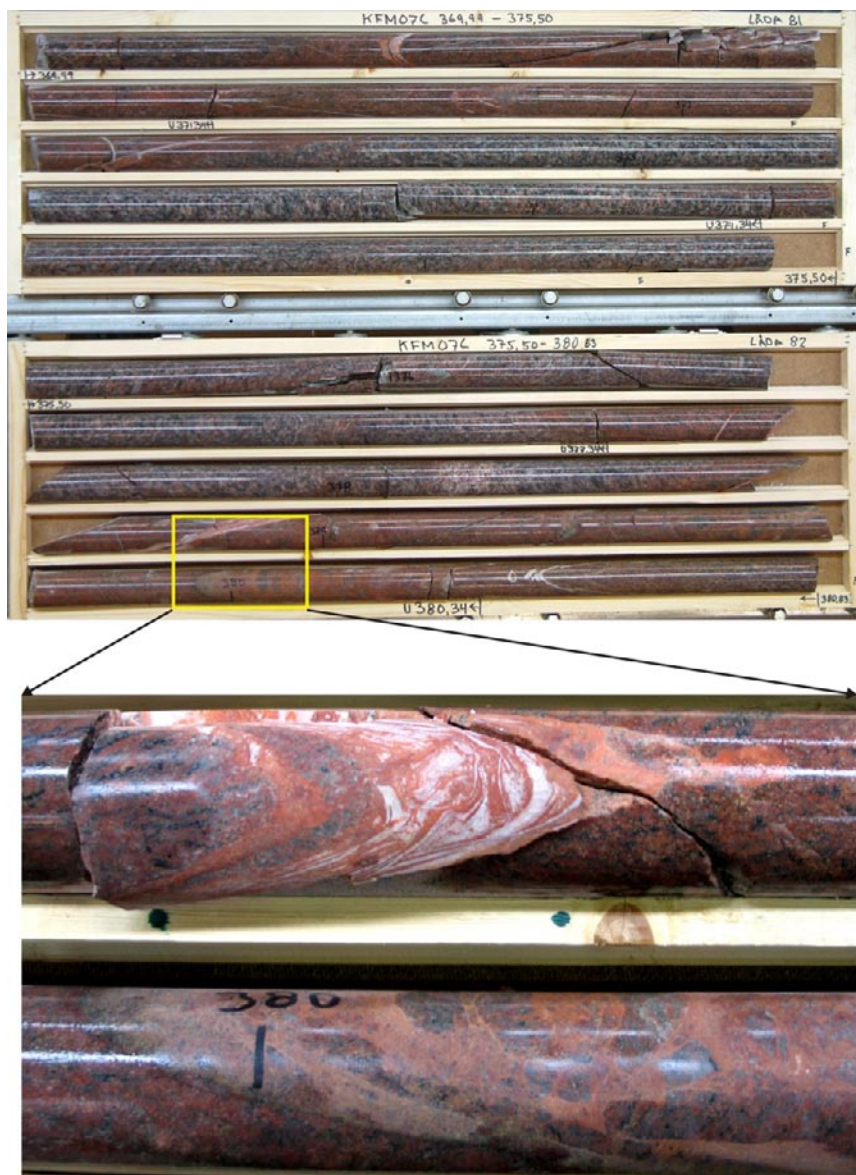


Figure 5-46. Above: overview of the drill core in the interval 370–375.5 m. Local breccias and cataclasites are associated with laumontite-rich fractures/networks with calcite and chlorite. The cataclasites contain angular fragments of quartz and feldspar in a matrix of laumontite and minor epidote + zoisite. Deformation products are particularly abundant in the interval 378.5–380.5 m and is considered fault core according to /Munier et al. 2003/. In contrast, note the low frequency of fractures at 373–375.5 m. Below: Detail from the drill core showing a laumontite-euhedral calcite-filled fracture cutting across an older laumontite-cemented proto-breccia at ca 379 m (upper core section) and a NE-SW steep cataclasite/proto-breccia cemented with laumontite at 380 m (lower core section).

Ten striated faults have been measured along DZ2 in KFM07C (Figure 5-47) with most of them located in amphibolitic bodies (see Figure 5-42). Two gently E-dipping fault planes are observed: one with nearly dip-slip striations (number 1 on stereonet in Figure 5-47) and another with oblique striations on calcite with a pitch of 41 degrees toward the south (number 2, Figure 5-47, and Figure 5-48A). Both have an undetermined sense of shear. An E-W steep strike-slip plane of unknown sense of shear is also present (number 3, Figure 5-47).

The 7 other fault slip data correspond to NW-SE and NNW-SSE strike-slip faults with striations marked mainly on chlorite and hematite. A sinistral sense of shear has been mostly determined using well-developed steps on the fault surface such as (1) calcite-steps (Figure 5-48B) that

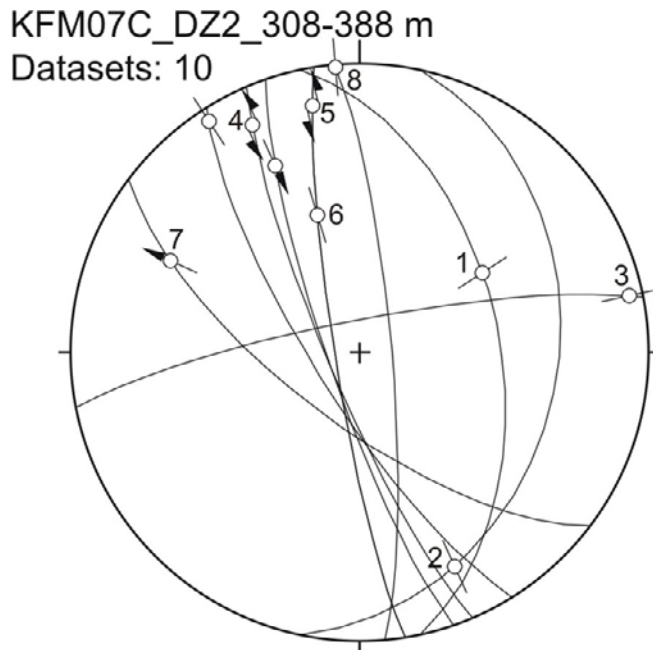


Figure 5-47. Stereonet of the striated faults in DZ2 of core KFM07C.

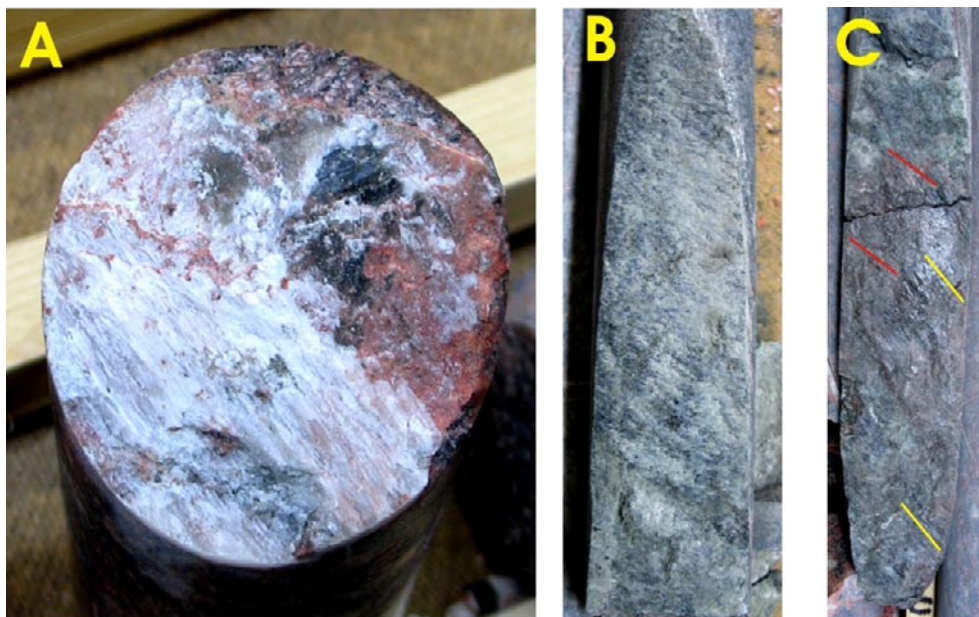


Figure 5-48. Examples of fault surfaces along DZ2 in KFM07C. A. Striations on calcite, undetermined sense of shear (strike/dip angle/pitch: 12/31/–41, number 2 on stereonet in Figure 5-47 (320.42 m). B. Striae on chlorite and calcite steps, sinistral sense of shear (strike/dip angle/pitch: 157/81/–14, number 4 on stereonet in Figure 5-47) (367.47 m). C. Two shear directions (highlighted with red and yellow lines) on the same fault surface: sinistral sense of shear with steps and fine striae on chlorite (strike/dip angle/pitch: 171/83/–14, number 5 on stereonet in Figure 5-47), and unknown sense of shear with polished chlorite and micro-grooves (pitch: –49, number 6 on stereonet in Figure 5-47) (367.12 m).

corresponds to slip number 4 on the stereonet in Figure 5-47, and (2) as chlorite-stepped surface (Figure 5-48C) that corresponds to slip number 5 on the stereonet in Figure 5-47. Two slips have been observed of one of these steep faults highlighting the reactivation of the fault possibly under successive tectonic phases (Figure 5-48C). One slip direction corresponds to a sinistral

shear sense as described previously (slip number 5 on the stereonet in Figure 5-47), and another shear is highly oblique on the plane with striae having a pitch of 49 degrees to the NNW (slip number 6 on the stereonet in Figure 5-47).

A NW-SE fault plane displays dextral striae on chlorite and hematite and is not consistent with the other slip data (slip number 7 on stereonet of Figure 5-47). Other minerals present on the fault surface, but not affected by shearing, are pyrite, sometimes laumontite, secondary calcite and oxides.

KFM07C: 429–439 m – DZ3

The rocks along DZ3 in KFM07C are amphibolites from the top of the zone to ca 434 m and metagranite-granodiorite in the lower part. Fractures strike WSW/SW and dip to the NNW/NW or are sub-horizontal. The upper part of the zone is characterized by abundant broken fractures and laumontite-euhedral calcite-sealed steep fracture networks in the amphibolites. From 432 m to the base of the amphibolite, gently dipping fractures with chlorite and some calcite are cut by steep calcite-sealed fractures (Figure 5-49). Between 434 and 439 m, there are several parallel fracture sets with laumontite, calcite and chlorite (Figure 5-49). Minor breccias occur along this fracture pattern, and the host rock is moderately oxidized. The nature of the brittle deformation along DZ3 resembles that in DZ2. In general, the DZ is considered a transition zone according to /Munier et al. 2003/. No fault slip data were obtained.

5.1.7 KFM08C

This drill hole is 951.1 m long and is located in the north-eastern part of the investigation area. The drill hole is oriented 036/60, i.e. directed towards the northeast away from the central part of the investigation area (Figure 5-1). Four deformation zones (DZ1, DZ2, DZ3, DZ4) defined by /Carlsten et al. 2006f/ with a combined length of 188 m were investigated (Table 5-1).



Figure 5-49. An overview of DZ3 in drill core KFM07C.

A total of 12 fault slip data were obtained from the investigated deformation zones (Figure 5-50). The predominant set consists of strike-slip faults with steep ca N-S orientations. The kinematic indicators are of high quality and have provided an excellent determination of the sinistral slip along these fault planes.

KFM08C: 161–191 m – DZ1

This deformation zone occurs in medium-grained metagranite-granodiorite with subordinate occurrences of pegmatitic granite. The interval exhibits a moderate increase in the frequency of sealed and open fractures that have highly variable orientations.

The fracture filling minerals are chlorite, calcite, adularia, laumontite, clay minerals, quartz, hematite, and pyrite. A fracture network with up to 10 mm wide veins filled with calcite, quartz and pyrite occurs at ca 168–169 m (Figure 5-51). Veins with coarse calcite and pyrite have steep to moderate dips towards the S to SSW. Minor crush zones are present at ca 177–178 and 186.5 m. The zone as a whole shows the character of a transition zone according to the definition of /Munier et al. 2003/.

One sinistral vertical N-S fault has been measured along DZ1 in KFM08C. The sense of shear has been determined using calcite steps on the chlorite- and hematite-striated surface (Figure 5-52).

KFM08C: 419–542 m – DZ2

The zone extends over a wide interval (123 m) in partly albitized medium-grained metagranite-granodiorite with subordinate occurrences of aplitic and pegmatitic rocks. The zone shows

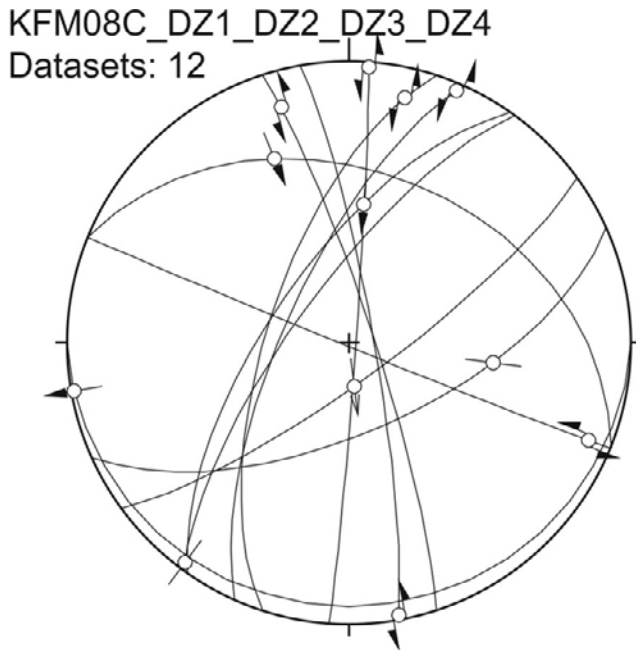


Figure 5-50. Stereoplot showing all the fault slip data collected along all the studied DZ in drill core KFM08C.

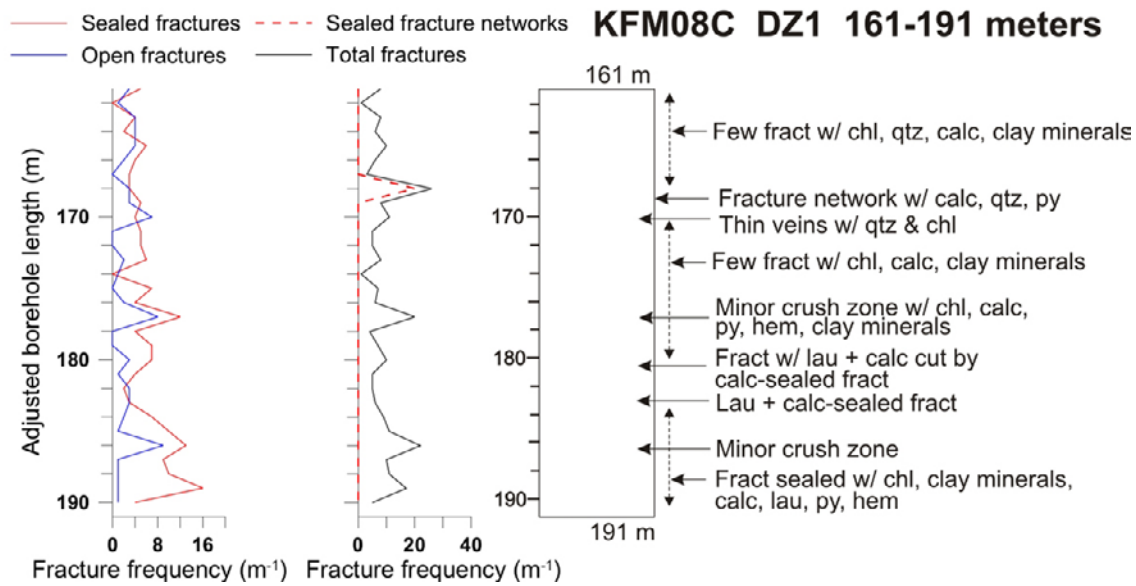


Figure 5-51. Simplified drawing of DZ1. Abbreviations as in Figure 5-3.

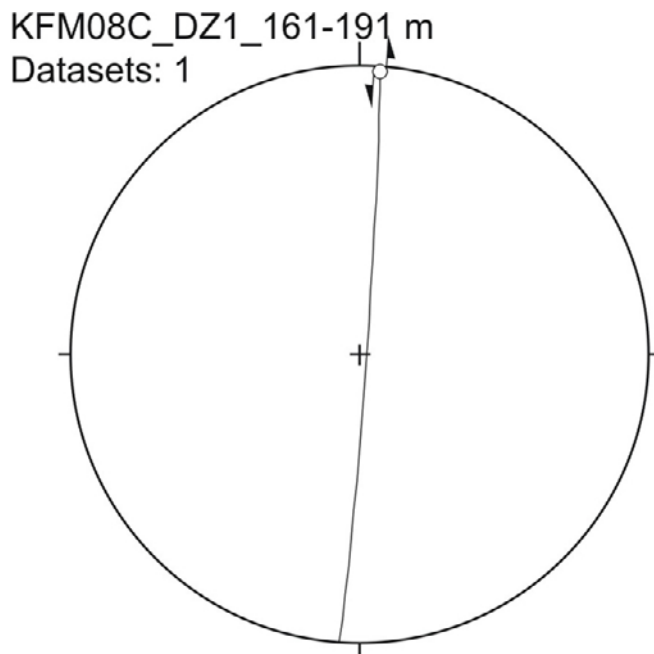


Figure 5-52. Stereoplot of fault slip data in DZ1 (KFM08C).

a moderately increased frequency of mainly sealed fractures (Figure 5-53). Open fractures generally have frequencies $< 5/m$ with minor peaks reflecting fairly narrow crush zones. The fractures show variable orientations. However, fractures with steep WNW dips and gently dipping to sub-horizontal fractures are most common (see /Carlsten et al. 2006f/). Calcite + adularia-filled veins and calcite-filled veins dip 60 degrees NW. The most frequent fracture-filling minerals include calcite, chlorite, hematite, adularia and quartz.

At ca 434.5 m, thin calcite-sealed fractures cut hairline fractures sealed with adularia + hematite. Altered vuggy rock that is variably oxidized occurs in the following intervals: 455–460 m, 498–499 m, 519–522 m and 522–524 m (Figure 5-53). Slightly vuggy rocks are sporadically present outside these intervals. The investigated interval shows the character of a transition zone according to /Munier et al. 2003/.

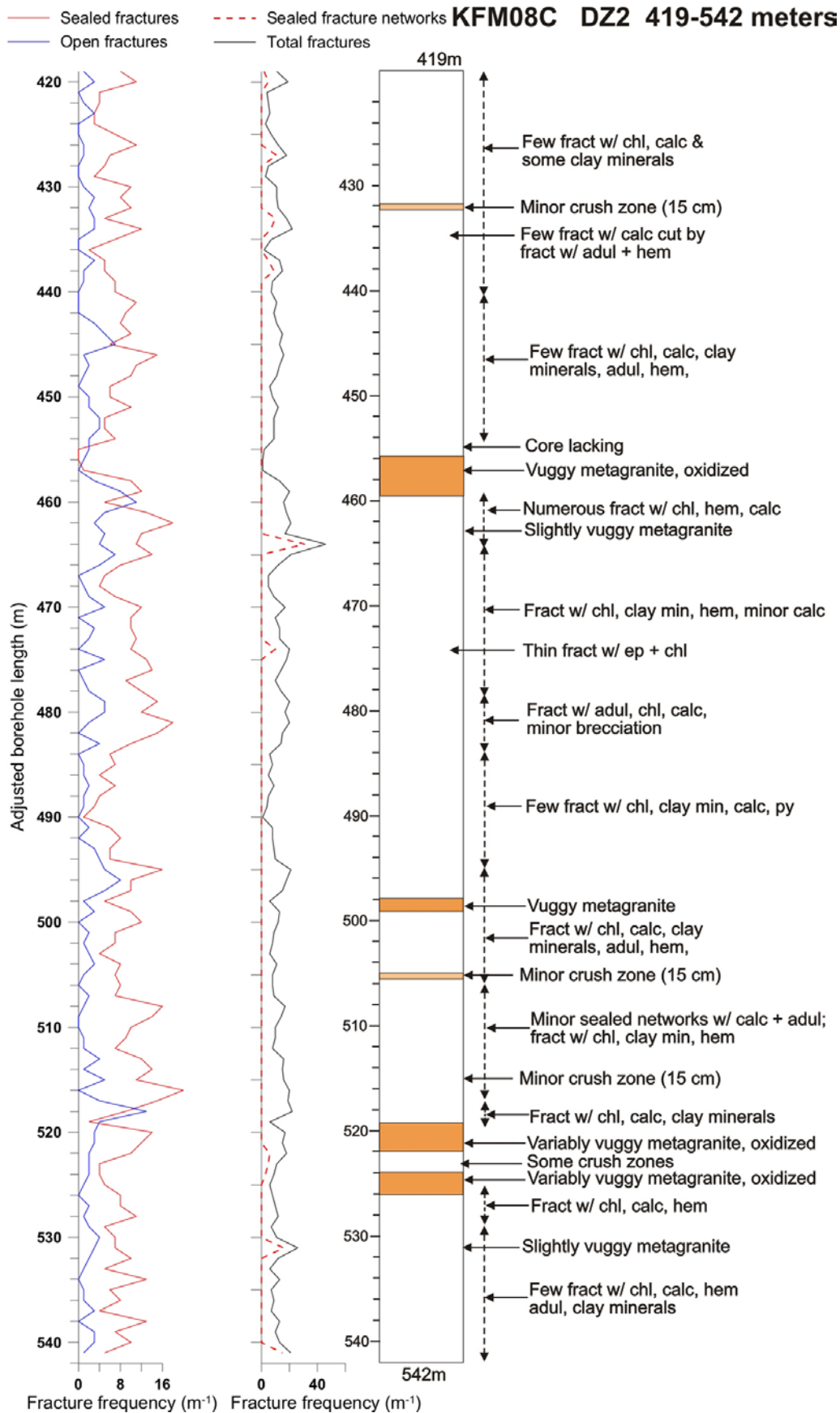


Figure 5-53. Simplified drawing of DZ2 in KFM08C. The fracture frequencies are moderately above the background level and DZ2 is considered a transition zone (Munier et al. 2003). Note that the intervals with vuggy and oxidized rocks do not have elevated fracture frequencies. Abbreviations as in Figure 5-3.

Eight striated faults are distributed along the zone (Figure 5-54). Steep SSW and steep NNW sinistral strike-slip faults are observed. Striations on chlorite and hematite, and calcite steps are the predominant kinematic indicators on these planes (Figure 5-54). One of these faults (strike-dip 216/74) shows striations on chlorite at the border of the fracture (pitch: 3 degrees to the SW) and a later infill with adularia and calcite in the middle of the fracture. A gently NE-dipping fault plane displays reverse oblique slip with calcite steps and grooves on the surface. A less well-defined NE-SW normal dip-slip fault is also recorded along the DZ and is characterised by hematite striations.

KFM08C: 673–705 m – DZ3

The rock types present in this zone are medium-grained metagranite-granodiorite with subordinate occurrences of pegmatitic granite, amphibolite and aplitic metagranite. As in the zones above, fractures are variable in orientation. Steep fractures that strike N-S to E-W are prominent; gently dipping fractures are also present. Fracture filling minerals include chlorite, calcite, clay minerals, adularia, epidote and quartz.

Sealed fractures exhibit a marked peak due to the occurrence of NW-SE thin, epidote-sealed fractures that cut oxidized metagranite in the interval 691–695.7 m (Figure 5-55). These are cut by thin fractures and minor networks sealed with adularia (see photograph in Figure 5-55). The deformation zone is predominantly a transition zone /Munier 2003/ with an interval with some epidote- and adularia-sealed fractures (691–695.7 m) defined as possible fault core.

Two striated faults have been measured along DZ3 in KFM08C (Figure 5-56). One corresponds to a vertical sinistral strike-slip fault trending WNW-ESE. The fault surface displays calcite steps and striations on quartz. The other very flat S-dipping fault has dextral movement shown by a chlorite-striated and calcite-stepped surface.

KFM08C_DZ2_419-542 m
Datasets: 8

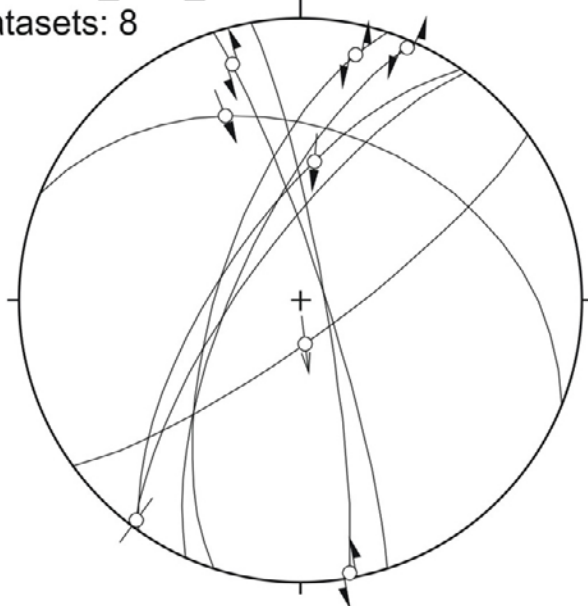


Figure 5-54. Left: Stereoplot of fault slip data in DZ2 (KFM08C). Right: Example of fault surface along DZ2 in KFM08C with sinistral steps of calcite and striations on chlorite (strike/dip angle/pitch: 204/71/-3) (537.19 m).

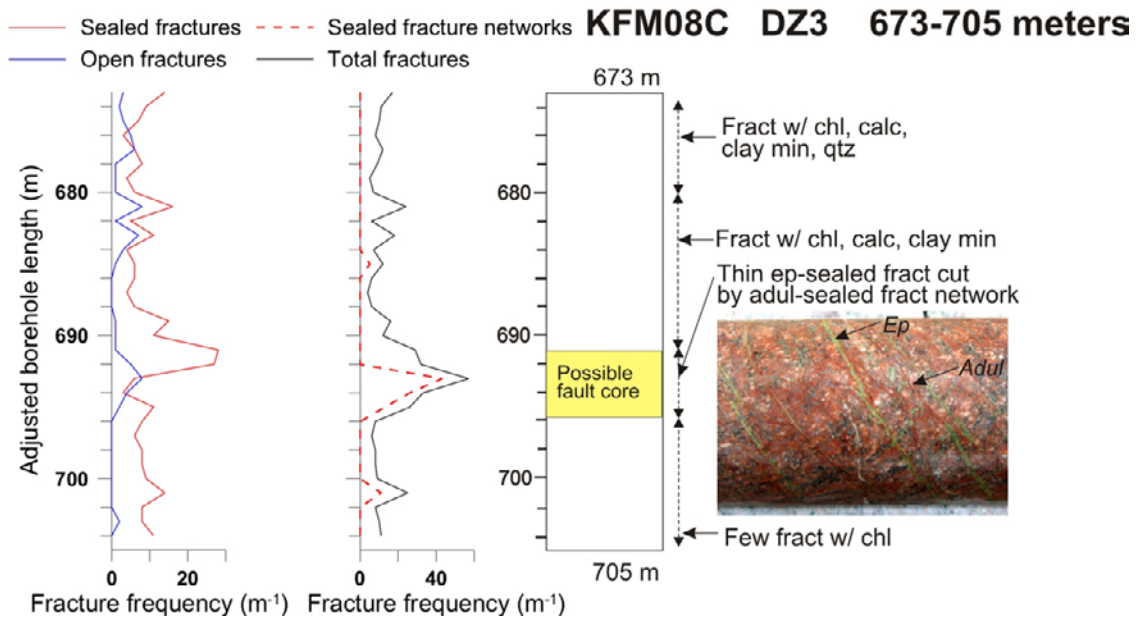


Figure 5-55. Simplified drawing of DZ3. The fracture frequencies are moderately above the background level and DZ3 is predominantly a transition zone according to (Munier et al. 2003/) with a possible fault core defined by an interval with some epidote- and adularia-sealed fractures at 691–695.7 m (see photo inset). Abbreviations as on Figure 5-3.

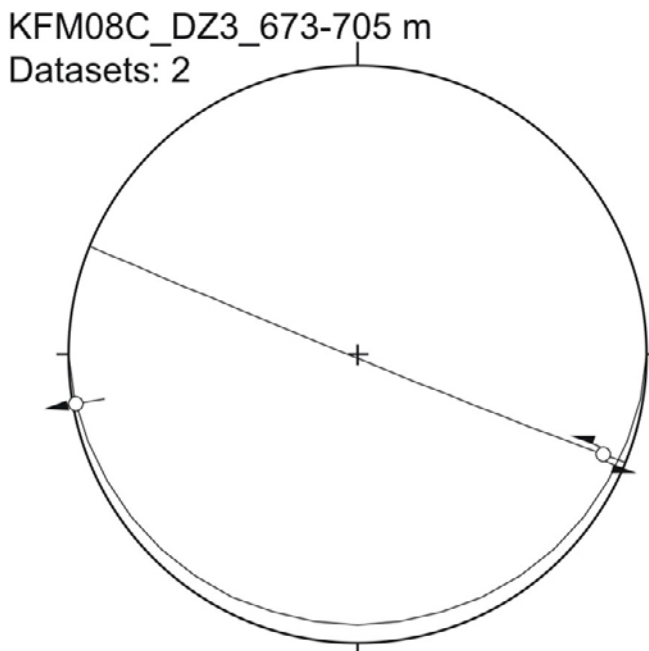


Figure 5-56. Stereoplot of fault slip data in DZ3 (KFM08C).

KFM08C: 829–832 m – DZ4

This is a very short deformation zone transecting slightly oxidized metagranite-granodiorite with subordinate occurrences of amphibolite. Fracture frequencies and orientations are variable. Fracture filling minerals include chlorite, calcite, clay minerals and hematite. A highly fractured zone including a ca 10 cm wide crush zone occurs at ca 830–830.5 m. This interval qualifies as fault core; otherwise DZ4 is a transition zone according to /Munier et al. 2003/.

One fault slip datum has been measured along DZ4 in KFM08C (Figure 5-57). It is a WSW-ENE steep plane displaying highly oblique striations on chlorite, hematite and calcite and with an undetermined sense of shear.

5.1.8 KFM09A

The borehole is 799.7 m long and is oriented 200/59. Five deformation zones /Carlsten et al. 2006a/, with a total length of 169 m were investigated. 46 kinematic data were retrieved from the inspected deformation zones. They are mainly NNW-SSE steep sinistral strike-slip faults (Figure 5-58).

KFM09A: 15–40 m – DZ1

The rocks along DZ1 are medium-grained metagranite-granodiorite with amphibolite until ca 20 m, after which pegmatitic granite is present to the base of the DZ. The brittle deformation in the DZ is characterised by several networks (Figure 5-59) with a complex mineralogy which comprises adularia, chlorite, calcite, laumontite and quartz (Figure 5-60). Brecciation and development of cataclasite and some ultra-cataclasite has occurred locally. The fracture frequency increases around 22–23 m and 30–31 m due to the presence of such networks. Calcite veins cut across the networks and all other brittle structures. Thin chlorite veins cut across hairline adularia veins. Most of the fractures are flat. Some steep fractures are present and preferentially trend ENE-WSW. Relatively few broken fractures are present. The DZ qualifies as a transition zone according to /Munier et al. 2003/.

Four steep strike-slip faults are observed along the upper part of DZ1 in KFM09A. Three of them trend NNW-SSE and one fault trend WSW-ENE (Figure 5-62). The kinematic indicators on the fault surfaces are slickensides on hematite, striae on chlorite and calcite and polished chlorite.

KFM08C_DZ4_829-832 m
Datasets: 1

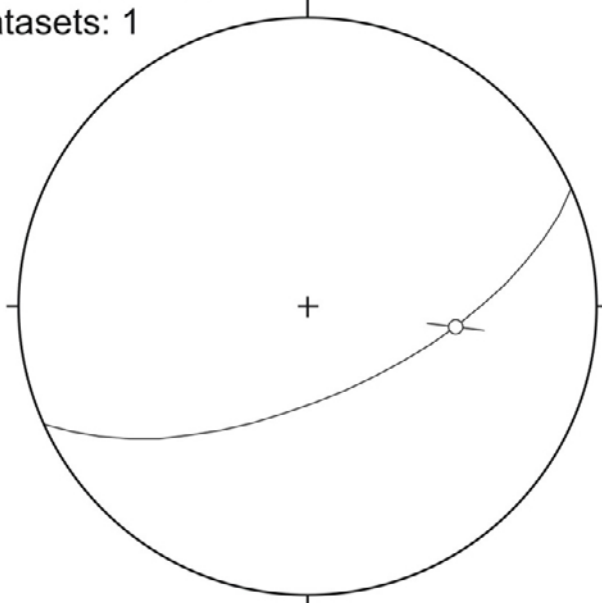


Figure 5-57. Stereoplot of fault slip data in DZ4 (KFM08C).

KFM09A_DZ1_DZ2_DZ3_DZ4_DZ5

Datasets: 46

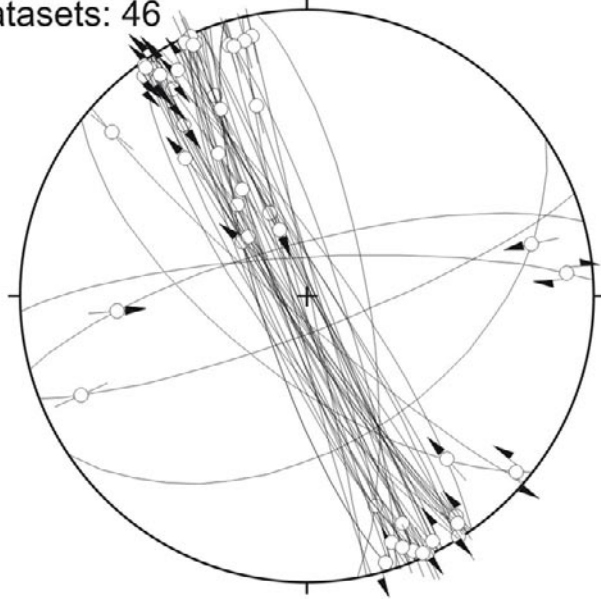


Figure 5-58. Stereoplot showing all the fault slip data collected along all the studied DZ of drill core KFM08C.

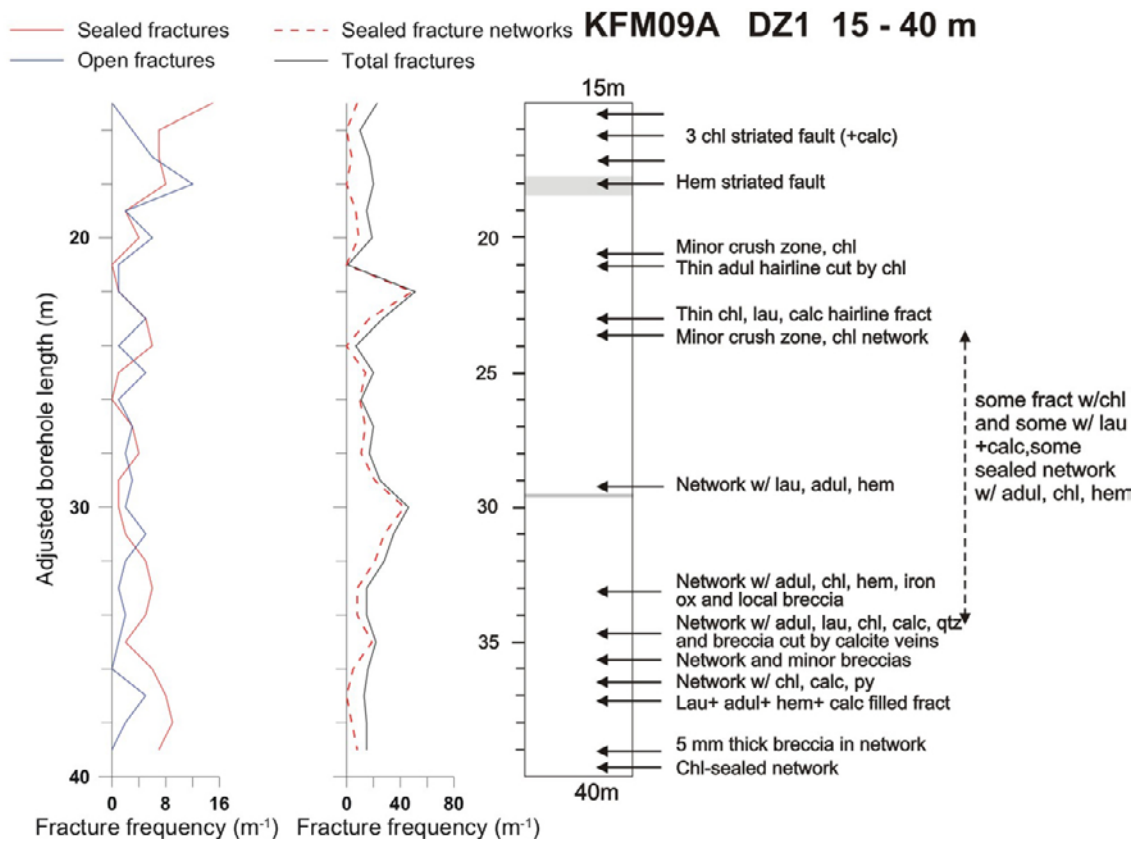


Figure 5-59. Simplified drawing of DZ1 showing brittle structures. Grey fields denote mafic amphibolite. Abbreviations as in Figure 5-3.

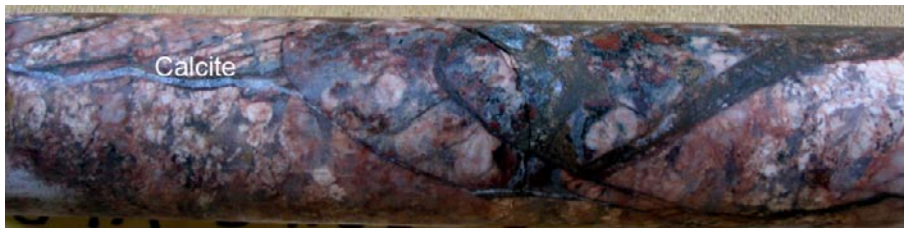


Figure 5-60. Section of drill core cut by fracture network with some brecciation and minor cataclasite. The fractures are sealed with adularia, laumontite, calcite, chlorite, and quartz. A late calcite-sealed vein (marked on the photograph) cuts across older structures (KFM09A, 34.80 m).

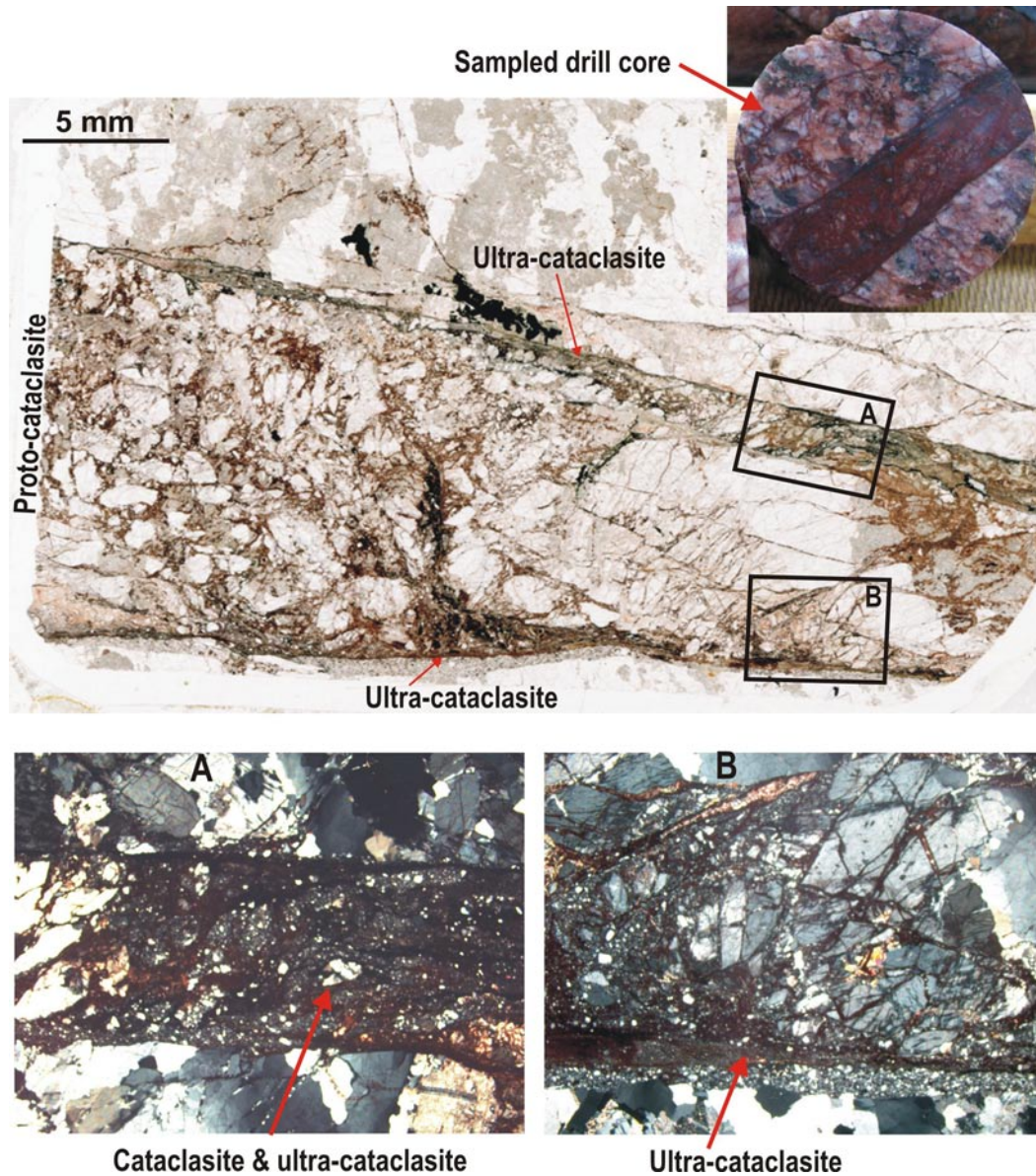


Figure 5-61. Scanned thin section (above) of with inset photograph of sampled drill core KFM09A_33.15 (upper right) showing metagranite cut by a sharply defined cataclasite with adularia, chlorite and hematite. Photomicrographs (A and B below) illustrate textural details of the squares marked A and B on the thin section. The metagranite is cut by a more than 10 mm wide proto-cataclasite with variable degrees of fracturing and grain size reduction. Angular fragments of the metagranite are present in a fine-grained matrix resulting from brittle grain size reduction. Along the boundaries of the proto-cataclasite, there is a distinct, marginal zone of cataclasites and extremely fine-grained ultra-cataclasites that appear to cut across other deformation products. Hematite occurs as a dusty impregnation in the fine-grained deformation products.

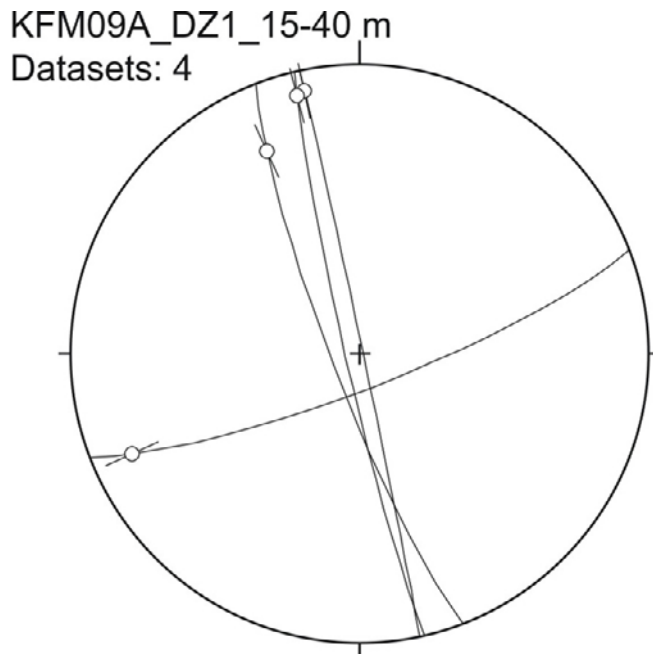


Figure 5-62. Stereoplot of fault slip data in DZ1 (KFM09A).

KFM09A: 86–116 m – DZ2

The rock types along DZ2 in KFM09A is a grey to pink-grey coarse-grained metagranite. The brittle deformation of DZ2 is characterized by a moderate frequency of broken fractures and chlorite-calcite-sealed networks and some quartz veins that predominate at 94–95 m, and a laumontite-calcite network at 109–110 m (Figure 5-63). Local brecciation occurred in the network observed between 94 and 95 m. This deformation is located along a thin amphibolite. Broken grains of altered feldspar occur in a foliated chlorite-rich lithology cut by thin veins filled with quartz and some chlorite (Figure 5-64).

The laumontite and/or calcite-filled veins cut across epidote-filled and chlorite-filled veins. Calcite and laumontite-sealed veins are steep and trend NE-SW and older epidote-filled veins are steep and trend NW-SE (Figure 5-65). However, most of the fractures are flat-lying. In general, the DZ qualifies as a transition zone according to /Munier et al. 2003/.

Two striated faults are present along DZ2 in KFM09A (Figure 5-66). One E-W steep dextral fault has been defined with striae on chlorite and hematite and calcite steps. The other datum is a N-S steep strike-slip fault with striae on hematite and a later coating of calcite and pyrite on the fault surface.

KFM09A: 217–280 m – DZ3

The rock types along DZ3 in KFM09A are coarse pegmatite down to 224 m, after which metagranitoids with occurrences of pegmatite at 237 m, 245.5 m, and 268–273 m, and amphibolite at 247.5 m, 261.5 m and 266.5 m are present.

The predominant fracture sets are laumontite-rich sealed network/veins with more or less calcite, and chlorite- and/or calcite-filled veins (Figure 5-67). Calcite-filled veins, laumontite-sealed veins and laumontite-calcite-filled and brecciated veins are all parallel and strike NE-SW with steep dips (Figure 5-68). Figure 5-69 shows an increase of broken chlorite- and calcite-filled fractures within a crush zone developed in amphibolite and metagranodiorite between 262 and 264.5 m. Quartz veins and epidote veins are also present from 260 to 280 m (Figure 5-70). DZ3 generally qualifies as a transition zone according to the definition of /Munier et al. 2003/. However, the intervals with the most abundant sealed networks and some breccias (230–235 m and 239–242 m), would qualify as fault core.

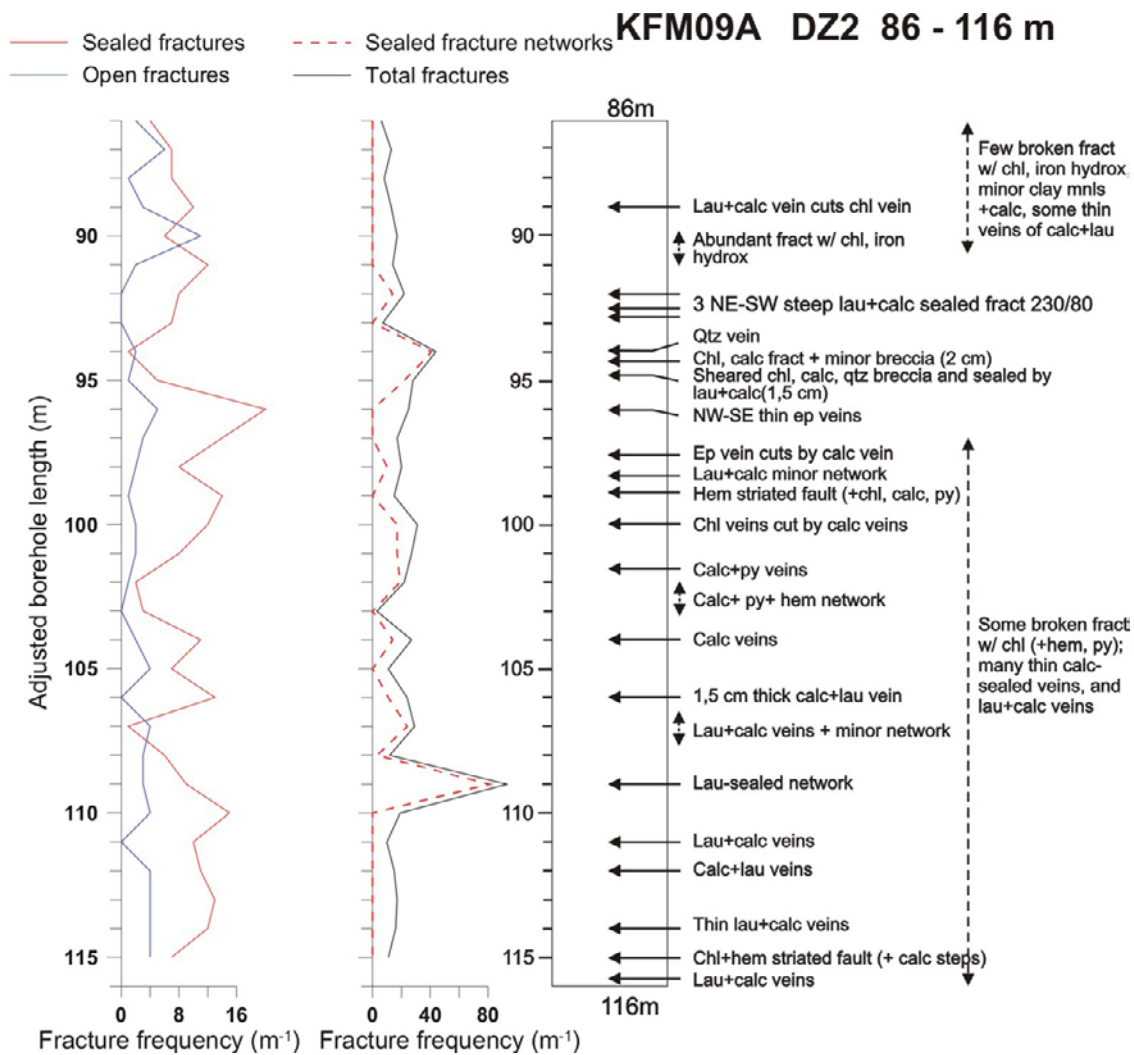


Figure 5-63. Simplified drawing of DZ2 showing brittle structures. Abbreviations as on Figure 5-3.

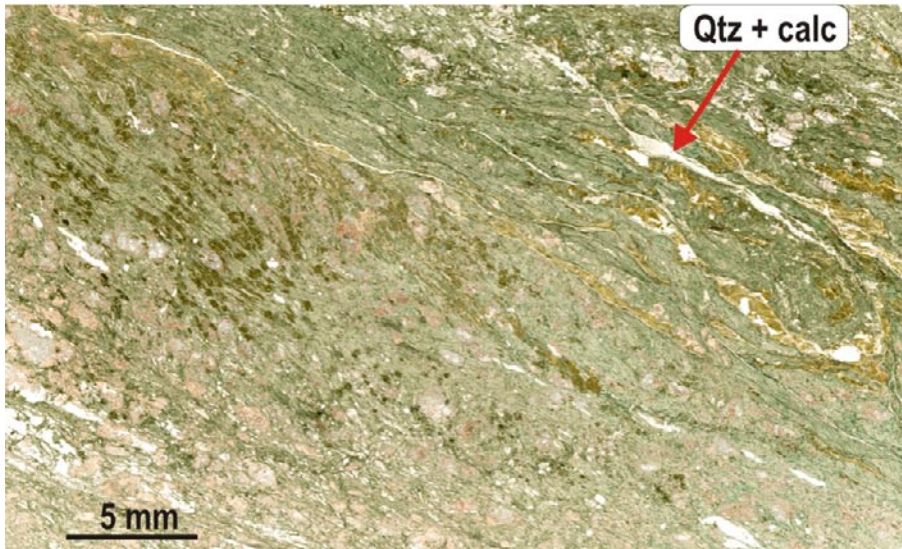
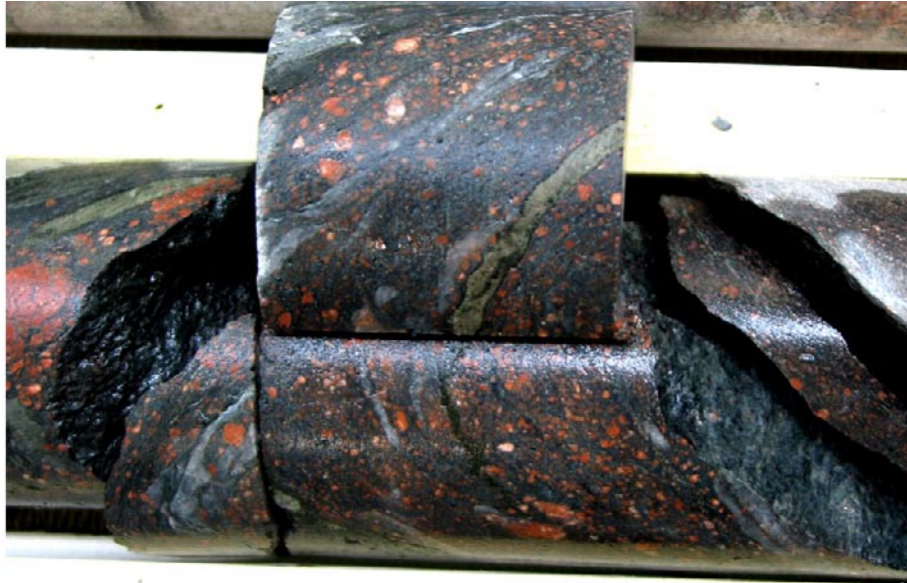


Figure 5-64. Sample KFM09A_94.74 of drill core (above) and scanned thin section (below) show a sheared fault rock with broken grains of altered feldspar in a foliated chlorite-rich lithology cut by thin veins filled with quartz and some calcite.

KFM09A_DZ2_86-116 m
Datasets: 4

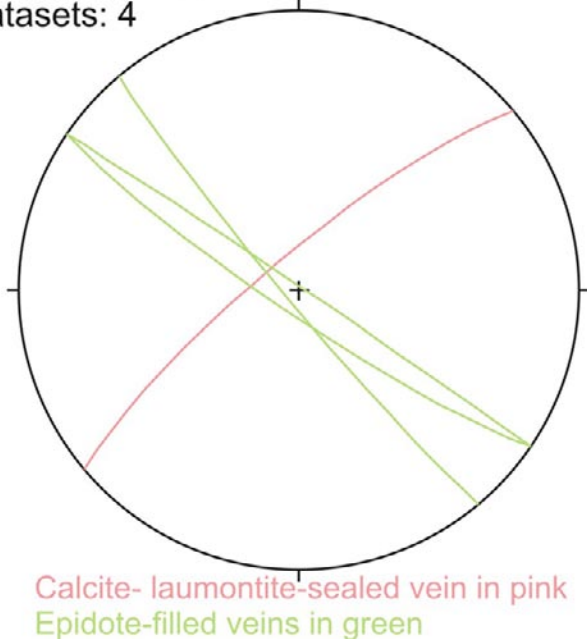


Figure 5-65. Stereonet of the most common steep mineralised fractures observed along DZ2 in KFM09A.

KFM09A_DZ2_86-116 m
Datasets: 2

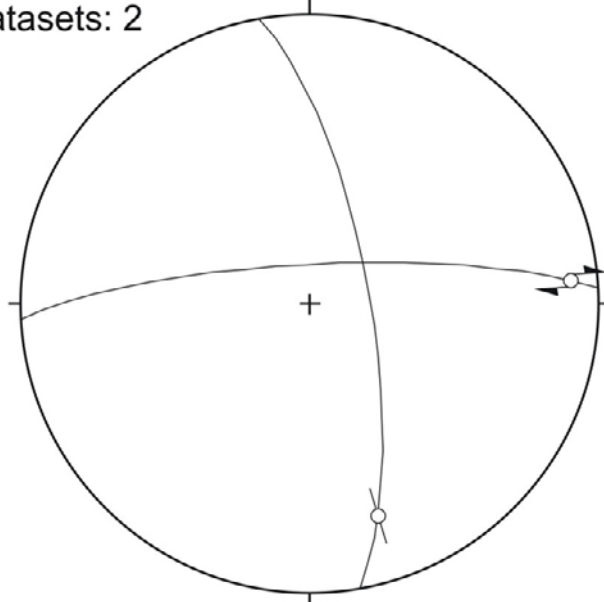


Figure 5-66. Stereoplot of fault slip data in DZ2 (KFM09A).

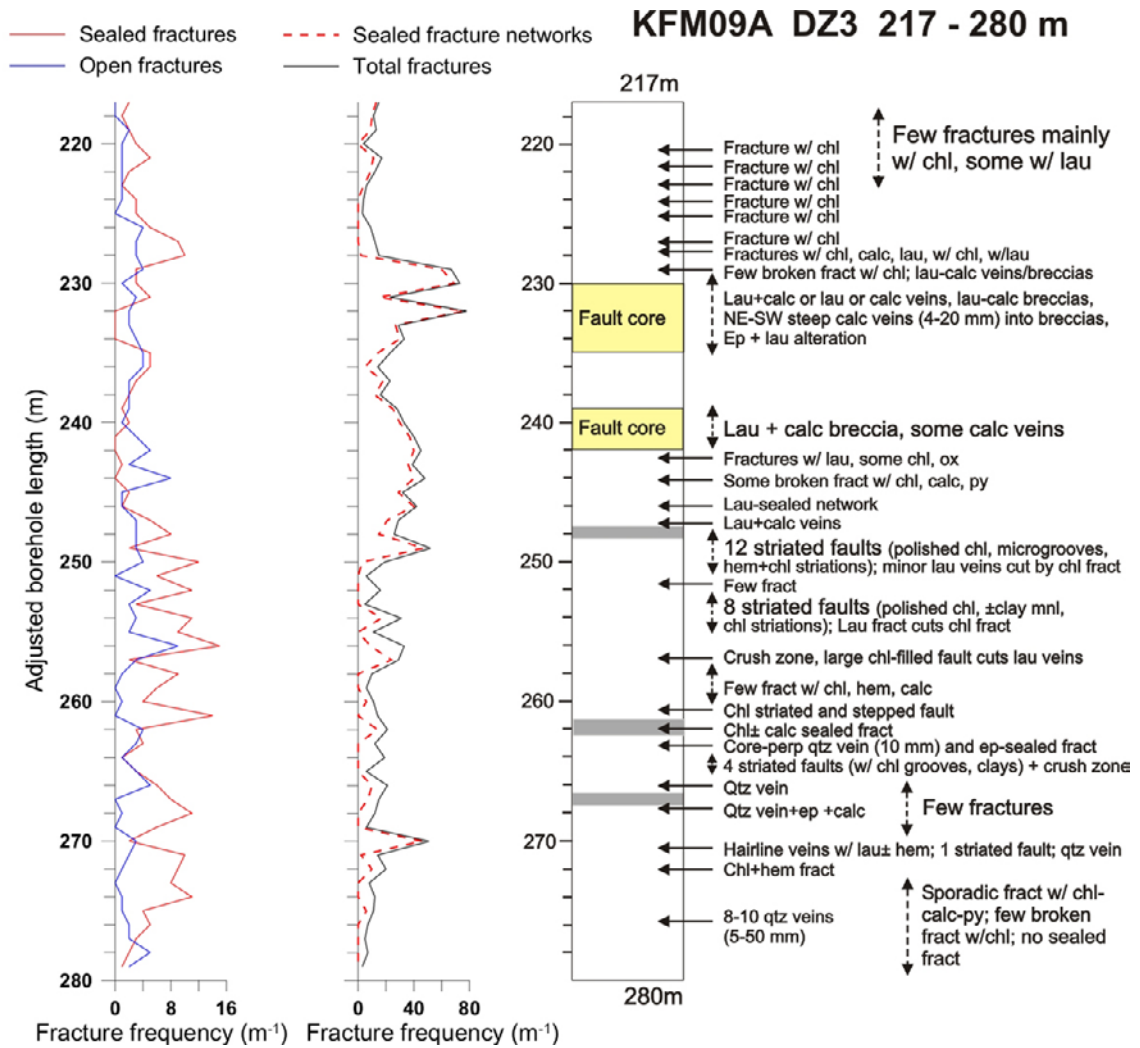
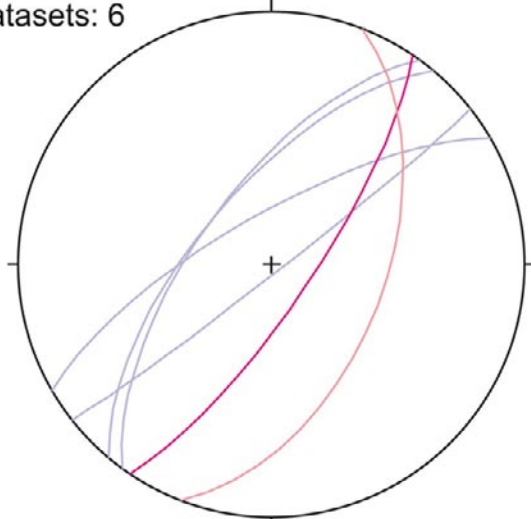


Figure 5-67. Simplified drawing of DZ3 showing brittle structures. Abbreviations as in Figure 5-3. Amphibolites are marked in grey. The intervals with the most abundant sealed networks and some breccias (230–235 m and 239–242 m), would qualify as fault core; otherwise DZ3 is considered a transition zone.

KFM09A_DZ3_217-280 m
 Datasets: 6



Calcite-filled veins in mauve
 Laumontite-sealed vein in pink
 Upper border of a wide laumontite-,
 calcite-filled and brecciated veins in dark pink

Figure 5-68. Trends of laumontite-filled and calcite-filled veins, and the upper border of the laumontite-calcite brecciated zone at 238 m.



Figure 5-69. Increase of broken chlorite-calcite-filled fractures in the interval 262.5–264 m. The rock types are metagranite and some amphibolite.



Figure 5-70. Quartz- and epidote-filled veins and to the right calcite and quartz veins in an amphibolitic part of the drill core.

Twenty-six fault slip data have been measured along DZ3 in KFM09A (Figure 5-71). NNW-SSE steep fault planes with strike-slip shears are the predominant data set (Figure 5-71 and picture A of Figure 5-72). Faults with a sinistral sense of shear have been observed in this set (pictures B and C in Figure 5-72). Some oblique-slip faults with the same trend are also present. One of these planes displays two sets of slips (picture C of Figure 5-72). The fault surfaces show polished and striated chlorite and calcite steps, occasionally striations on clay minerals and on hematite, and grooves on chlorite (Figure 5-72). A gently SE-dipping dextral-reverse fault is also observed and kinematic indicators are calcite steps on a surface of polished chlorite. Striated faults are mainly located in the mafic rocks along the core (amphibolitic and dioritic components).

KFM09A: 723–754 m – DZ4

The rock types along DZ4 in KFM09A are grey metagranodiorite with coarse pegmatite at 725.5–726.3 m, 753–754 m, amphibolite at 727–728 m and 751–752 m, and alternating amphibolite-metagranodiorite at 728–732.5 m and 744–749 m.

The deformation along DZ4 (Figure 5-73) is characterised by a variety of brittle features distributed throughout the zone. Open and sealed fractures are both abundant around 730 m with chlorite-coated fractures cutting the laumontite-sealed networks. Laumontite-calcite-sealed networks occur sporadically at ca 732.5–733.5 m, ca 738–740 m, 741.3 m and ca 743.5–747 m (Figure 5-73), with some minor breccia. An example of such laumontite-sealed breccia occurs from 732 to 733.50 m with a chlorite-laumontite-calcite-pyrite sealed breccia at the upper end of the interval (Figure 5-74). The laumontite-sealed breccia is cut by calcite-sealed veins (Figure 5-74). Another network of laumontite-calcite sealed fractures occurs in the amphibolites at around 744.5 m (Figure 5-75). Other interesting relative chronologies between fractures have been determined in the drill core. A chlorite-striated fault cuts a laumontite-calcite-filled vein at 724.50 m (Figure 5-76). From 740 to 744 m, there are good examples of epidote-filled veins cut by calcite veins. DZ4 qualifies as a transition zone according to the definition of /Munier et al. 2003/.

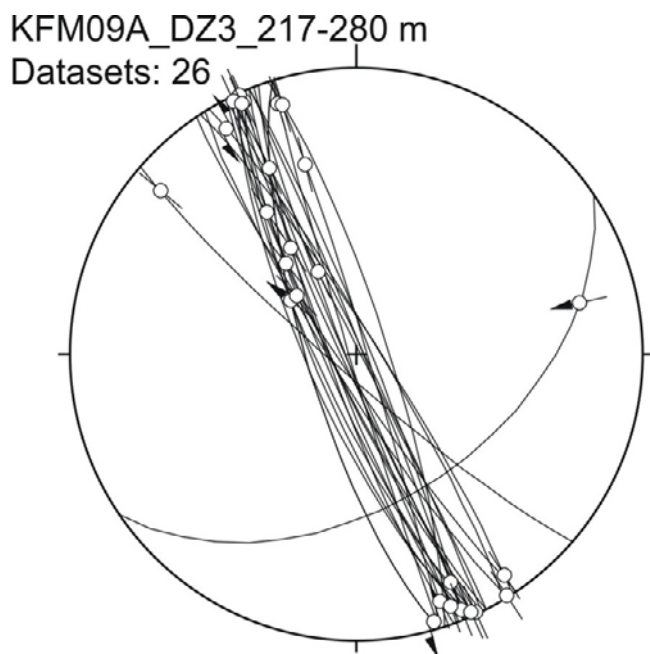


Figure 5-71. Stereoplot of fault slip data in DZ3 (KFM09A).



Figure 5-72. Examples of fault surfaces in KFM09A_DZ3. A. Polished surface with clays and chlorite and grooves, unknown sense of shear (strike/dip angle/pitch: 159/87/7) (265.03 m). B. Sinistral sense of shear with smooth and polished chlorite and clays (strike/dip angle/pitch: 329/84/10) (250.03 m). C. Two shears on the same fault surface: sinistral sense of shear with small steps and polished chlorite and hematite (strike/dip angle/pitch: 163/76/3) and undetermined oblique sense of shear with striae on chlorite and hematite (pitch: -30) (247.53 m).

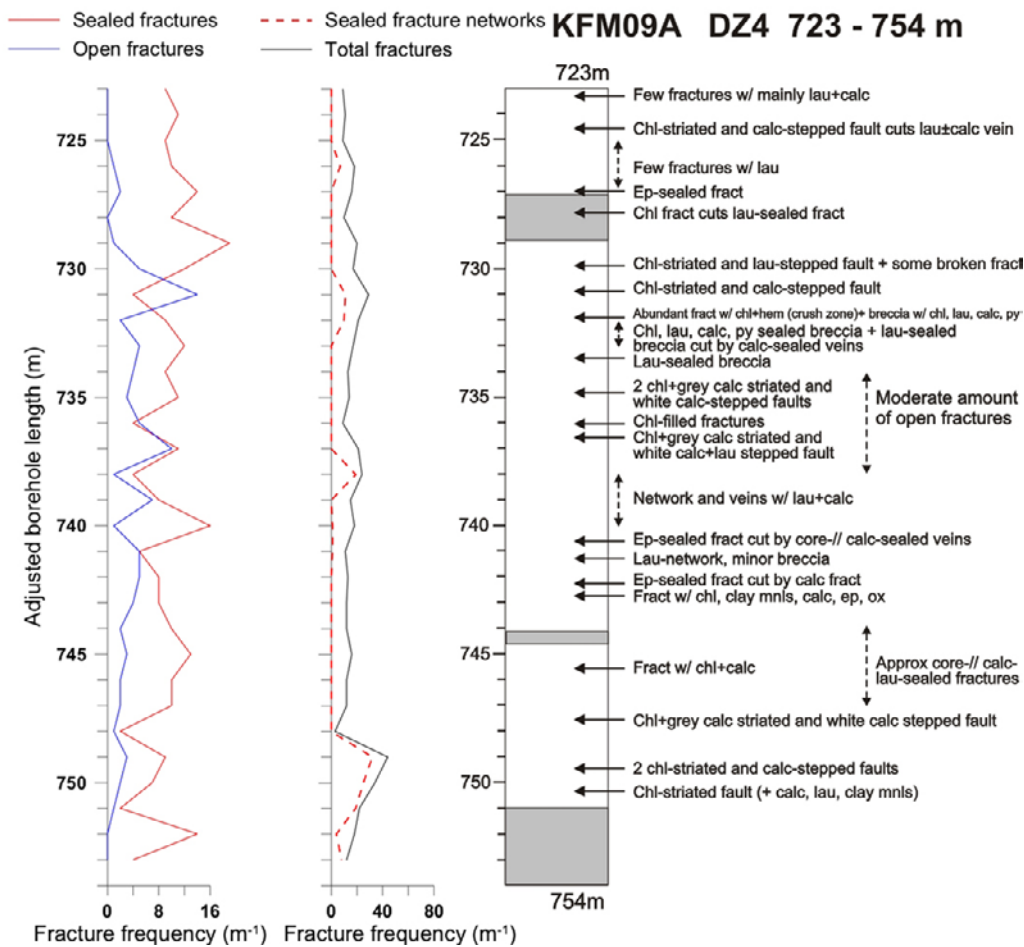


Figure 5-73. Simplified drawing of DZ4 showing brittle structures. Amphibolites are marked in grey. Abbreviations as in Figure 5-3.



Figure 5-74. Left: A chlorite-laumontite-calcite-pyrite-sealed breccia (in green on picture) at the top of a laumontite-sealed breccia (at 732.5 m). Right: calcite-sealed veins cutting the laumontite-rich breccia.

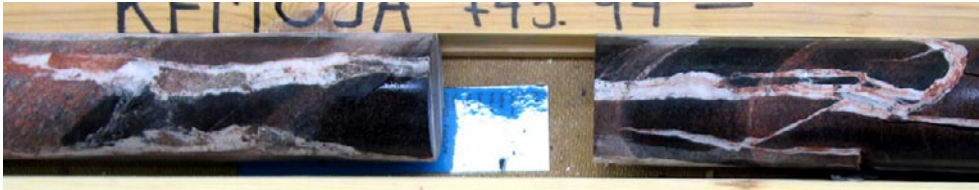


Figure 5-75. Laumontite-calcite sealed fractures at 744 m.

KFM09A_DZ4_723-754 m

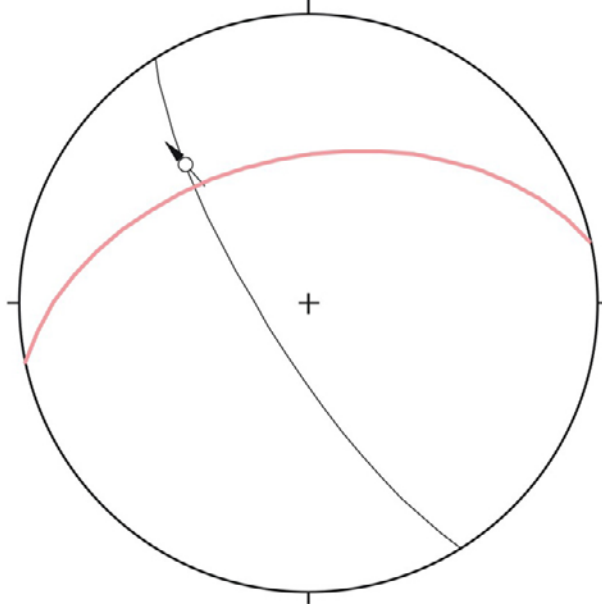


Figure 5-76. A chlorite-striated dextral fault cuts a laumontite-calcite-filled vein at 724.50 m.

Ten fault slip data have been measured along DZ4 in KFM09A (Figure 5-77). Kinematic indicators are well preserved and the sense of shear was confidently determined on all the planes. The faults display striae on chlorite, quartz, grey calcite, and clay minerals, and steps of a white calcite, and also, but less commonly, steps of laumontite (Figure 5-78). The set of NNW-SSE to NW-SE trending sinistral faults is very well represented. An ENE-WSW steep dextral fault is also present (Figure 5-77 and picture B of Figure 5-78).

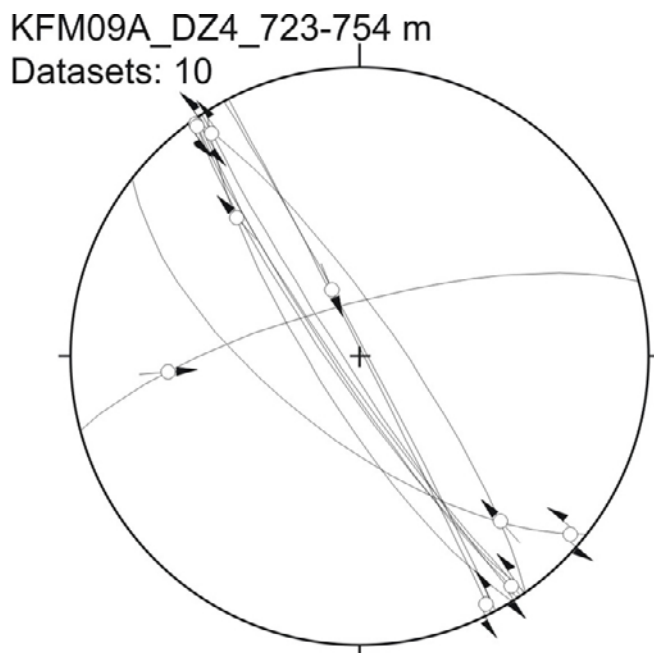


Figure 5-77. Stereoplot of fault slip data in DZ4 (KFM09A).

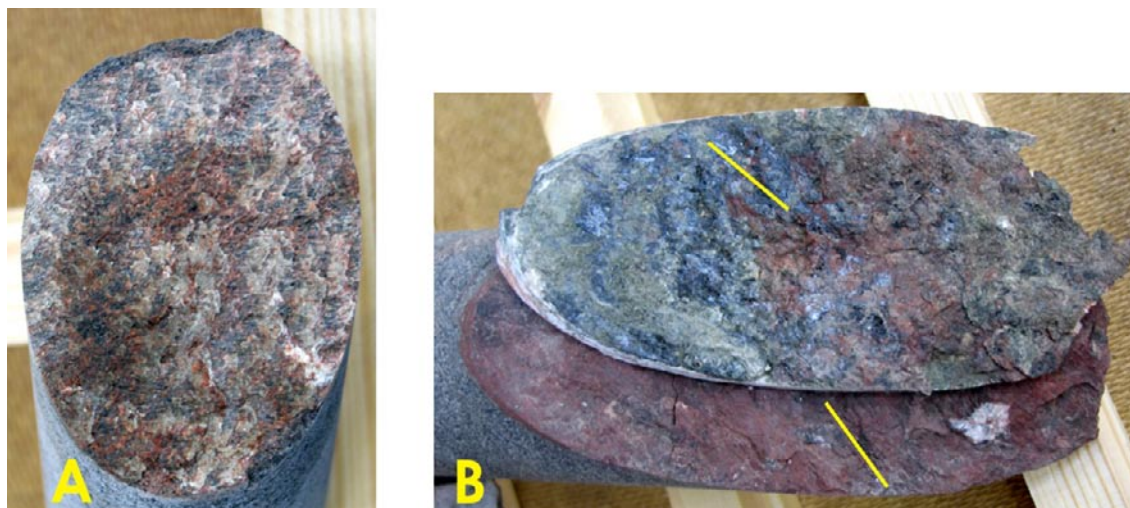


Figure 5-78. Two examples of fault surfaces in KFM09A_DZ4. A. Sinistral steps of white calcite and laumontite, striae on grey calcite and chlorite (strike/dip angle/pitch: 147/86/-8) (736.50 m). B. Oblique dextral reverse striations on chlorite and calcite steps (strike/dip angle/pitch: 255/75/35) (730.92 m).

KFM09A: 770–790 m – DZ5

The rock types along DZ of KFM09A are mainly dark grey foliated fine-grained metagranites. DZ5 shows an increased of fracture density at 775 m (Figure 5-79). At this depth, laumontite hairline fractures cut chlorite fractures. Fractures are coated/filled with calcite, laumontite, chlorite, pyrite, clay minerals, and oxides. They trend NW-SE and are steep or are sub-horizontal. DZ5 qualifies as a transition zone according to the definition of /Munier et al. 2003/.

Four fault slip data are present along DZ5 in KFM09A (Figure 5-80). They form a consistent set of NW-SE trending sinistral faults. Striations are on chlorite and clay minerals and calcite steps allow unambiguous determination of the sense of shear.

5.1.9 KFM09B

This borehole is located in the northwest part of the investigation area (Figure 5-1). The borehole is oriented 141/55 and has a length of 616.5 m /Carlsten et al. 2006d/. Four deformation zones were investigated with a combined length of 216 m (Table 5-1).

A total of 15 fault slip data were obtained from the investigated deformation zones along the drill core (Figure 5-81). NNW-SSE sinistral faults are predominant but some dextral slip has been also determined along the same fault trend. Some steep strike-slip WSW-ENE oriented faults are also present with one dextral slip observed. The latter fault may form a conjugate system with the sinistral NNW-SSE faults.

KFM09B: 9–132 m – DZ1

This deformation zone transects 121 m of medium- to fine-grained metagranite and some amphibolite. The zone is characterized by an increased frequency of open, predominantly gently dipping fractures as well as sealed fractures and fracture networks that are gently dipping, steeply dipping with mainly SW strike, and steeply WSW-dipping. The central part of the zone (ca 43–106 m) has a notably lower fracture frequency than the upper and lower parts of the zone (Figure 5-82). Fracture minerals are calcite, chlorite, laumontite, hematite, clay minerals, prehnite and asphalite.

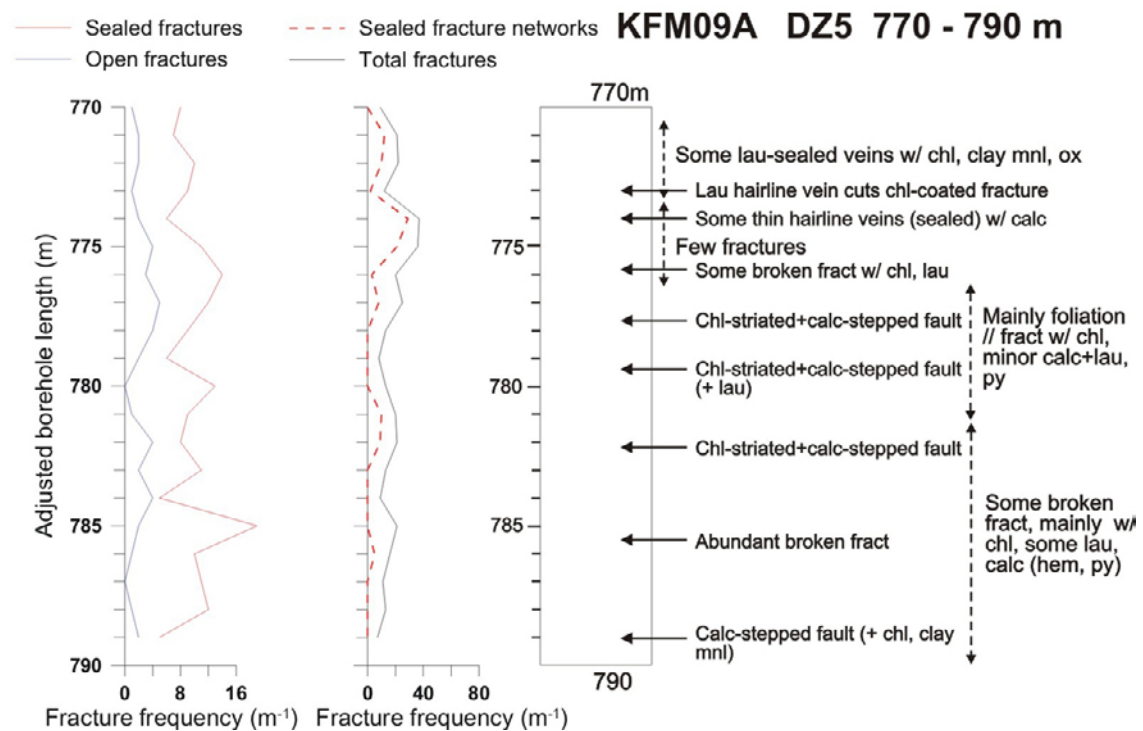


Figure 5-79. Simplified drawing of DZ5 showing brittle structures. Abbreviations as in Figure 5-3.

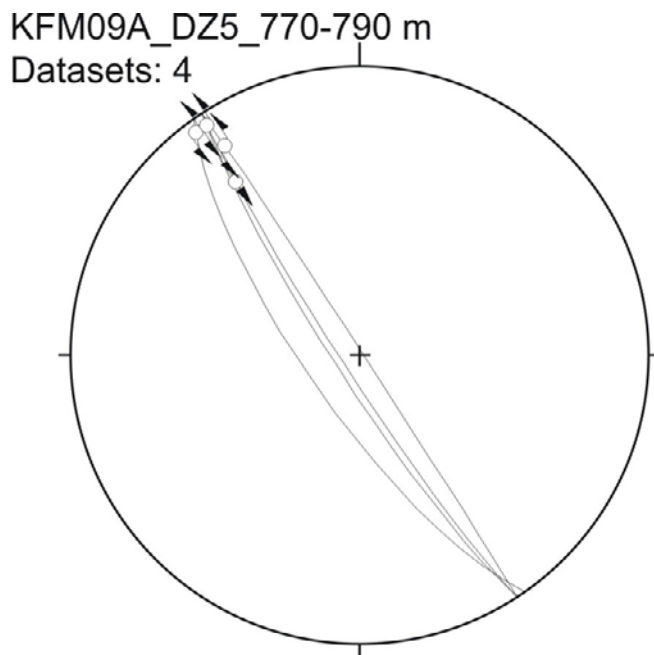


Figure 5-80. Stereoplot of fault slip data in DZ5 (KFM09A).

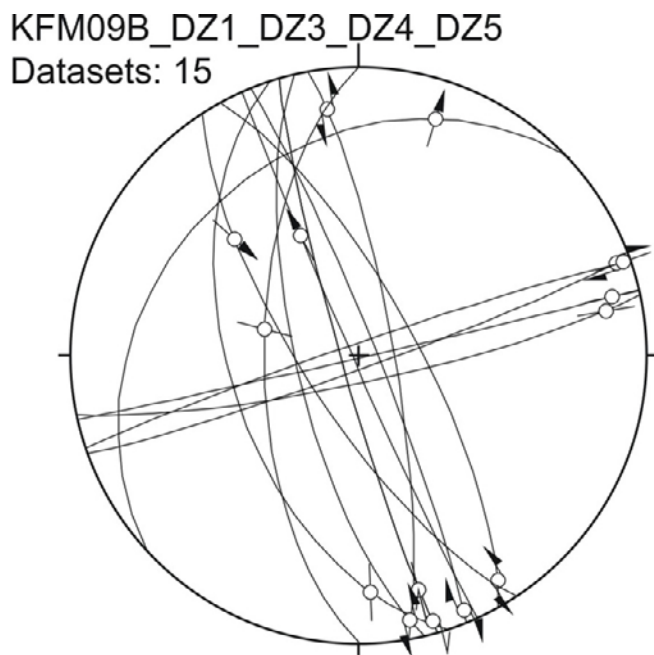


Figure 5-81. Stereoplot showing all the fault slip data collected along all the studied DZ of drill-core KFM09B.

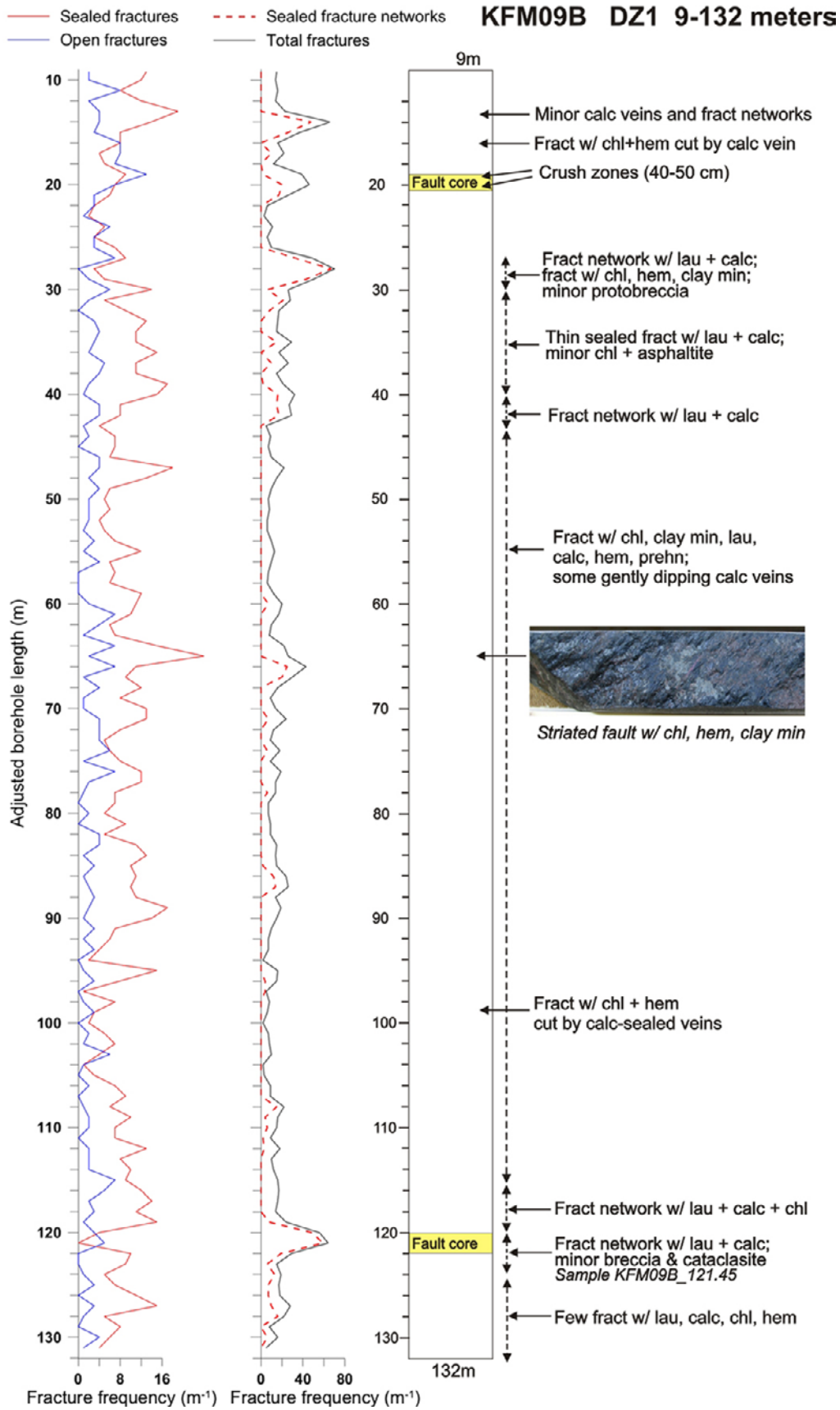


Figure 5-82. Simplified drawing of KFM09B, DZ1, showing the occurrences of the most significant brittle deformation features. One interval with crush zones (19–20.5 m) and one interval with abundant sealed fractures networks are defined as fault core according to /Munier et al. 2003/. Abbreviations as in Figure 5-3.

In the interval 14–17 m, WSW-striking calcite veins post-date fractures sealed with chlorite + hematite. At 19–20.5 m, two crush zones (ca 4–50 cm) are present with chlorite, hematite and calcite. This interval is defined as fault core according to /Munier et al. 2003/.

At 27–30 m, several deformation products occur, including thin fractures and networks sealed with laumontite + calcite. At ca 27.5 m, the drill core shows some hematite alteration, fractures are coated with chlorite, clay minerals and hematite, and there are some breccias sealed with chlorite + calcite + laumontite (Figure 5-83). A local increase in fractures sealed with calcite + laumontite also occurs at 40–42 m.

In the central interval (43–106 m), there is a reduced frequency of fractures with chlorite, clay minerals, laumontite, calcite, hematite, and prehnite. Some gently-dipping calcite veins are present. Together with a second set of WSW-ENE steep calcite veins, they cut across all other brittle structures (Figure 5-85). Rare occurrences of minor sealed network (laumontite) and thin proto-breccias also occur. Some of the faults in this interval are striated (Figure 5-88B).



Figure 5-83. KFM09B_27.5 m. The drill core shows some hematite alteration, fractures are coated with chlorite, clay minerals and hematite, and there are some breccias sealed with chlorite + calcite + laumontite.

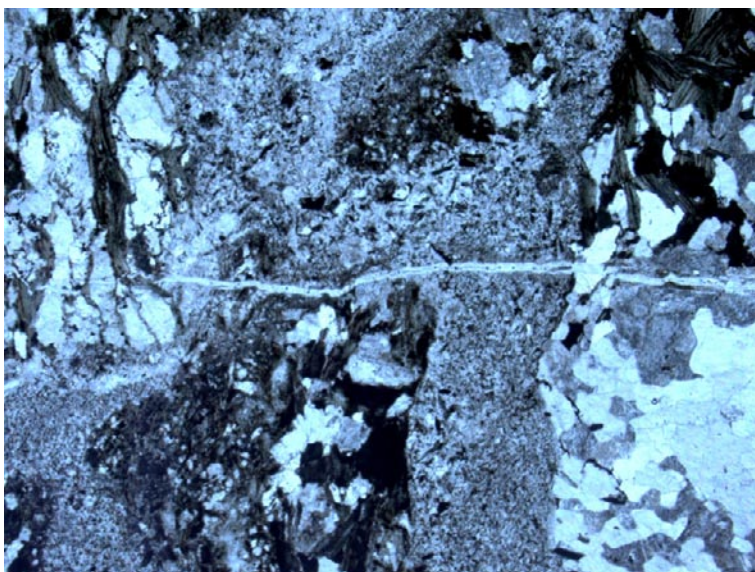


Figure 5-84. Photomicrograph of sample KFM09B_121.45 showing fine-grained cataclasite with fragments of foliated metagranite. A thin vein filled with prehnite cuts across the cataclasite. The field of view is 4.5 mm wide.

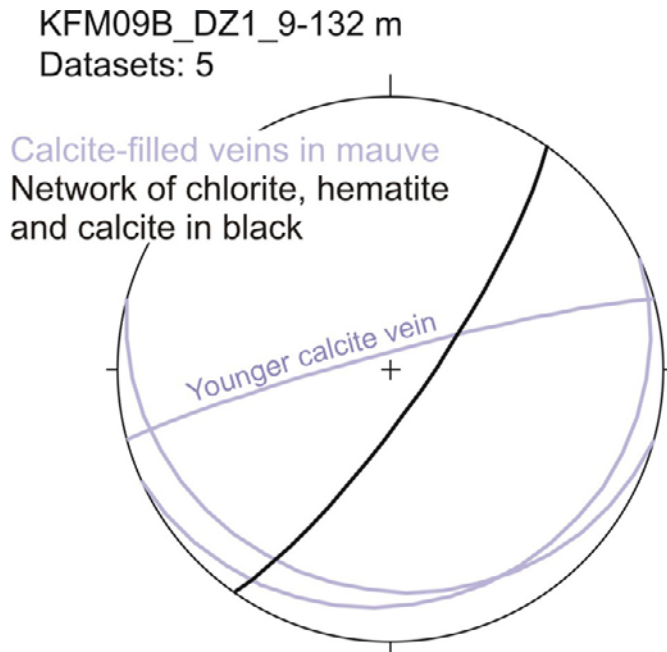


Figure 5-85. The WSW-ENE steep and the flat-lying calcite veins cut across all other brittle structures.

The lower part of the zone shows a return to higher fracture frequencies with the main fractures and fracture networks being sealed with predominantly laumontite and calcite. Sealed networks with some breccia and cataclasite are fairly abundant at ca 120–122 m, and this interval is defined as fault core according to /Munier et al. 2003/. At 121.45 m, there is an occurrence of breccia and cataclasite (Figure 5-86). A photomicrograph from sample KFM09B_121.45 (Figure 5-84) shows an example of fine-grained cataclasite with fragments of foliated metagranite.

Generally, the intervals with abundant, mainly sealed fractures are considered transition zones with subordinate, locally developed fault core at 19–20.5 m and at 120–122 m. In the central part of DZ3, the brittle deformation features are only slightly above the background level and have the character of a transition zone according to /Munier et al. 2003/.

Five striated faults are present along DZ1 in KFM09B (Figure 5-87). They correspond to steep strike-slip faults trending NNW-SSE. Striations are on chlorite, hematite, clay minerals and calcite. Calcite steps define one sinistral and two dextral senses of shear on three of the fault surfaces (pictures A and B of Figure 5-88 as examples). It follows from this inconsistency that different stress regimes have been active during geological time along the NNW-SSE faults.

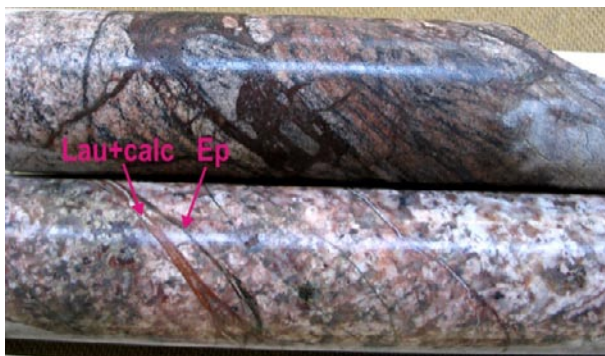


Figure 5-86. Photo of drill core sections from ca 121 m. In the drill core section above, a laumontite-rich cataclasite fills the space in a brecciated part of the core (sample KFM09B_121.45). Below, the metagranite contains thin fractures sealed with epidote that are cut by veins sealed with reddish laumontite and white calcite.

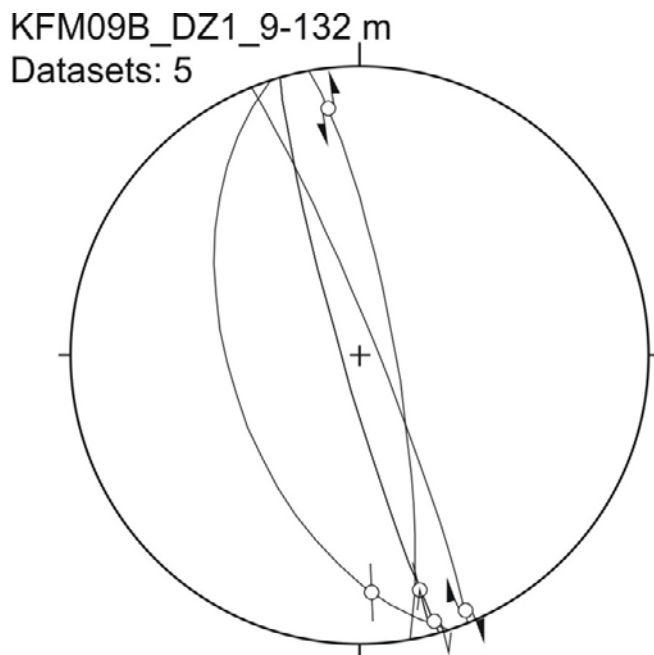


Figure 5-87. Stereoplot of fault slip data in DZ1 (KFM09B).

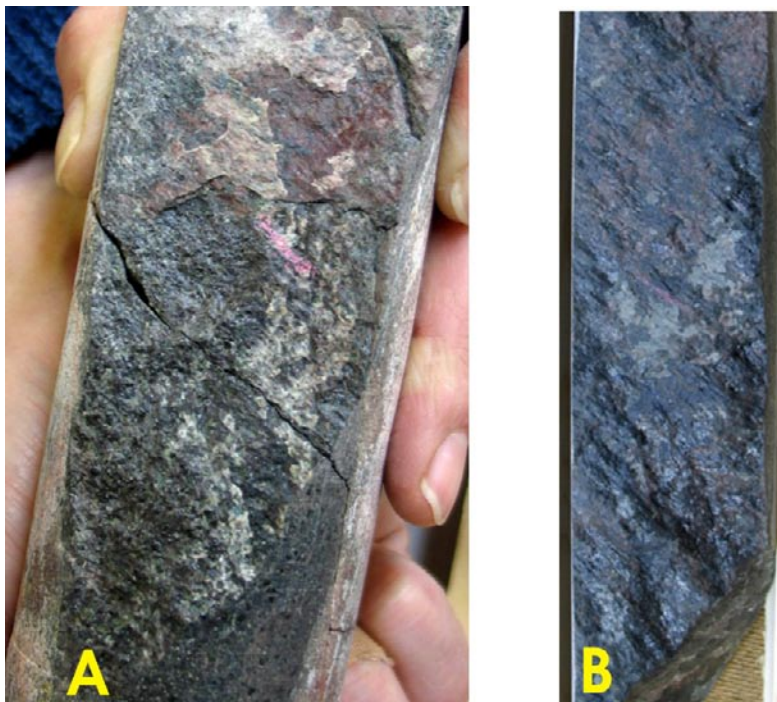


Figure 5-88. Two examples of fault planes along DZ1 in KFM09B. A. Sinistral calcite steps and striations on hematite (strike/dip angle/pitch: 350/80/15) (20.035 m). B. Dextral striations on chlorite, hematite, clay mineral (strike/dip angle/pitch: 338/85/-5) (65.043 m).

KFM09B: 363–413 m – DZ3

Deformation zone DZ3 occurs in medium-grained metagranite-granodiorite with minor occurrences of pegmatitic granite and amphibolite. It is characterized by an increased frequency of sealed and open fractures and sporadic sealed fracture networks (Figure 5-89). Prominent brittle deformation features are NE-striking fractures with steep dips and gently dipping fractures with variable, but mainly NW dips. Fracture filling minerals include chlorite, calcite, laumontite, clay minerals, hematite and pyrite.

The highest fracture frequencies in the zone are related to intervals with fracture networks sealed with laumontite and less abundant calcite. Some fault breccias are associated with the sealed networks, including a 40 cm wide zone at ca 391 m (see photo inset in Figure 5-89). Cross-cutting relationships between different fracture sets were observed in several places. At ca 372 m, laumontite-sealed fractures cut a chlorite-coated fracture. Calcite-filled veins cut fractures with chlorite + laumontite ± hematite at 377.4 and 408.6 m.

A 10 mm wide cataclasite occurs in the lower part of a thin amphibolite at ca 402 m (Figure 5-90). A scanned thin section and a photomicrograph shows angular fragments of the host rock in the cataclasite, whereas reddish brown ultra-cataclasite post-dates the cataclasite (Figure 5-90). At ca 406 m, a fracture network sealed with laumontite and calcite cuts an epidote-altered zone with thin quartz veins (Figure 5-91).

DZ3 is generally a transition zone according to the definition of /Munier et al. 2003/. The 40 cm wide sealed fault breccia that occurs at ca 390.5 m (see photo) constitutes a minor interval of fault core.

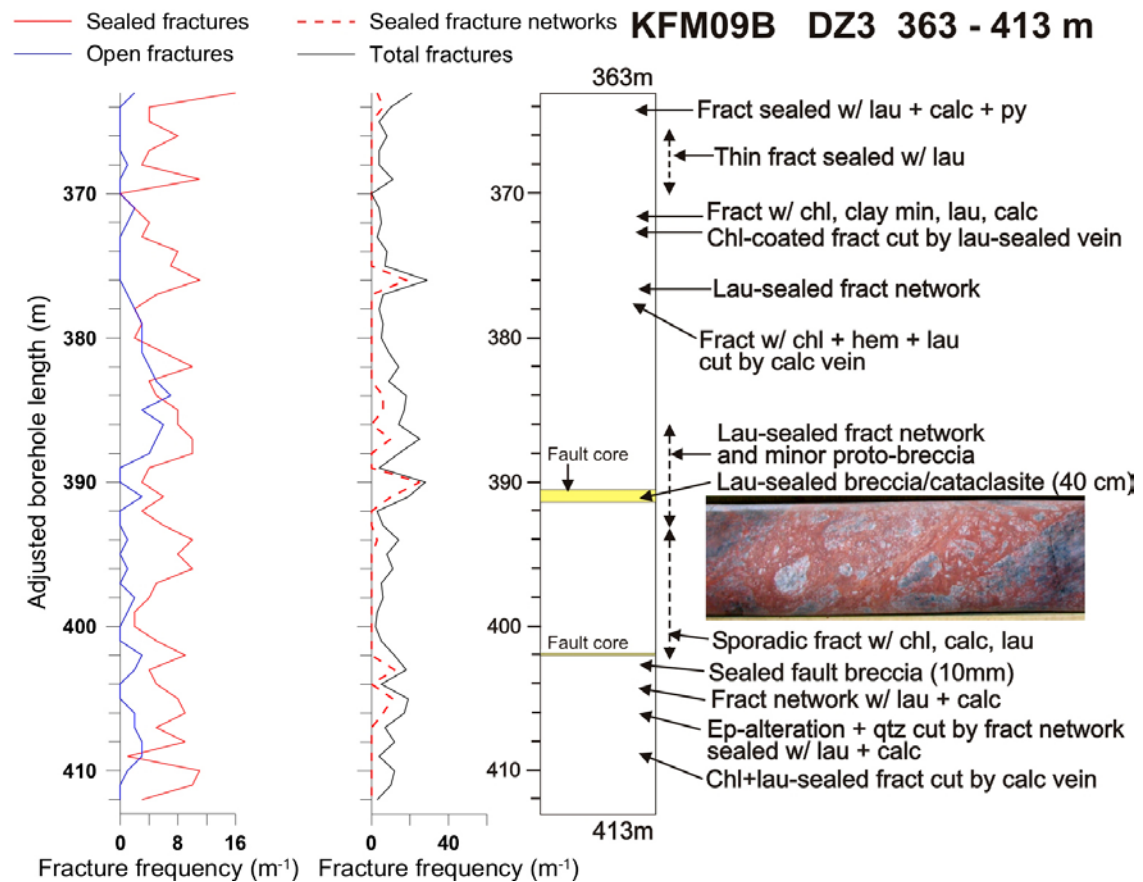


Figure 5-89. Simplified drawing of KFM09B, DZ3, showing the occurrences of the most significant brittle deformation features. A 40 cm wide sealed fault breccia that occurs at ca 390.5 m (see photo) constitutes a minor interval of fault core; otherwise DZ3 is a transition zone /Munier et al. 2003/. Abbreviations as in Figure 5-3.

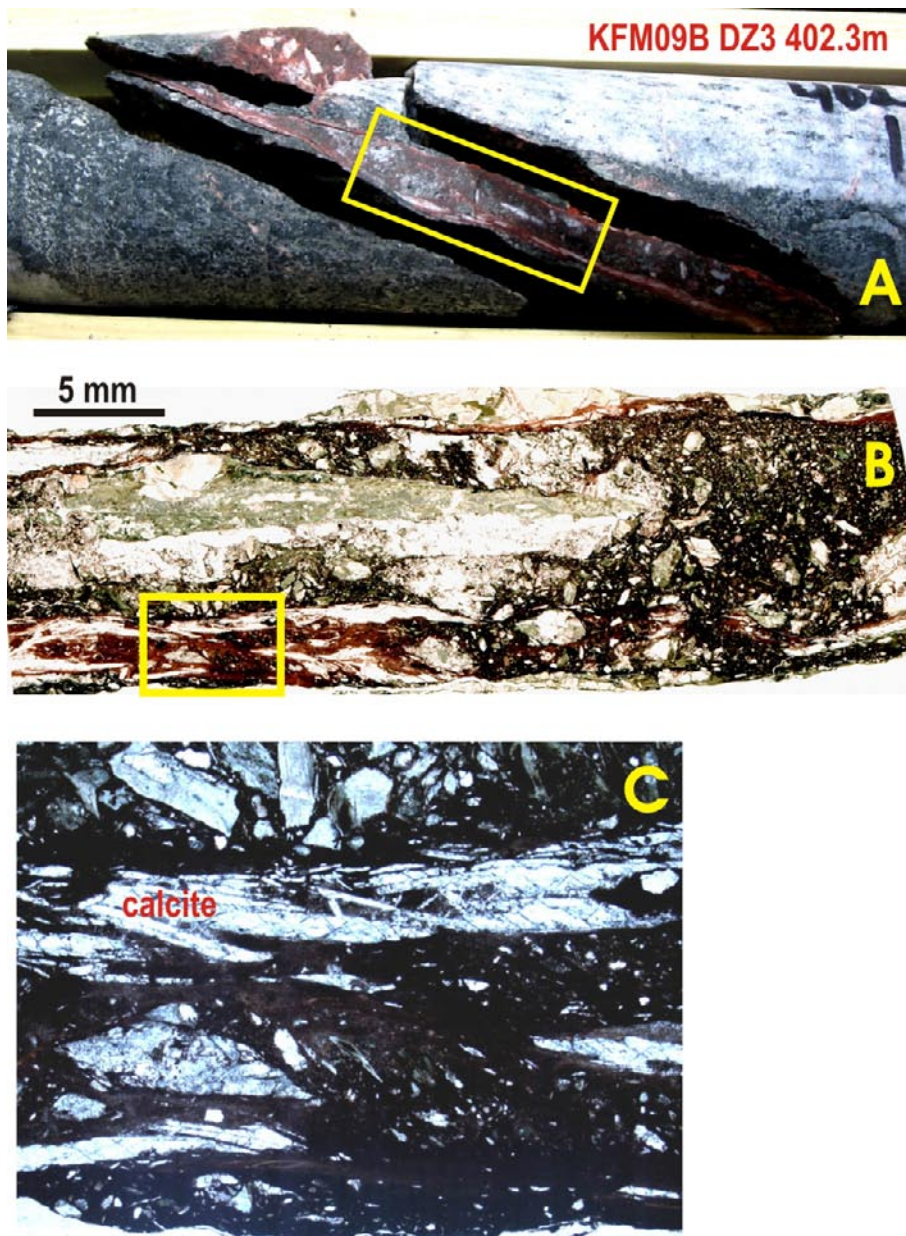


Figure 5-90. *A: Photo of drill core showing a ca 10 mm wide cataclasite. The fault rock (framed) was sampled for thin section (KFM09B_402.3). B: Scanned thin section of the fault rock shown in A. Dark cataclasite contains variably sized, angular fragments of the host rock. The reddish brown and extremely fine-grained rock is an ultra-cataclasite which appears to post-date the cataclasite. C: Photomicrograph showing the extremely fine-grained ultra-cataclasite and a small part of the cataclasite with host rock fragments in the upper part of the photograph. Euhedral blade-shaped calcite post-dates the development of the fault rocks.*



Figure 5-91. Photo of the drill core at ca 406 m showing an epidote-altered zone with quartz cut by a network of WSW-ENE steep fractures sealed with laumontite and calcite.

Four striated strike-slip faults have been observed along DZ3 in KFM09B (Figure 5-92). Striations are on chlorite, hematite, calcite and later calcite, pyrite and laumontite crystallized on the fault surfaces. Sinistral slip was determined on a NW-SE steep fault. Two strike-slip faults are striking WSW-ENE. Their sense of shear was not determined. A gently NW-dipping dextral normal fault is also observed along DZ3 with striae plunging to the north.

KFM09B: 520–550 m – DZ4

Deformation zone DZ4 occur in and medium-grained metagranite-granodiorite with notable intervals of pegmatite and subordinate occurrences of amphibolite.

The major part of the zone exhibits an increased frequency of sealed and open fractures and sealed fracture networks (Figure 5-93). Gently dipping fractures are rare.

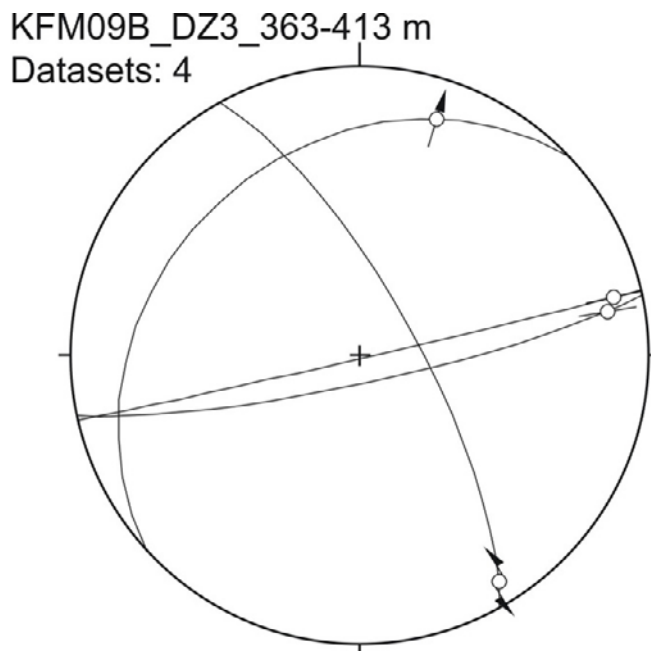


Figure 5-92. Stereoplot of fault slip data in DZ3 (KFM09B).

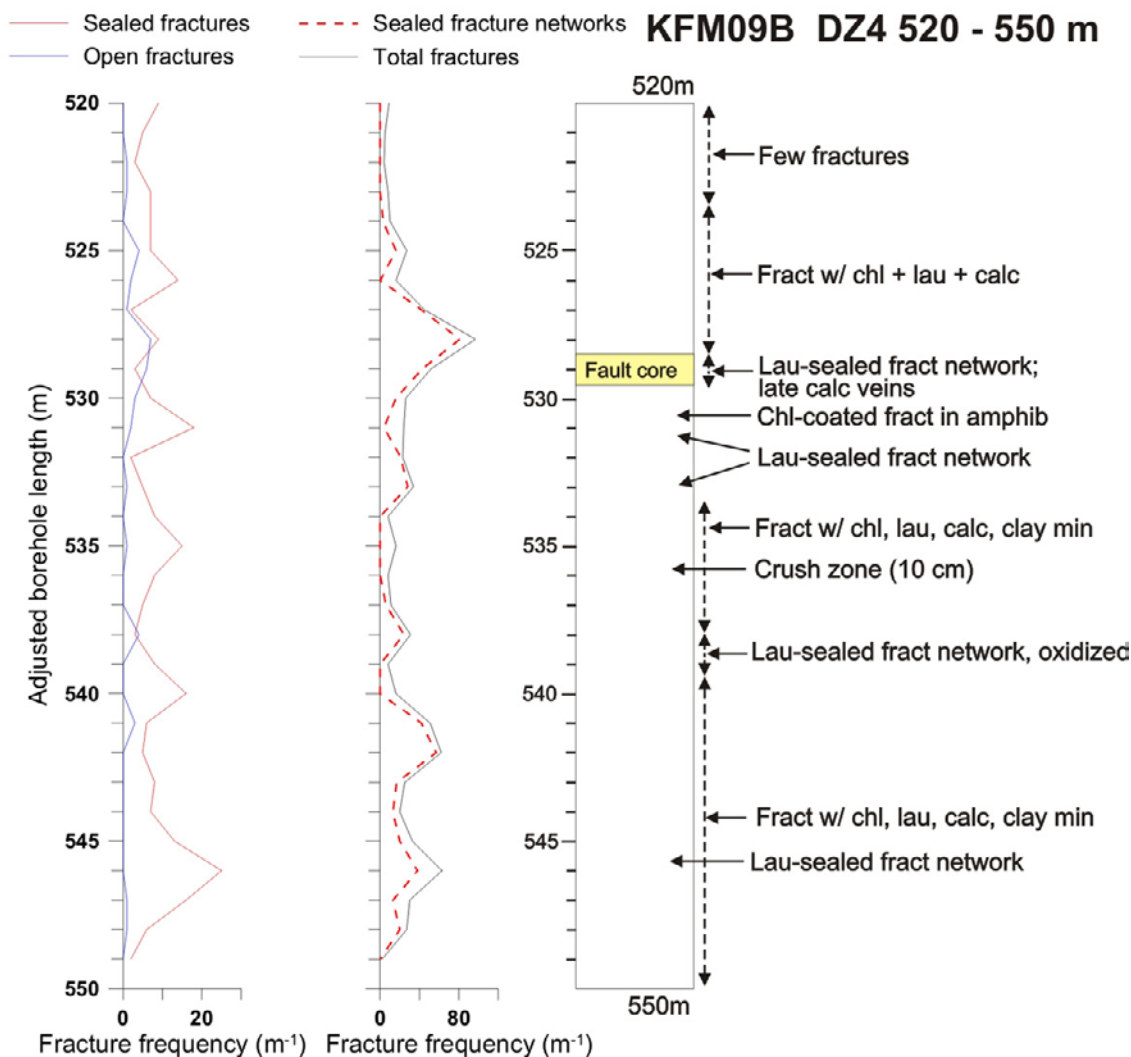


Figure 5-93. Simplified drawing of KFM09B, DZ4, showing the occurrences of the most significant brittle deformation features. The interval 528.5–529.5 m contains sealed fracture networks and and/or breccias and is considered fault core according to /Munier et al. 2003/. Abbreviations as in Figure 5-3.

Steeply dipping fractures with a strike that varies from NNW to EW are present.

The main fracture filling minerals are chlorite, calcite, laumontite and hematite.

The highest fracture frequencies are present where there are crush zones and fracture networks sealed with laumontite and calcite (Figure 5-93). Late calcite veins (< 10 mm) are present in places. Local proto-breccia is also present, e.g. at 529.0 m (Figure 5-94). A thin section collected from this lithology shows early brittle fracturing and cataclasis followed by cementation with laumontite and growth of calcite (Figure 5-95).

The fracture frequency /Carlsten et al. 2006d/ and brittle deformation features shows that DZ4 is a transition zone (/Munier et al. 2003/) with a short interval of fault core associated with sealed fracture networks and and/or breccias at 528.5–529.5 m.

Kinematic data were obtained from five faults (Figure 5-96). Striations are on chlorite, hematite, and calcite. The sense of shear was confidently determined using well-formed calcite steps. The following faults sets are present: (1) a WSW-ENE steep dextral strike-slip fault and a NNW-SSE steep sinistral strike-slip fault that may form a conjugate system of strike-slip faults, and (2) two steep NNW-SSE faults displaying highly oblique striae with opposite senses of movement (sinistral and dextral slips with pitches of 43 and 52 degrees to the NNW, respectively). A N-S steep dip-slip fault with unknown sense of shear is also present along DZ4.



Figure 5-94. Laumontite-sealed network and proto-breccia. Sample KFM09B_529.0 was collected in this lithology.

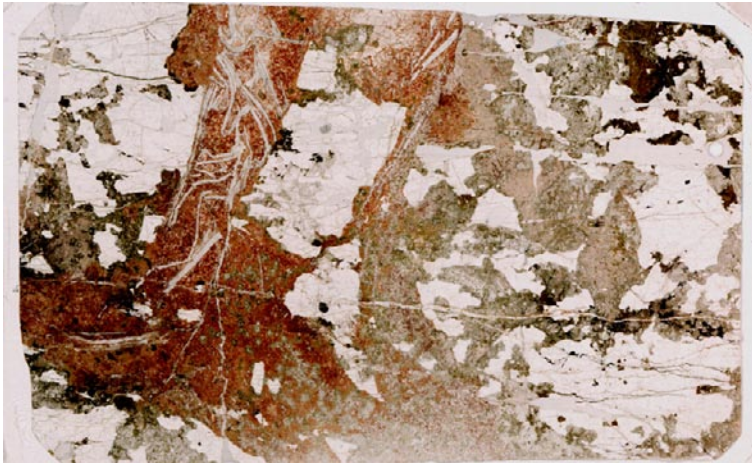


Figure 5-95. Scanned thin section of laumontite-sealed network and proto-breccia at 529.0 m (Sample KFM09B_529.0).

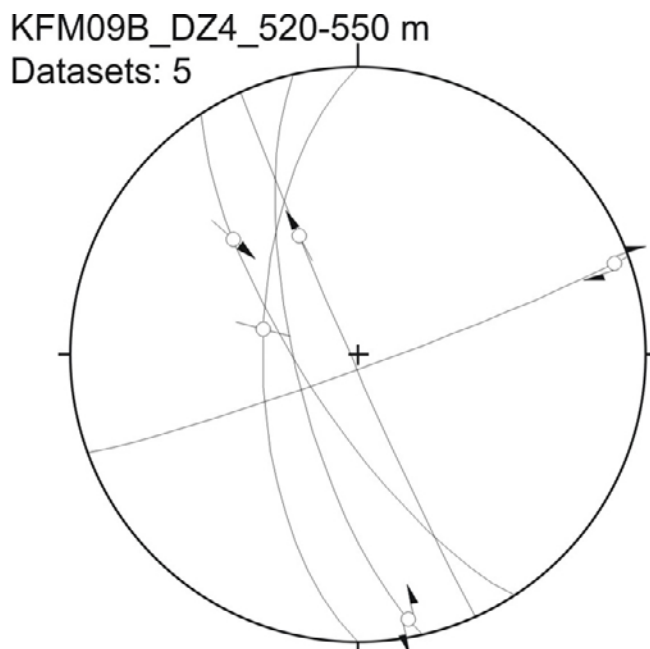


Figure 5-96. Stereoplot of fault slip data in DZ4 (KFM09B).

KFM09B: 561–574 m – DZ5

DZ5 is fairly short and is situated in medium-grained metagranite-granodiorite with subordinate pegmatite. Most of the zone shows an increased frequency of sealed and open fractures striking mainly ENE. From 569 m and downwards to the base of the zone vuggy granite with very few fractures is present (photo inset in Figure 5-97). Fracture filling minerals are mainly chlorite and subordinate calcite, clay minerals and laumontite. Laumontite-sealed fractures with minor fracture networks occur at 562.5 m. To summarize, DZ5 is a transition zone according to the definition of /Munier et al. 2003/.

Only one steep WSW-ENE strike-slip and chlorite-striated fault has been measured along DZ5 in KFM09B (Figure 5-98).

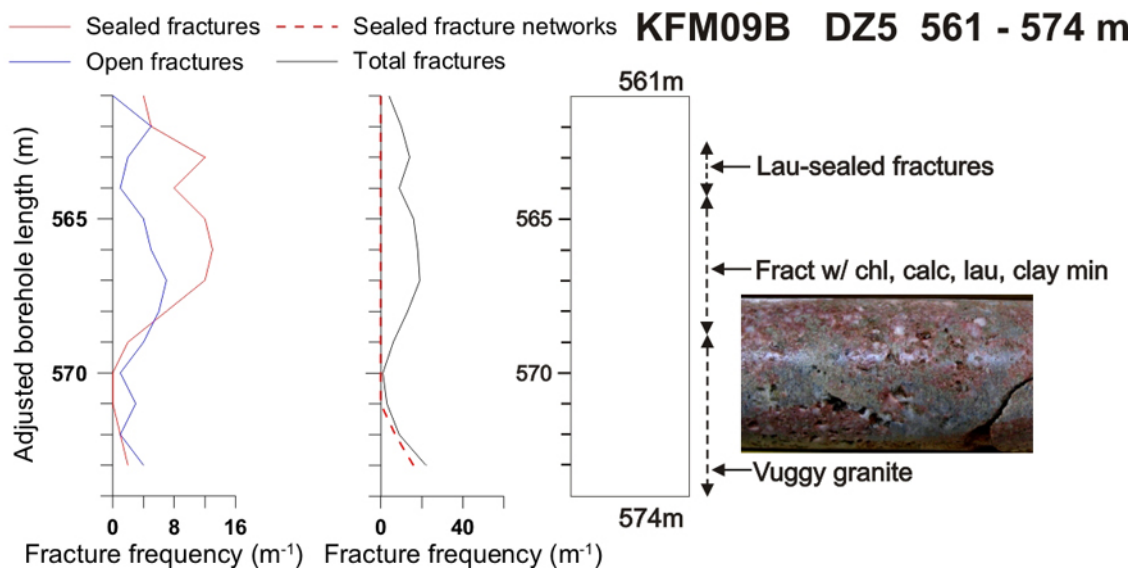


Figure 5-97. Simplified drawing of KFM09B, DZ5, showing the occurrences of significant brittle deformation features. Abbreviations as in Figure 5-3.

KFM09B_DZ5_561-574 m
 Datasets: 1

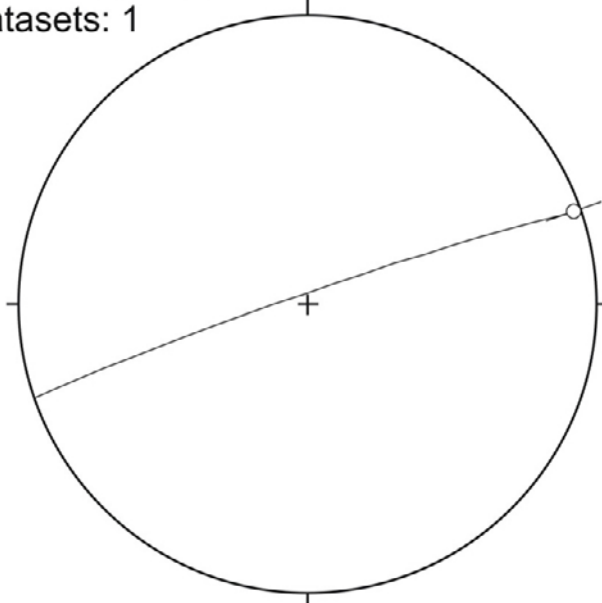


Figure 5-98. Stereoplot of fault slip data in DZ5 (KFM09B).

5.1.10 KFM10A

This borehole is located northeast of the Eckarfjärden deformation zone along the south-western border of the candidate area (Figure 5-1). The borehole is oriented 010/50 and has a length of 500 m (Carlsten et al. 2006f). Three deformation zones were investigated with a combined length of 113 m (Table 5-1). 40 kinematic data are collected in the studied part of the core (Figure 5-99). Apart from some gently southward- and northward-dipping, probably reverse faults, the main trend corresponds to NW-SE steep strike-slip faults that display a predominant sinistral sense of shear.

KFM10A: 63–145 m – DZ1

The rock types along DZ1 are mainly strongly foliated fine- to medium-grained metagranite-granodiorite with occurrences of pegmatitic granite and amphibolite. Some vuggy granites are also present (Figure 5-100). The geometry of fractures is variable. Three sets are apparent: (1) strike NW-SE and dip steeply to the SW, (2) gently dipping to sub-horizontal and, (3) strike NE-SW and dip variably to the SE.

From the top of the zone to ca 90 m, there are mainly single fractures with moderate frequency (Figure 5-101). Fractures are coated with chlorite and sometimes with clay minerals and minor calcite. At 78.50 m a thick calcite-cemented micro-breccia occurs in an amphibolitic body. At 82 m, a 1 cm thick fine-grained laumontite-calcite-sealed breccia is observed. A crush zone occurs at ca 86 m.

The fracture frequency increases slightly between 100 and 110 m. The fractures are coated with calcite, chlorite, hematite, asphaltite, and clay minerals. Abundant open/broken fractures with calcite are observed in the interval 103–104 m. A crush zone is developed at ca 106 m. At ca 109 m, a vein with calcite-chlorite-clay mineral is cut by a quartz-calcite-filled fracture and the latter is roughly parallel to a chlorite-pyrite-coated fracture (Figure 5-102). A set of thin calcite-laumontite sealed fractures is also present (Figure 5-102).

KFM10A_DZ1_DZ2_DZ3 Datasets: 40

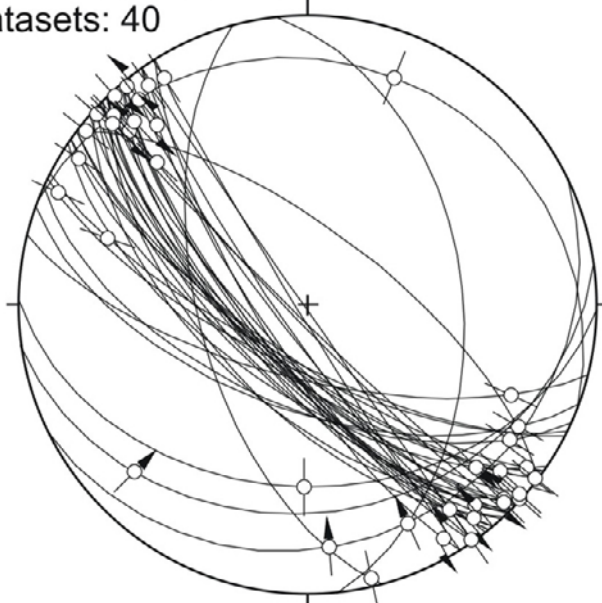


Figure 5-99. Stereoplot showing all the fault slip data collected along all the studied deformation zones in drill core KFM10A.

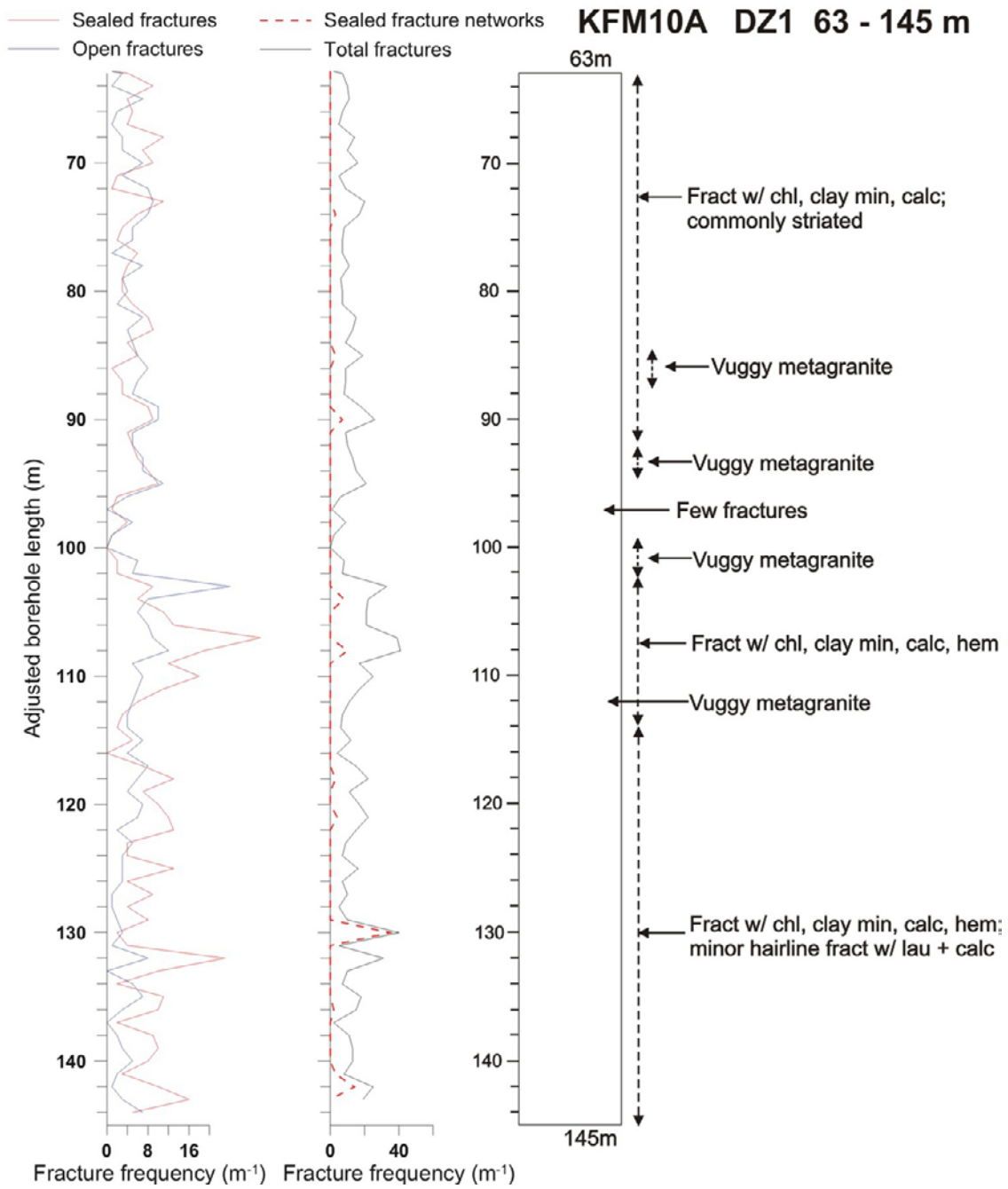


Figure 5-100. Simplified drawing of DZ1 showing brittle structures. Abbreviations as in Figure 5-3.



Figure 5-101. An overview of the upper part of DZ1 in KFM10A. A moderate frequency of single fractures coated with chlorite, clay minerals and minor calcite dominates.

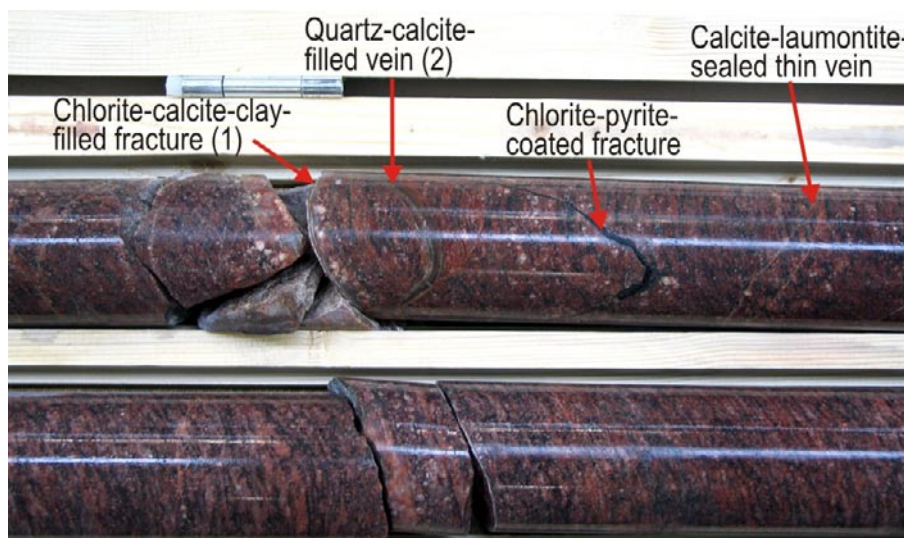


Figure 5-102. At 109 m (KFM10A, DZ1), a calcite-chlorite-clay filled fracture (1) is cut by a quartz calcite-filled vein (2). The latter is roughly parallel to a chlorite-pyrite coated fracture. Hairline laumontite-calcite-sealed fractures are also present.

The lower half of the zone displays some fractures with chlorite, chlorite + hematite, calcite + chlorite, chlorite + hematite + clay minerals. Rare sealed hairline fractures with laumontite and calcite occur and are responsible for the increase of fracture frequency at 130 m (Figure 5-100). Based on the overall nature and distribution of brittle deformation features, DZ1 qualifies as a transition zone according to /Munier et al. 2003/.

The density of striated faults along DZ1 in KFM10A is the second highest encountered in this study with on average one fault every two metres of drill core. 37 fault slip data have been measured (Figure 5-103). Striations are observed on chlorite, calcite and clay minerals. Most of the data were obtained from steeply SW-dipping strike-slip faults. Eight sinistral slips have been determined using well-formed steps of calcite on these surfaces (Figure 5-103). Two faults are gently N- and S-dipping dip-slip faults with a reverse slip determined on the S-dipping plane (Figure 5-103).

KFM10A: 430–449 m – DZ2

The rock types along DZ2 in KFM10A are medium to coarse-grained metagranite- granodiorite with some amphibolite. Three main sets of fractures exist: (1) steep north-dipping fractures, (2) sub-horizontal fractures, and (3) steep to gently dipping NW-SE fractures.

The upper part of the zone is characterised by open fractures with mainly chlorite and clay minerals (Figure 5-104) and at 435 m, by sealed fractures with laumontite that are oriented parallel to the drill core (Figure 5-105). At 440 m, the fracture frequency is the highest in the zone and due to the presence of thin fractures sealed with chlorite (Figure 5-104). The lower part of the zone displays a moderate amount of fractures coated with chlorite, clay minerals, calcite and laumontite (Figure 5-104). DZ2 qualifies as a transition zone according to /Munier et al. 2003/.

KFM10A_DZ1_63-145 m
Datasets: 37

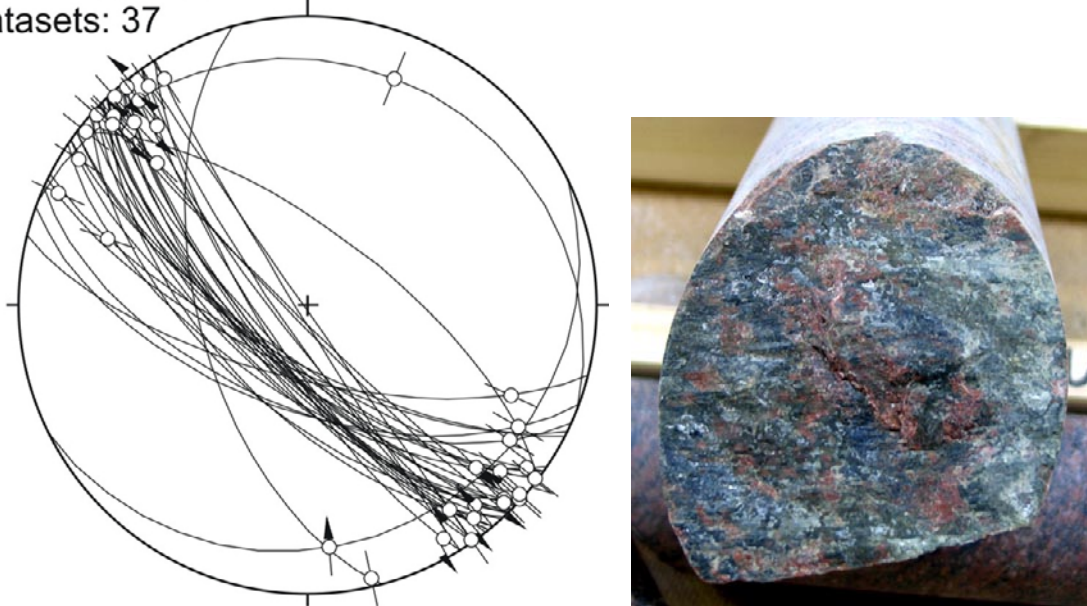


Figure 5-103. Left: Stereonet of the striated faults along DZ1 in KFM10A. Right: Example of fault surface with sinistral calcite steps and striations on hematite, chlorite and clay minerals (strike/dip angle/pitch: 147/76/7) (63.89 m).

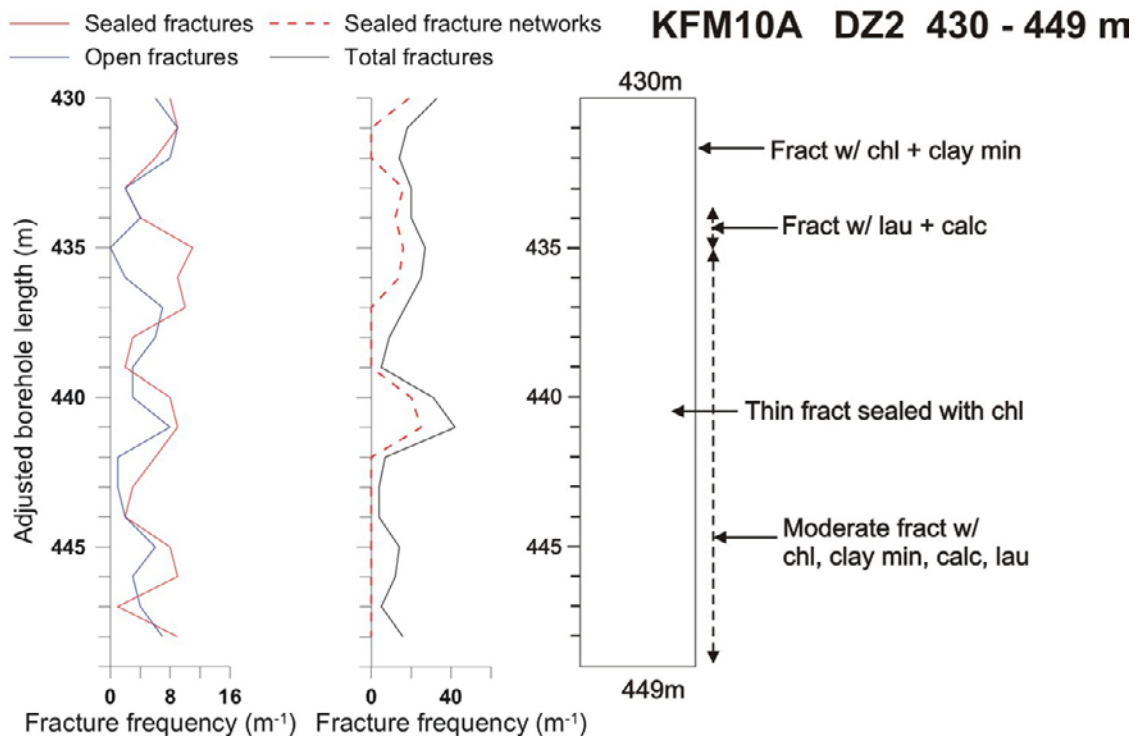


Figure 5-104. Simplified drawing of DZ2 showing brittle structures. Abbreviations as in Figure 5-3.



Figure 5-105. Left: Fractures with calcite-laumontite in grey metagranite-granodiorite that are oriented parallel to the drill core in DZ2 of KFM10A. Right: Example of fault plane with greenish calcite steps showing a reverse/sinistral sense of shear (strike/dip angle/pitch: 354/44/-26) (436.36 m).

Only two faults with fault-slip data have been measured along DZ2 in KFM10A (Figure 5-106): a 44 degrees E-dipping reverse, sinistral fault and 30 degrees S-dipping reverse/sinistral fault. Both fault surfaces contain steps of greenish calcite as illustrated in Figure 5-105.

KFM10A: 478–490 m – DZ3

The rock types along DZ3 in KFM10A are metagranite-granodiorite with minor pegmatite and amphibolite. Gentle to steep SSW-dipping fractures are the main set encountered along the zone. The fractures are mainly with chlorite, clay minerals, hematite, calcite, prehnite and oxides (Figure 5-107). The fracture frequency increases at ca 485 m (Figure 5-107). DZ3 qualifies as a transition zone according to /Munier et al. 2003/.

One gently S-dipping dip-slip fault with an undetermined sense of slip has been measured along DZ3 in KFM10A (Figure 5-108). Striations affect chlorite and prehnite.

KFM10A_DZ2_430-449 m
Datasets: 2

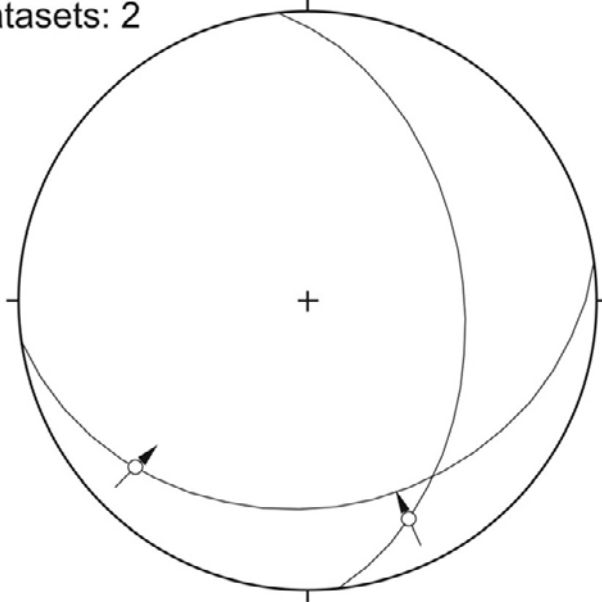


Figure 5-106. Stereonet of the striated faults along DZ2 in KFM10A.

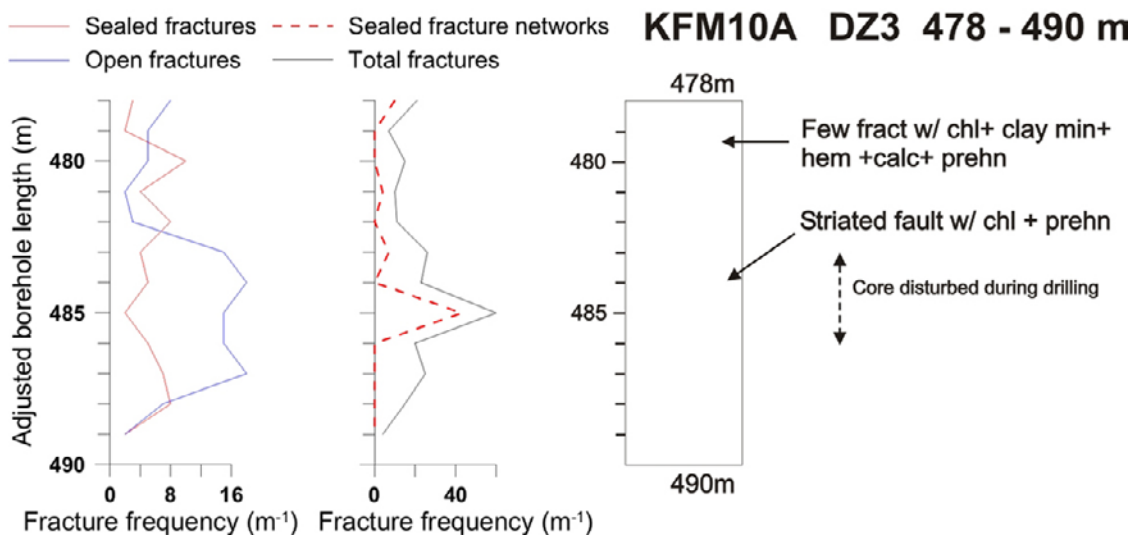


Figure 5-107. Simplified drawing of DZ3 showing brittle structures. Abbreviations as in Figure 5-3.

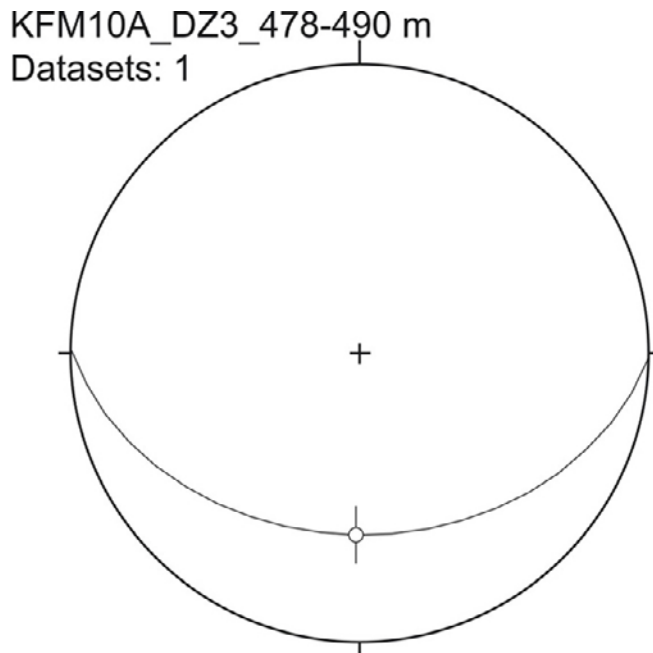


Figure 5-108. Stereonet of the striated fault in DZ3 of core KFM10A.

5.2 Summary of the results of the borehole data

Seven boreholes (KFM01C, KFM01D, KFM07B, KFM07C, KFM08C, KFM09A and KFM09B) are situated in the northwest part of the investigation area (Figure 5-1). Kinematic data were mainly obtained from a population of steep faults in KFM09A (especially in DZ3) that strike NW-SE to NNW-SSE. Slickensides on these faults show mainly sinistral strike-slip sense of movement. This trend is also observed in KFM09B, again with mainly sinistral sense of shear. In both of these cores, a minor proportion of the NW-SE to NNW-SSE faults are showing dextral strike-slip movement. The cores also exhibit a set of steep ENE-WSW-trending dextral faults that may form a conjugate set with the sinistral NW-SE to NNW-SSE faults. However, these faults are less abundant than the NW-SE to NNW-SSE faults.

The steep NNW-SSE-striking set of sinistral faults is also observed in drill core KFM01C, mainly in DZ2 of the drill core. However, the possible conjugate set of dextral faults displays a slight deviation in orientation to NE-SW for most of the planes and is focused in DZ3 of the drill core. It may be noted that DZ3 of KFM01C is the zone with the highest observed frequency of striated fault (more than 1 striated fault per metre) of all the investigated deformation zones in the present study.

In drill core KFM08C (DZ2), NNE-SSW sinistral faults that dip 70 degrees to the west are observed in addition to steep NNW-SSE sinistral faults.

During the first phase of the study /Nordgulen and Saintot 2006/, the predominant set of NW to NNW steep faults was largely observed in KFM04A, KFM07A, KFM08A and KFM08B. The steep ENE-WSW striking faults were also identified in KFM04A KFM06A and KFM07A. The strike-slip character of both fault sets was also recorded. The data presented in this study suggest that the NW-SE/NNW-SSE sinistral faults and ENE-WSW dextral faults define a conjugate system of strike-slip faults. However, the fact that a minor proportion of opposite shear sense have been observed on both fault sets, suggests that the effects of different stress regimes can be seen along these faults.

KFM10A and KFM06C are located some distance away from the group of boreholes mentioned above (Figure 5-1). KFM10A is located northeast of the major EDZ, along the south-western border of the candidate area. KFM10A and more specifically DZ1 of KFM10A (DZ1 of core

KFM10A showing the second highest frequency of striated faults, with one fault every two meters of core in average), displays a set of steep strike-slip faults with an important population of sinistral striae. KFM06C is located in the central part of the candidate area. The main set of faults is oriented NNE-SSW and comprises roughly vertical sinistral faults, resembling those observed along DZ2 in KFM08C.

In many of the studied deformation zones, there is a small but significant population of gently dipping to flat-lying faults trending E-W to NE-SW. They are reminiscent of the important population of reverse faults identified during the first phase of the study, especially in KFM02A /Nordgulen and Saintot 2006/. As such, they may also represent the faults similar to those imaged as the large seismic reflectors interpreted as thrusts by /Juhlin and Stephens 2006/.

Among the oldest observed fractures are the epidote- and quartz-sealed veins with some chlorite. Epidote has not been observed on any of the fault surfaces. Striated fault surfaces are commonly coated with chlorite, hematite and calcite, and calcite may also form steps on many faults. In some deformation zones, it is observed that a fairly large proportion of the striated fault planes have been recorded along sections of drill core with amphibolitic and in dioritic bodies (e.g. DZ3 of drill core KFM09A). Chlorite-coated faults are commonly reactivated and/or cut by faults and fractures with laumontite, calcite, adularia and prehnite. In many cases these minerals have sealed breccias and cataclasites. Late fracture minerals include quartz, calcite, fluorite, pyrite and clay minerals. Rare asphaltite occurs on some of the fractures in the upper parts of the boreholes. These observations suggest that the main faults and fracture systems have been reactivated and coated/filled with a variety of minerals in response to changes in hydrothermal regime and stress conditions.

References

- Braathen A, 1999.** Kinematics of brittle faulting in the Sunnfjord region, western Norway. *Tectonophysics* 302, 99–121.
- Braathen A, Gabrielsen R H, 2000.** Bruddsoner i fjell- oppbygning og definisjoner. *Gråstein*, 7, 1–20. Norges geologiske undersøkelse, ISSN 0807-4801.
- Braathen A, Osmundsen P T, Nordgulen Ø, Roberts D, Meyer G B, 2002.** Orogen-parallel extension of the Caledonides in northern Central Norway: an overview. *Norwegian Journal of Geology*, 82, 225–241.
- Braathen A, Osmundsen P T, Gabrielsen R, 2004.** Dynamic development of fault rocks in a crustal-scale detachment; an example from western Norway. *Tectonics*, 23, TC4010, doi:10.1029/2003TC001558.
- Caine J S, Evans J P, Forster C B, 1996.** Fault zone architecture and permeability structure. *Geology*, 24, 11, 1025–1028.
- Carlsten S, Gustafsson J, Keisu M, Peterson J, Stephens M B, 2006a.** Geological single-hole interpretation of KFM09A and KFM07B. SKB P-06-134, Svensk Kärnbränslehantering AB.
- Carlsten S, Gustafsson J, Mattson H, Peterson J, Stephens M B, 2006b.** Geological single-hole interpretation of KFM06C. SKB P-06-83, Svensk Kärnbränslehantering AB.
- Carlsten S, Gustafsson J, Mattson H, Peterson J, Stephens M B, 2006c.** Geological single-hole interpretation of KFM01D, HFM24, FM25, HFM27 and HFM29. SKB P-06-210, Svensk Kärnbränslehantering AB.
- Carlsten S, Gustafsson J, Petersson J, Stephens M B, Thunehed H, 2006d.** Geological single-hole interpretation of KFM09B and KFM01C. SKB P-06-135, Svensk Kärnbränslehantering AB.
- Carlsten S, Peterson J, Samuelsson E, Stephens M B, Thunehed H, 2006e.** Geological single-hole interpretation of KFM07C and HFM26. SKB P-06-208, Svensk Kärnbränslehantering AB.
- Carlsten S, Peterson J, Stephens M B, Thunehed H, 2006f.** Geological single-hole interpretation of KFM08C, KFM10A, HFM23, HFM28, HFM30, HFM31, HFM32 and HFM38. SKB P-06-207, Svensk Kärnbränslehantering AB.
- Evans J P, Forster C B, Goddard J V, 1997.** Permeability of fault-related rocks, and implications for hydraulic structure of fault zones. *Journal of Structural Geology*, 19, 1393–1404.
- Gudmundsson A, Berg S S, Lyslo K B, Skurtveit E, 2001.** Fracture networks and fluid transport in active fault zones. *Journal of Structural Geology*, 23, 2–3, 343–353. 0191–8141.
- Juhlin C, Stephens M B, 2006.** Gently dipping fracture zones in Paleoproterozoic metagranite, Sweden: Evidence from reflection seismic and cored borehole data and implications for disposal of nuclear waste. *Journal of Geophysical Research*, B09302, doi: 10.1029/2005JB003887.
- Munier R, Stanfors R, Milnes A G, Hermanson J, Triumf C-A, 2003.** Geological Site Descriptive Model. A strategy for model development during site investigations. SKB R-03-07, Svensk Kärnbränslehantering AB.
- Nordgulen Ø, Braathen A, Corfu F, Osmundsen P T, Husmo T, 2002.** Polyphase kinematics and geochronology of the Kollstraumen detachment, north-central Norway. *Norwegian Journal of Geology*, 82, 299–316.

Nordgulen Ø, Braathen A, 2005. Structural investigations of deformation zones (ductile shear zones and faults) around Forsmark – a pilot study. SKB P-05-183, Svensk Kärnbränslehantering AB.

Nordgulen Ø, Saintot A, 2006. The character and kinematics of deformation zones (ductile shear zones, fault zones and fracture zones) at Forsmark – report from phase 1. SKB P-06-212, Svensk Kärnbränslehantering AB.

Osmundsen P T, Braathen A, Nordgulen Ø, Roberts D, Meyer G B, Eide E A, 2003. The Nesna shear zone and adjacent gneiss-cored culminations, North-central Norwegian Caledonides. *Journal of the Geological Society, London* 160, 1–14.

Petit J P, 1987. Criteria for the sense of movement on fault surfaces in brittle rocks. *Journal of Structural Geology* 9, 597–608.

Sandström B, Savolainen M, Tullborg E L, 2004. Fracture mineralogy. Results from fracture minerals and wall rock alteration in boreholes KFM01A, KFM02A, KFM03A and KFM03B. Forsmark site investigation. SKB P-04-149, Svensk Kärnbränslehantering AB, 93 pp.

Sandström B, Tullborg E L, 2005. Fracture mineralogy. Results from fracture minerals and wall rock alteration in boreholes KFM01B, KFM04A, KFM05A and KFM06A. SKB P-05-197, Svensk Kärnbränslehantering AB, 151 pp.

Twiss R J, Moores E M, 1992. *Structural geology*. W.H. Freeman & Company, New York, 592 pp.

Samples for microscope studies

ID	Adjusted SecUp	Possible deformation zone	Sample
KFM01C	312.66	DZ3	Vein sealed with calcite + prehnite
KFM01C	329.9	DZ3	Vein sealed with calcite + prehnite
KFM06C	429.4	DZ3	Fault rock sealed with laumontite
KFM07B	234.2	DZ4	Fault rock sealed with laumontite + calcite
KFM07C	348.8	DZ2	Fault rock sealed with laumontite + calcite
KFM07C	380.64	DZ2	Laumontite-sealed fault rock with epidote + zoisite
KFM09A	33.15	DZ1	Laumontite-sealed fault breccia
KFM09A	94.74	DZ2	Green chlorite-rich fault rock, foliated
KFM09B	121.45	DZ1	Chlorite-rich fault rock
KFM09B	402.3	DZ3	Cataclasite and ultra-cataclasite with calcite
KFM09B	529.0	DZ4	Fault rock sealed with laumontite + calcite